

REPUBLIC OF IRAQ

MINISTRY OF HIGHER EDUCATION

AND SCIENTIFIC RESEARCH

AL-FURAT AL-AWSAT TECHNICAL  
UNIVERSITY

ENGINEERING TECHNICAL  
COLLEGE- NAJAF



# A NOVEL DESIGN AND ANALYSIS STUDY OF OPTICAL MICROSTRIP NANOANTENNA

A THESIS

SUBMITTED TO THE COMMUNICATION TECHNIQUES  
ENGINEERING DEPARTMENT

IN PARTIAL FULFILLMENT OF THE REQUIREMENTS FOR  
THE MASTER OF TECHNIQUES DEGREE IN  
COMMUNICATION TECHNIQUES ENGINEERING

BY

**Bassam Raof Mohammed Ali**

Supervised by

**Prof. Abdulkadhum Jaafar Alyasiri, Ph.D.**

**Asst. Prof. Faris Mohammed Ali, Ph.D.**

September 2019

بِسْمِ اللَّهِ الرَّحْمَنِ الرَّحِيمِ

﴿ نرفع درجات من نشاء وفوق كل ذي علم عليم ﴾

صَدَقَ اللَّهُ الْعَلِيُّ الْعَظِيمُ

الآية (76) من سورة يوسف

## **DEDICATION**

**To the greatest person in this world**

**AL-IMAM AL-MAHDI AL-MUNTATHAR**

**Alayhi Alsalam**

**To the one I am so proud to carry his name, to the one who  
taught me giving, to my father.**

**To my love, devoted, tender, affectionate, merciful, to life's  
smile, to the essence of existence, to my beloved mother.**

**To loyalty and sincerity, to that encouraged me, in my life, to  
my family.**

**BASAM**

**2019**

## Acknowledgment

In the beginning, I would like to thank *Allah* Almighty, the most gracious, the most merciful, for giving me the determination and the strength to complete this research in the field of communications technology engineering.

I appreciate the guidance and advice that I have received from the supervisors **Prof. Dr. Abdulkadhum Jaafar Alyasiri** and **Assistant Prof. Dr. Faris Mohammed Ali** and their continued support and encouragement.

I extend my sincere thanks to the **AL-FURAT AL-AWSAT TECHNICAL UNIVERSITY, ENGINEERING TECHNICAL COLLEGE- NAJAF** and **COMMUNICATION TECHNIQUES Eng. Dept.** for their supports throughout my studies.

I would like also to express my thanks to **Asst. Prof. Dr. Ali Jabbar Salim** and **Ph.D. Gufran Mahdi** for providing advice throughout the research period.

I am very grateful to my **family** for their help, understanding, patience, and encouragement. Finally, I would like to thank my **father** and **mother** for their patience, long-suffering and great encouragement. To them, I owe everything in my life from birth to death.

## Supervisors Certifications

We certify that this thesis titled “**A Novel Design and Analysis Study of Optical Microstrip Nanoantenna**” which is being submitted by **Bassam Raof Mohammed Ali** was prepared under my/our supervision at the Communication Techniques Engineering Department, Engineering Technical College-Najaf, AL-Furat Al-Awsat Technical University, as a partial fulfillment of the requirements for the Communication Techniques Engineering.

Signature:  
Name: **Prof. Dr. Abdulkadhum Jaafar Alyasiri**  
(Supervisor)  
Date:     /     / 2019

Signature:  
Name: **Asst. Prof. Dr. Faris Mohammed Ali**  
(Supervisor)  
Date:     /     / 2019

In view of the available recommendation, we forward this thesis for debate by the examining committee.

Signature:  
Name: **Dr. Salim M. Wadi**  
(Head of Comm. Tech. Eng. Dept.)  
Date:     /     / 2019

## Committees Report

We certify that we have read this thesis titled “**A Novel Design and Analysis Study of Optical Microstrip Nanoantenna**” which is being submitted by **Bassam Raof Mohammed Ali** and as Examining Committee, examined the student in its contents. In our opinion, the thesis is adequate for award of Master Science degree in Communication Techniques Engineering.

Signature:  
Name: **Prof. Dr. Abdulkadhum Jaafar Alyasiri**  
(Supervisor and member)  
Date:     /     / 2019

Signature:  
Name: **Asst. Prof. Dr. Faris Mohammed Ali**  
(Supervisor and member)  
Date:     /     / 2019

Signature:  
Name: **Asst. Prof. Dr. Musa H. Wali**  
(Member)  
Date:     /     / 2019

Signature:  
Name: **Dr. Salim M. Wadi**  
(Member)  
Date:     /     / 2019

Signature:  
Name: **Asst. Prof. Dr. Ali Albakry**  
(Chairman)  
Date:     /     / 2019

### Approval of the Engineering Technical College- Najaf

Signature:  
Name: **Asst. Prof. Dr. Ali Albakry**  
Dean of Engineering Technical College- Najaf  
Date:     /     / 2019

## Abstract

Several sensing and scientific applications interest the attention of researchers in the area of microstrip nanoantenna design toward the terahertz frequency range. The invention of new components in the nanotechnology as well as optical spectroscopic techniques also leads to the development of the THz region applications.

In this work, the various geometrical parameters such as the feeding, dimensions of patch, substrate and ground plane are inserted with different sizes and shapes in Nanoantennas have been conducted.

In this thesis, design, simulate and analyze a new microstrip nanoantenna that operates in THz region and covers a lot of optical communication bands or frequencies range from (100-150) THz. we have designed and simulated six Microstrip Nanoantenna shapes, where getting a several frequency bands which operate in THz region. All the dielectric substrate of the six microstrip Nanoantenna designs are composed the silicon dielectric material since it contains high dielectric constant  $\epsilon=11.9$ . The feeding type that has been used for exciting these types of Nanoantennas were waveguide feed at  $50 \Omega$ . All dimensions of the substrate that have been used in the Microstrip Nanoantenna designs are in the range of  $(950 \times 950) \text{ nm}^2$  with a thickness of 50 nm and the dimensions of the ground plane are in the range of  $(950 \times 950) \text{ nm}^2$  with a thickness of 20 nm. The patch dimensions are in the range of  $(450 \times 450) \text{ nm}^2$  with a thickness of 20 nm. In order to evaluate the performance of each proposed Nanoantenna, a commercially available software simulator called CST STUDIO SUITE 2018 has been utilized to achieve the desired goals. The first and second Microstrip

Nanoantenna designs take the form of Hash and Hash Slot, so it is called Microstrip Hash Nanoantenna (MHNA) and Microstrip Hash Slot Nanoantenna (MHSNA). These Nanoantennas works at bandwidth from (125.3 - 133.3) THz and (126.39 - 132.99) THz respectively. While the third and fourth Microstrip Nanoantenna designs take the form of Bluetooth and Bluetooth Slot, so it is called Microstrip Bluetooth Nanoantenna (MBNA) and Microstrip Bluetooth Slot Nanoantenna (MBSNA). These Nanoantennas works at bandwidth of (115.54 - 124.47) THz and (128.97 - 135.97) THz respectively. Finally, the fifth and sixth Microstrip Nanoantenna design takes the form of Wi-Fi and Wi-Fi Slot, so it is called Microstrip Wi-Fi Nanoantenna (MWNA) and Microstrip Wi-Fi Slot Nanoantenna (MWSNA), these Nanoantennas operate in the range of bandwidth of (103.31 - 110.31) THz and (103.31 - 110.31) THz respectively.



# Contents

Title	Page No.
Acknowledgment	I
Supervisors Certification	II
Committees Reports	III
Abstract	V
Contents	VII
Nomenclatures (Symbols)	XI
Abbreviations	XII
List of Figures	XIII
List of Tables	XV
List of Publications	XVI
<b>Chapter One: Introduction</b>	
1.1 Background	1
1.2 Microstrip Antenna	3
1.3 Applications of the Nanoantenna	3
1.4 Motivation	5
1.5 Problem Statement	5
1.6 Aim of the work	6
1.7 Objective	6
1.8 Thesis Contribution	6
1.9 Thesis layout	7
<b>Chapter Two: Literatures Review</b>	
2.1 Introduction	8
2.2 Literature survey	8
<b>Chapter Three: Theory and Design Configuration</b>	
3.1 Introduction	23
3.2 Microstrip Antenna layers	24
3.2.1 Patch Antenna (first layer)	24
3.2.2 Substrate (second layer)	24
3.2.3 Ground (third layer)	25

3.3 Feeding Technique	26
3.3.1 Microstrip line feed	27
3.3.2 Coaxial feed	28
3.3.3 Aperture coupled feed	29
3.3.4 Proximity coupled feed	30
3.3.5 Co-Planer Waveguide (CPW) feed	31
3.3.6 Waveguide feed	32
3.4 Antenna parameters	32
3.3.1 Reflection Coefficient	32
3.3.2 Gain	33
3.3.3 Directivity	34
3.3.4 Current distribution	34
3.3.5 Radiation pattern	35
3.3.6 Efficiency	35
3.3.7 Bandwidth	35
3.5 The proposed model I; Microstrip Hash Nanoantenna (MHNA)	36
3.6 The proposed model II; Microstrip Hash Slot Nanoantenna (MHSNA)	38
3.7 The proposed model III; Microstrip Bluetooth Nanoantenna (MBNA)	41
3.8 The proposed model V; Microstrip Bluetooth Slot Nanoantenna (MBSNA)	44
3.9 The proposed model VI; Microstrip Wi-Fi Nanoantenna (MWNA)	46
3.10 The proposed model VII; Microstrip Wi-Fi Slot Nanoantenna (MWSNA)	49
3.11 Analysis Formulation of the Microstrip Nanoantenna Structures.	51
<b>Chapter Four: Results, Discussions and Performance Evaluation</b>	
4.1 Introduction	53
4.2 Characteristics of the Microstrip Hash-shape Nanoantenna and Microstrip Hash-shape Slot Nanoantenna.	53
4.2.1 Reflection Coefficient for MHNA & MHSNA	53

4.2.2 Gain for MHNA & MHSNA	55
4.2.3 Directivity for MHNA & MHSNA	57
4.2.4 Current distribution MHNA & MHSNA	58
4.2.5 Radiation patterns for MHNA & MHSNA	59
4.2.6 Efficiency for MHNA & MHSNA	62
4.2.7 Bandwidth for MHNA & MHSNA	62
4.2.8 Validation between MHNA, MHSNA and other references.	64
4.3 Characteristics of the Microstrip Bluetooth-shape Nanoantenna and Microstrip Bluetooth-shape Slot Nanoantenna.	65
4.3.1 Reflection Coefficient for MBNA & MBSNA	65
4.3.2 Gain for MBNA & MBSNA	66
4.3.3 Directivity for MBNA & MBSNA	68
4.3.4 Current distribution for MBNA & MBSNA	70
4.3.5 Radiation Patterns for MBNA & MBSNA	71
4.3.6 Efficiency for MBNA & MBSNA	74
4.3.7 Bandwidth for MBNA & MBSNA	74
4.3.8 Validation between MBNA, MBSNA and other references.	76
4.4 Characteristics of the Microstrip Wi-Fi-shape Nanoantenna and Microstrip Wi-Fi-shape Slot Nanoantenna.	77
4.4.1 Reflection Coefficient for MWNA & MWSNA	77
4.4.2 Gain for MWNA & MWSNA	78
4.4.3 Directivity for MWNA & MWSNA	81
4.4.4 Current distribution for MWNA & MWSNA	82
4.4.5 Radiation Patterns for MWNA & MWSNA	83
4.4.6 Efficiency for MWNA & MWSNA	86
4.4.7 Bandwidth for MWNA & MWSNA	86
4.4.8 Validation between MWNA, MWSNA and other references.	88
4.5 Comparison between overall six proposed designs.	89
<b>Chapter Five: Conclusions and Suggestions for Future Work</b>	
5.1 Introduction	92

5.2 Conclusion	92
5.3 Suggestion for Future Scope	93
References	95

### Nomenclatures (Symbols)

Symbol	Meaning
$E_+$	Amplitude of incident wave
$E_-$	Amplitude of reflected wave
$f_c$	Center frequency
$\epsilon$	dielectric constant
D	Directivity
$\epsilon_{\text{reff}}$	Effective dielectric constant
R1	First Patch circle
R4	Fourth Patch circle
$v_o$	free space velocity of light
G	Gain
Lg	Ground length
Wg	Ground width
t	Patch thickness
U	Radiation intensity
U	Radiation intensity
$S_{11}$	Reflection coefficient
$f_r$	Resonant frequency
R2	Second Patch circle
h	Substrate height
L	Substrate length
W	Substrate width
T	Thickness of Ground & Thickness of patch
H	Thickness of Substrate
R3	Third Patch circle
P <sub>in</sub>	Total input power
P <sub>rad</sub>	total power radiation

## List of Abbreviations

Abbreviation	Meaning
BW	Bandwidth
BT	Bluetooth
CST	Computer Simulation Technology
CPW	Coplanar Waveguide
dB	decibel
FDTD	Finite Difference Time Domain
FDFD	Finite Deference Frequency Domain
FR4	Flame Resistant
HFSS	High-Frequency Structural Simulator
IR	Infrared
IEEE	Institute of Electrical and Electronics Engineers
MBNA	Microstrip Bluetooth Nanoantenna
MBSNA	Microstrip Bluetooth Slot Nanoantenna
MHNA	Microstrip Hash Nanoantenna
MHSNA	Microstrip Hash Slot Nanoantenna
MWNA	Microstrip Wi-Fi Nanoantenna
MWSNA	Microstrip Wi-Fi Slot Nanoantenna
NbN	Niobium Nitride
MgO	Oxide manganese
PBG	Photonic Band Gap
PEC	Perfect Electric Conductor
SPP	Surface Plasmon Polaritons
THz	Terahertz
VSWR	Voltage Standing Wave Ratio
Wi-Fi	Wireless Fidelity

## List of Figures

<b>Figure No.</b>	<b>Figure Title</b>	<b>Page No.</b>
Fig. 1.1	The electromagnetic spectrum	5
Fig. 3.1	Basic structure of Microstrip	24
Fig. 3.2	Common shapes of patch	25
Fig. 3.3	Microstrip Line Feed	26
Fig. 3.4	Coaxial feed	27
Fig. 3.5	Aperture coupled feed	28
Fig. 3.6	Proximity coupled feed	29
Fig. 3.7	CPW feed	30
Fig. 3.8	Waveguide feed	31
Fig. 3.9	a: MHNA front view, b: MHNA side view, c: MHNA perspective view, d: MHNA bottom view.	36
Fig. 3.10	a: MHSNA front view, b: MHSNA side view, c: MHSNA perspective view, d: MHSNA bottom view.	39
Fig. 3.11	a: MBNA front view, b: MBNA side view, c: MBNA bottom view, d: MBNA perspective view.	41
Fig. 3.12	a: MBSNA front view, b: MBSNA side view, c: MBSNA perspective view, d: MBSNA bottom view.	44
Fig. 3.13	a: MWNA front view, b: MWNA side view, c: MWNA perspective view, d: MWNA bottom view.	46
Fig. 3.14	a: MWSNA front view, b: MWSNA side view c: MWSNA bottom view, d: MWSNA perspective view.	49
Fig. 4.1	$S_{11}$ of MHNA	53
Fig. 4.2	$S_{11}$ of MHSNA	53
Fig. 4.3	Gain of MHNA (a) 3D and (b) 2D	54
Fig. 4.4	Gain of MHSNA (a) 3D and (b) 2D	54
Fig. 4.5	Directivity of MHNA	55

Fig. 4.6	Directivity of MHSNA	55
Fig. 4.7	Current distribution, (a) MHNA & (b) MHSNA	56
Fig. 4.5	Radiation pattern of the MHNA at $f=129.44$ THz.	58
Fig. 4.6	Radiation pattern of the MHSNA at $f=129.74$ THz.	59
Fig. 4.10	Bandwidth of MHNA	61
Fig. 4.11	Bandwidth of MHSNA.	61
Fig. 4.12	$S_{11}$ of MBNA	63
Fig. 4.13	$S_{11}$ of MBSNA	64
Fig. 4.14	Gain of MBNA (a) 3D and (b) 2D	64
Fig. 4.15	Gain of MBSNA (a) 3D and (b) 2D	65
Fig. 4.16	Directivity of MBNA	66
Fig. 4.17	Directivity of MBSNA	66
Fig. 4.18	Current distribution, (a) MBNA & (b) MBSNA	67
Fig. 4.19	Radiation pattern of the MBNA at $f=120$ THz.	69
Fig. 4.20	Radiation pattern of the MBSNA at $f=133$ THz.	70
Fig. 4.21	Bandwidth of MBNA	72
Fig. 4.22	Bandwidth of MBSNA	72
Fig. 4.23	$S_{11}$ of MWNA	74
Fig. 4.24	$S_{11}$ of MWSNA	75
Fig. 4.25	Gain of MWNA (a) 3D and (b) 2D	76
Fig. 4.26	Gain of MWSNA (a) 3D and (b) 2D	76
Fig. 4.27	Directivity of MWNA	77
Fig. 4.28	Directivity of MWSNA	77
Fig. 4.29	Current distribution of (a) MWNA & (b) MWSNA	78
Fig. 4.30	Radiation pattern of the MWNA at $f=106$ THz	80
Fig. 4.31	Radiation pattern of the MWNA at $f=126.28$ THz	81
Fig. 4.32	Bandwidth of MWNA	83
Fig. 4.33	Bandwidth of MWSNA	83
Figure 4.34	Values of six proposed nanoantennas.	87



### List of Tables

<b>Table No.</b>	<b>Table Title</b>	<b>Page No.</b>
Table 2.1	The Microstrip Nanoantenna designs references	15
Table 3.1	MHNA dimensions	37
Table 3.2	MHSNA dimensions	40
Table 3.3	MBNA dimensions	42
Table 3.4	MBSNA dimensions	45
Table 3.5	MWNA dimensions	47
Table 3.6	MWSNA dimensions	50
Table 4.1	Characteristics of the far-field radiation pattern for the MHNA & MHSNA.	60
Table 4.2	Comparison between MHNA, MHSNA and references	62
Table 4.3	Characteristics of the far-field radiation pattern for the MBNA & MBSNA.	71
Table 4.4	Comparison between MBNA, MBSNA and references	73
Table 4.5	Characteristics of the far-field radiation pattern for the MWNA & MWSNA.	82
Table 4.6	Comparison between MWNA, MWSNA and references	84
Table 4.7	Comparison between the sixth proposed Nanoantennas.	86

### List of Publications

<b>Paper No.</b>	<b>Paper Title</b>	<b>Paper Status</b>
Paper 1	A New Design of Microstrip Hash-shape Nanoantenna & Microstrip Hash-shape Slot Nanoantenna at THz Spectroscopy for Imaging Application	Published In International Journal of Engineering & Technology
Paper 2	Comparison between a New Designs of Microstrip Wi-Fi-shape Nanoantenna (MUNA) & Microstrip Wi-Fi-shape Slot Nanoantenna (MWSNA) at THz region	Published In Journal of Physics: Conference Series, World Engineering, Science and Technology Conference 2019

# CHAPTER ONE

## INTRODUCTION

### 1.1 Background

The antenna is defined by IEEE Standard Definitions of Terms for Antennas defines the aerial or antenna as “a means for radiating or receiving radio waves.” In other words, the antenna is the transitional structure between free-space and a guiding device [1].

The nanoantenna is called the optical antenna. Optical antenna is like the traditional antenna, so it manages electromagnetic waves with the exception of that nanoantenna works in the optical frequency segment of the electromagnetic spectrum. Antenna measurements are comparable to the working wavelength so as to achieve resonance at optical frequencies. Antennas must be shrinking to the nanoscale size. Nanoantenna can be defined as "a nanometer scale metallic structure that is capable of enhancing the optical radiation interaction with the matter" [2].

In 1959, Richard Feynman presented an imaginative paper titled "There's Plenty of Room at the Bottom". He discussed the problem of controlling materials on nanoscale measurements. This paper proposed a scientific idea added to open researcher's eyes on the nanotechnology a little decades later. He talked about the likelihood of building nanoscale electric circuits as he asked "is it possible to emit light from nanoantenna array, like we emit radio waves from antenna array to beam the radio programs to Europe? Which is similar to beam the light out in a definite direction with high directivity" [2] [3].

The progress made by Feynman in nanofabrication techniques and nanotechnology studies turned Feynman's suggestion into a fact, and many nanoantennas for several applications have been fabricated [4] [5] [6] [7].

The general features of radiofrequency and microwave counterparts are compatible with the optical antenna. On the other word, the conventional antennas and nanoantennas are limited in light that the physical properties that materials have and materials reaction to the optical frequencies are various from that at RF/microwave frequencies. So, the design and the direct scaled-down interpretation of conventional antenna theory is impossible. Thus the new Nano scaled-down antenna theory should take into consideration the various phenomena at the optical frequencies [8].

The first concept of Nano optical is introduced by K.B.Crozier group in Stanford University to the Nano photonic device which connects optical-frequency electromagnetic waves to sub-wavelength scale effectively by using surface Plasmon effects [9]. So, Nanoantennas are designed to discover the light in the visible part, infrared part and farther, perhaps applied in Polari-metric imaging systems, optical sensors, and for other applications [10].

Newly Nanoantennas have received growing attention in nanotechnology research. They can be used in many applications like microscopy, data-communication, spectroscopy, and even solar energy harvesting [11].

## 1.1 Microstrip Antenna

The idea of Microstrip antenna starts in 1950 and it was presented by Deschamps, and for several years later Microstrip based antenna was presented by Gutton and Baissino, Despite the spread of the Microstrip concept, where there was little activity to develop in 15 years [12] [13]. So, the early of 1970, the development of Microstrip antenna began to increase with the need for thin antennas for spacecraft, conformal, and missiles [14].

## 1.2 Applications of the Nanoantenna

In this part, Microstrip antennas have been attracted much consideration from engineers, researchers and designers. Indeed, they have been utilized widely in RF and microwave systems, for example, biomedical systems, radar, communications, navigation, and remote sensing. Also, they can take several shapes, for example, dipole, patch, traveling-wave structure, or a slot, intended for specific applications [15].

**A. Microscopy:** Nanoantenna empowers scientists to create what is called near field optical microscopy. This optical imaging strategy can be utilized to break, as far as possible, around  $\lambda/2$ . In near field optical microscopy mapping of the near field distribution of nanoscale antenna or nanostructure can be acquired by identifying the scattering response from a sharp probing tip (for this reason, bowtie

Nanoantenna is usually utilized) oscillating over the surface of a sample [4].

**B. Sensing:** Nanostructures are considered smooth to the environment; subsequently any change in refractive index of the surrounding medium leads to red or then again blue move in the situation of the far field resonance peak [16].

**C. Energy harvesting applications:** notwithstanding the known potential utilizations of Nanoantenna array in sun oriented panels, Nanoantenna array has potential applications in the Cooling frameworks by changing over infrared warmth radiation "IR" into another type of radiation, Exploiting our bodies' radiation for power creation, Cooling or heating inside dress and cooling devices and energy collectors that draw squander warm from car engines, The middle of the range, electronic devices that can be utilized in cooling PCs/workstations as an option in contrast to the regular fans [2].

**D. Spectrograph:** It has been discovered that the Raman signal can be improved by a factor of larger than  $10^{13}$  when particles are absorbed on plasmonic Nanostructure which is named as Surface Enhanced Raman Scattering (SERS). Therefore Nanoantennas can be utilized to improve the location limit to a single molecule [2].

### 1.3 Motivation

The researchers and scientists are very important in the THz visible regions, the familiar studies offer frequency bands in the field of GHz. So decided to introduce a set design of Microstrip Nanoantenna to operate in the THz region to cover the visible region and infrared (IR) [17].

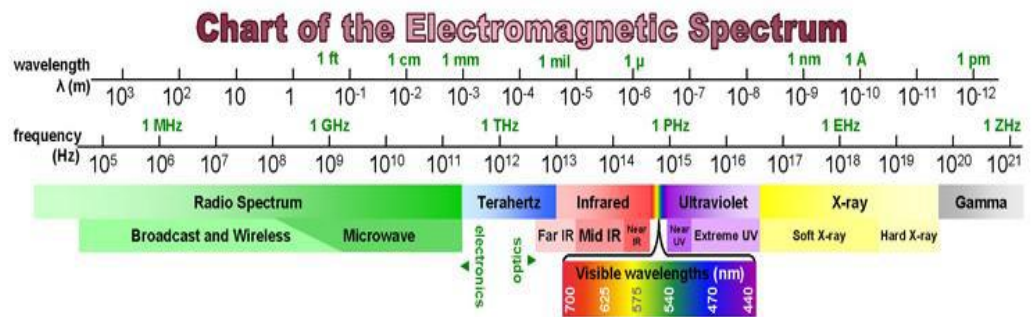


Figure 1.1: The electromagnetic spectrum [18]

### 1.4 Problem Statement

Size and power are two of the main design choices for any antenna system. Often there is tradeoff between these two as smaller antennas lead to a decrease antenna gain and therefore less power. So, by minimizing the antenna size, the antenna gain can be enhanced without changing the structure of the antenna.

## **1.5 Aims of the work**

The aim of this thesis to design and simulate a Microstrip Nanoantenna to cover a lot of optical communication bands starting from O-band (1260-1360) nm, E-band (1360-1460) nm, S-band (1460-1530) nm, C-band (1530-1565) nm, L-band (1565-1625) nm and lastly U-band (1625-1675) nm, or frequencies range from (80-300) THz. These values can be specified with the design of Microstrip Nanoantenna, and by applying the CST Microwave Studio 2018 simulator will get a band of frequency range of (106-133) THz.

## **1.6 Objective**

The objective of this thesis is to design, simulate and analyze a new Microstrip Nanoantenna that operates in THz region and covers a lot of optical communication bands or frequencies range from (100-150) THz.

## **1.7 Thesis Contribution**

A novel six nanoantennas designs has been done based on the CST Microwave Studio 2018 simulator to obtain the suitable values for the parameters of the antenna to extract the best one for overall designs.



## 1.8 Thesis layout

**Chapter One:** It is an introduction to the Nanoantenna, applications of the Nanoantenna, motivation, aim of this thesis and thesis layout.

**Chapter Two:** It includes a literature review of several types of Microstrip Nanoantennas.

**Chapter Three:** It includes the theory and design configuration of the proposed Microstrip Nanoantennas.

**Chapter Four:** It in this chapter, discussing the simulation and the results obtained from the proposed Microstrip Nanoantennas.

**Chapter Five:** It presents the conclusions of the proposed Microstrip Nanoantennas and recommendations for future work.

# CHAPTER TWO

## LITERATURE REVIEW

### 2.1 Introduction

In this chapter, the literature review about the previous works and related works in Nanoantenna will be presented, in particular the Microstrip Nanoantenna will be studied and analyzed in this thesis. Therefore, the substrate and the frequency bands of the Nanoantennas will be discussed in the layout review.

### 2.2 Literature Review

- **In 2011, A. Kawakami *et.al*** [19] proposed a way to enhance the reaction execution of infrared detectors by building up a fabrication process for Nanoantennas and measuring the progress temperature to the superconducting strips. A Nanoantenna comprises of a dipole antenna built with aluminum strips, and an NbN thin film strip is put in the antenna's center. The operation frequency is required to be at around 40 THz. The assessed antennas dimension was separately set at (L=2400 nm and W=400 nm); the antennas were put at the area of 1 mm<sup>2</sup>. The dielectric material of the substrate is MgO.

- **In 2011, Kumud R. and G. Singh [20]** investigated a Microstrip Nanoantenna at THz frequency. The designed Nanoantenna is proposed to radiate at the frequency range of 0.5-0.7 THz with high radiation efficiency and gain. The effect of different substrate parameters of the proposed Nanoantenna has been simulated and analyzed. The CST Microwave Studio simulator has been used to perform the simulation process, a commercial simulator based on limited options. The radiation efficiency of the proposed Nanoantenna is 94.50% at 0.6 THz.
- **In 2011, Mario Bareib *et.al* [21]** proposed a “Nano Antenna Array for Terahertz Detection” an infrared (IR). Identifiers have been manufactured comprising of Antenna-Coupled Metal Oxide Metal Diodes (ACMOMDs). These identifiers were characterized by utilizing electron beam lithography. They are intended to be touchy to the IR range and work at room temperature without cooling. The printed antenna structures comprise of gold and aluminum. The Nanoantenna design has used silicon as a dielectric material substrate.
- **In 2013, Lechen Yang *et.al* [22]** discussed two-dimensional photonic precious stones working at THz frequency. A multi-frequency THz Microstrip patch Nanoantenna on crystal substrate is exhibited and its electromagnetic wave engendering wonder is researched. The proposed design can operate at five frequency scope at the THz region, and the radiation efficiency is up to 96%. The photonic crystal structure of the substrate is utilized to improve the directivity, radiation efficiency and the gain of the Nanoantenna.

- **In 2013, Junsei Horikawa *et.al*** [23] proposed in “Study of Mid-Infrared Superconducting Detector with Phased Array Nano-Slot Antenna” a Nano-slot antenna with a micro-detector. Depending on the properties of antenna and Microstrip for the design of a mid-infrared detector with antenna. The Microstrip line and antenna were designed for operating at a wave center near 5  $\mu\text{m}$ . In the substrate, using the MgO dielectric material. The resonant frequency of the proposed antenna is 54 THz.
- **In 2013, Evgeny G. Mironov** [24] presented a High-Power Pulsed Operation using titanium Nanoantenna. Nanoantenna is composed of the gold metal (or titanium). Devices are made by utilizing gold or titanium. So, gold is a common choice that is used in plasmonic because of its relatively low losses. The dielectric substrate made from Quartz. The wavelength for this work is 1053 nm correspond to the resonant frequency 284 THz. The Nanoantenna application is used in nonlinear optics, photovoltaics, sensing and imaging.
- **In 2014, Ameneh Nejati *et.al*** [25] studied the “Effect of photonic crystal and frequency selective surface implementation on gain enhancement in the Microstrip patch antenna at terahertz frequency” on the Microstrip patch antenna, in the range of frequencies (0.5–0.7) THz. The arrangement of holes on an antenna and the effects of substrate thickness in both Photonic Band Gap (PBG) forms are studied. The tools that are used for simulations and designs are CST Microwave Studio and Ansoft HFSS.

- **In 2014, B. Mehta and Zaghoul [26]** discussed the tuning of optical Nanoantennas in visible range utilizing graphene. Setting monolayer and bilayers of graphene sheets over the optical Nanoantennas will result in an adjustment in resonating wavelength. The FDTD (Finite Difference Time Domain) simulation is used to check the experiment results. Gold was utilized for the creation of the dipole Nanoantennas. Fused silica is utilized as the substrate and titanium is utilized as layer between fused silica substrate and gold. So, used a gap to isolate to the two sequential dipole nanoantennas. A result is a large number of dipole Nanoantennas in array. The manufacture was done in  $1 \times 1$  mm zone to disentangle the optical estimation setup expected to test the device.
- **In 2015, Amandeep S. and Surinder S. [27]** proposed a “Trapezoidal microstrip patch antenna on photonic crystal substrate for high speed THz applications” Microstrip line is utilized to provide the coupling among source and Nanoantennas. The proposed design is created to be used in wider bandwidth of 0.88–1.62 THz. It is observed that the VSWR (Voltage Standing Wave Ratio), gain and return loss achieved show large improvement.
- **In 2015, Behzad Ashrafi *et.al* [28]** proposed a “Nanoantenna System Utilized a Plasmonic Rotman Lens with Five Switchable Beams” operating at the standard telecommunication wavelength of  $1.55 \mu\text{m}$ . The array consists of six plasmonic nanoantennas fed by plasmonic waveguides. The substrate layer material is  $\text{SiO}_2$ . The resonant

frequency is 193.5 THz. high gain and suitable bandwidth achieve from this work. The designed Nanoantenna is used for optical wireless communication and low-cost integrated systems applications.

- **In 2015, Fatemeh Taghian *et.al*** [29] proposed “Enhanced Thin Solar Cells Using Optical Nanoantenna Induced Hybrid Plasmonic Travelling-Wave” to trap the light inside solar cells. In this technique, a Nanoantenna structure is presented and executed in the silicon based solar cells, to redirect the light. The structure of proposed antenna is numerically explain utilizing limited FDFD (Finite Deference Frequency Domain) method. Simulation results demonstrate that by utilizing the proposed Nanoantenna as the back contact of the solar cells. So, the resonant frequency is 333 THz. The antenna has been used silicon in the dielectric substrate material.
- **In 2015, Luke Zakrajsek *et.al*** [30] discussed the Graphene-based plasmonic antenna could empower ultra-broadband correspondence among Nano-device in the Terahertz band (0.1– 10 THz). The manufacture, control, and situation of exactly shaped graphene-based Nano-structures still stance numerous commonsense difficulties. So, demonstrating that lithographically characterize graphene antennas. The material of substrate is SiO<sub>2</sub>.
- **In 2017, Mai *et.al*** [31] proposed a new circularly polarized Nanoantennas intended for optical media transmission applications. In this paper “Novel Wire-Grid Nano-Antenna Array with Circularly Polarized Radiation for Wireless Optical Communication Systems”.

The array comprises two groups of radiators which are symmetrical to each other. The antenna produce a high directivity 10.8 dBi and a wide bandwidth transfer speed that covers the range from 188.2 THz to 197.8 THz. The efficiency of the antennas is 82.75% at the resonant frequency of 193.55 THz.

- **In 2017, Divesh M. & Ekambir S.** [32] proposed a “THz Rectangular Microstrip Patch Antenna Employing Polyimide Substrate for Video Rate Imaging and Homeland Defense Applications”. So, for Microstrip copper (Cu) is used in the patch and ground, substrate uses the dielectric polyimide. The proposed Microstrip has been fed by feedline having impedance of 49.78  $\Omega$ . The antenna gain is 5.22 dB and directivity is 5.08 dBi at resonant frequency of 0.67 THz. CST Microwave Studio 2014 has been used to simulate results. The range of frequencies are (0.6-0.8 THz) for homeland defense applications and (0.6 THz) for a vide-rate imaging system.
- **In 2018, Ritesh Kumar *et.al*** [33] studied a novel Microstrip patch antenna configuration, utilizing the photonic crystal for THz spectral band applications. The material of the substrate is polyimide that utilizes Photonic Band Gap (PBG) and the Gain and Directivity shows good results at frequency 0.6308 THz. Additionally, the working frequency is different from 0.6152 THz to 0.6514 THz. So, it is used for detection of explosive and material characterization applications.

- **In 2018, Qudsia Rubani *et.al*** [34] a Microstrip patch antenna at THz region had been structured and investigated. The material used in the substrate is RT/Duriod6010 ( $\epsilon_r=10.2$ ). So, the resonant frequency of this design is 0.852 THz which should be executed in Wireless Body Area Networks for the transmission. Furthermore, the measure of power transmission at different distance among transmitter and receiver has been analyzed at various modulation cases.
- **In 2018, Abdel-Karim *et.al*** [35] a novel Nanoantenna with two radiation modes is presented. The structure of this Nanoantenna comprises of a ring coupler and two patch antennas put on a  $\text{SiO}_2$  substrate. The proposed Nanoantennas is advanced to limit the losses in radiation efficiency. There are two optimization techniques, in particular multi-objective particle swarm method and configuration focusing method. The resonant frequency of this design is 193 THz.
- **In 2018, Yuyao Chen *et.al*** [36] proposed a plasmonic Nanoantenna absorber together with a metal-insulator-metal (MIM) tri-layer structure, the best layer of metallic Nanoantennas, a center layer of dielectric spacer and a metallic base layer with thickness considerably bigger than the depth skin of incident electromagnetic waves. The substrate is composed of Silicon. Finally, in this work the resonant frequency is 2 THz. The shape design of the antenna is similar to the new Q-code.

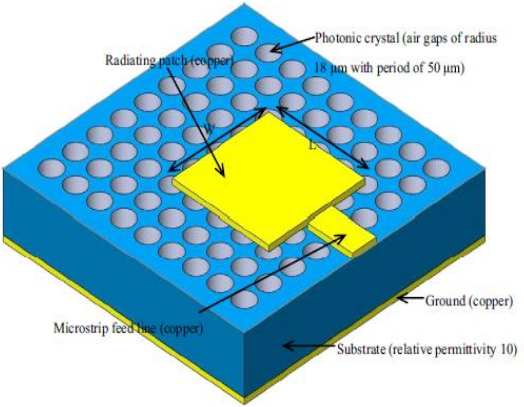
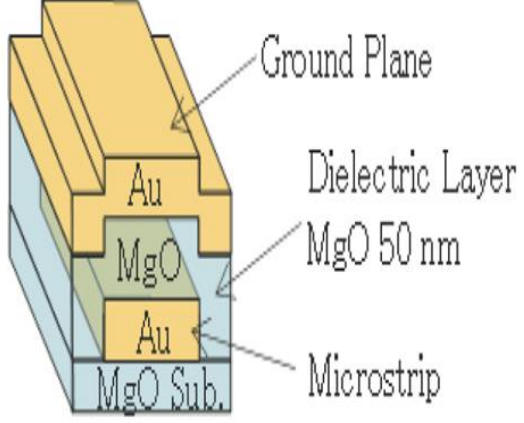
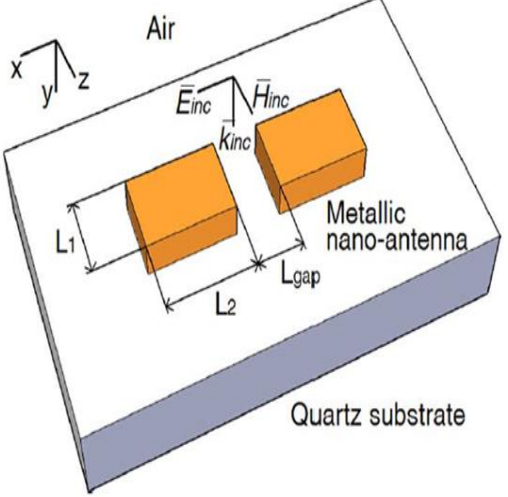


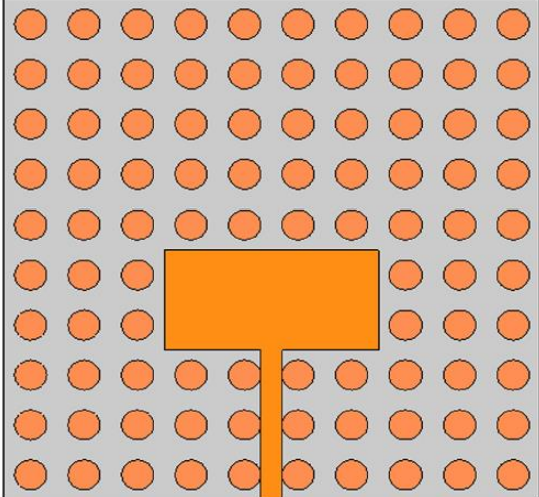
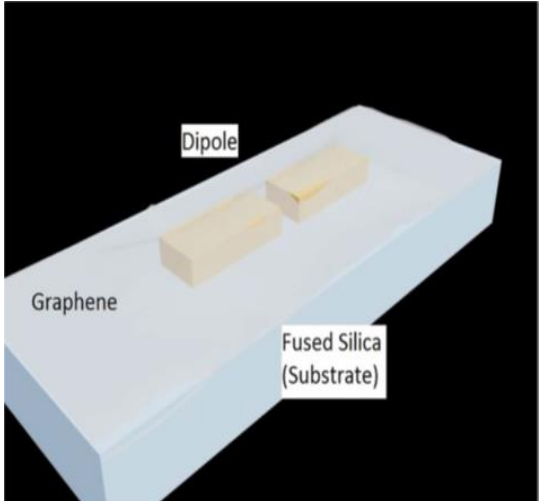
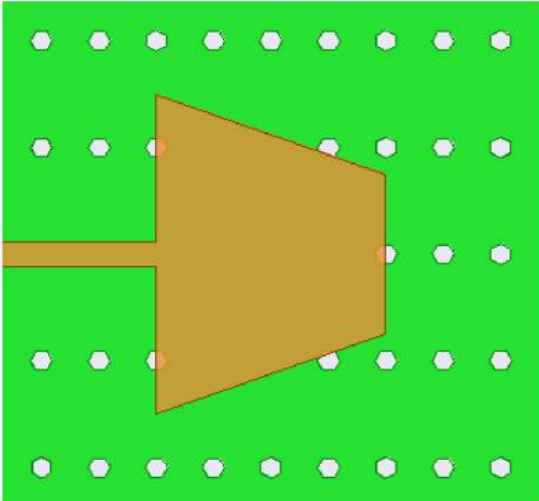
- **In 2019, Seyed Arash and Gholamreza Moradi** [37] proposed a novel design using graphene with patch operating at THz band. Graphene helps Surface Plasmon Polaritons (SPP) and gives good conductors. Computer Simulation Technology (CST) simulator program is applied to the proposed antenna. Microstrip line feeding is utilized to exciting antenna. A null fill improvement method of (H-plane) radiation pattern has been analyzed and studied.
- **In 2019, Göktug Isıklar *et.al*** [38] proposed the “Design and Analysis of Nanoantenna Arrays for Imaging and Sensing Applications at Optical Frequencies” a Nanoantenna operate in THz region using dielectric particles in the dialectical substrate. The shape that has been designed is called the bowtie. They notice the range of frequency band will start from 400 THz and end approximately at 500 THz.

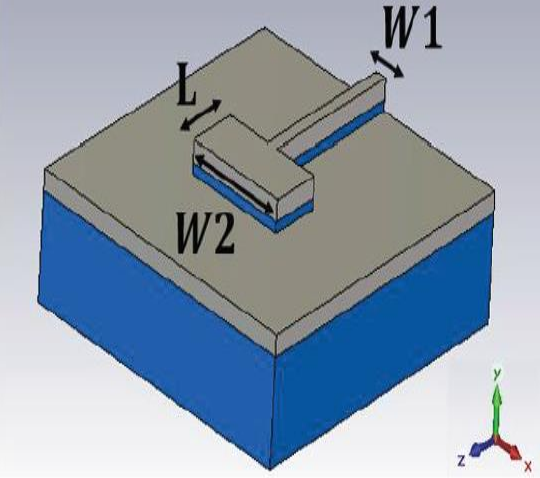
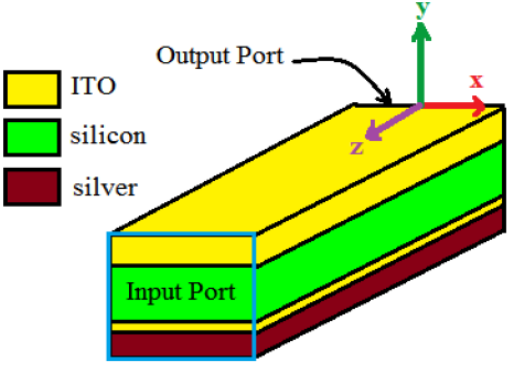
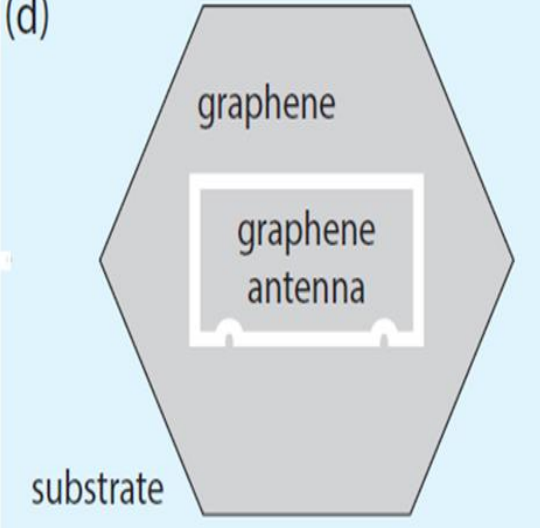
All previous studies referenced in the literature study (are concluded in Table 2.1) are expected to design an antenna with a smaller size, good gain, suitable bandwidth and good directivity. So, in order to plan an appropriate Microstrip Nanoantenna with an ideal detail and best outcomes like reduced reflection coefficient  $S_{11}$  smaller than usual, wide bandwidth, high gain and high directivity. So, many of the proposed models in Nanoantennas are designed to operating in the field of terahertz region.

**Table 2.1 The Microstrip Nanoantenna design references.**

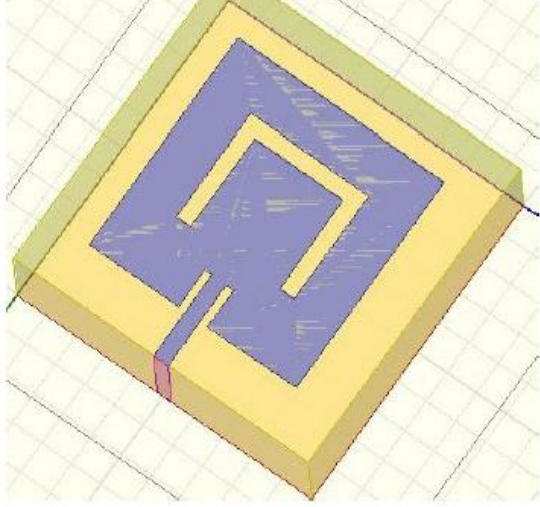
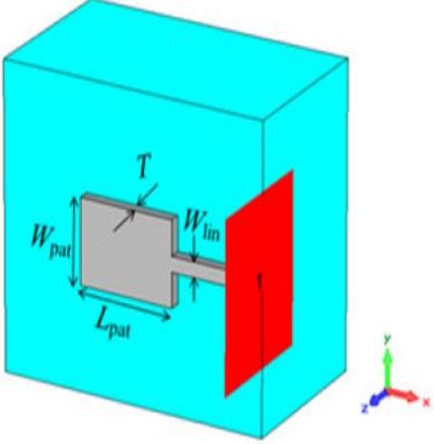
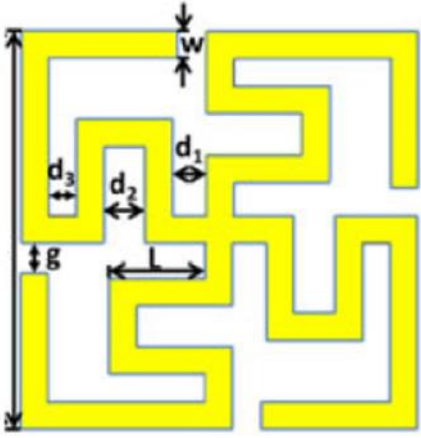
No.	Ref. No.	Frequency Band (THz)	Substrate Material	Nanoantenna design
1	[19]	40	MgO	
2	[20]	0.5-0.7	different substrate	
3	[21]	---	Silicon	

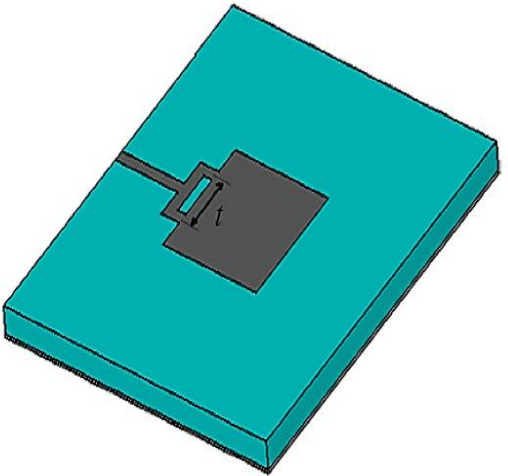
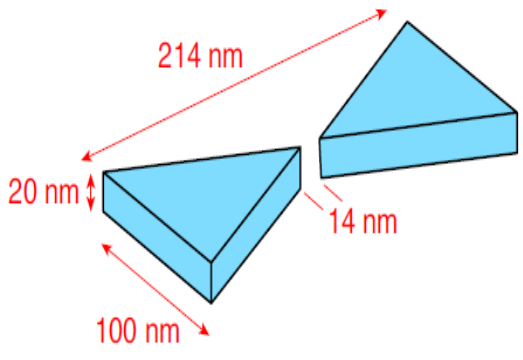
4	[22]	1.46-1.94	Crystal	
5	[23]	54	MgO	
6	[24]	---	Quartz	

7	[25]	0.5–0.7	Crystal	
8	[26]	315	SiO <sub>2</sub>	
9	[27]	0.88–1.62	Crystal	

10	[28]	193.5	SiO <sub>2</sub>	
11	[29]	333	Silicon	
12	[30]	0.1–10	SiO <sub>2</sub>	

<p>13</p>	<p>[31]</p>	<p>188.2 - 197.8</p>	<p>SiO<sub>2</sub></p>	
<p>14</p>	<p>[32]</p>	<p>0.6-0.8</p>	<p>Polyimide</p>	
<p>15</p>	<p>[33]</p>	<p>0.615-0.651</p>	<p>Polyimide</p>	

<p>16</p>	<p>[34]</p>	<p>0.852</p>	<p>RT/Durio d6010</p>	
<p>17</p>	<p>[35]</p>	<p>193</p>	<p>SiO<sub>2</sub></p>	
<p>18</p>	<p>[36]</p>	<p>2</p>	<p>Silicon</p>	 <p><b>Meander Line Nanoantenna</b></p>

19	[37]	1.4-1.5	SiO <sub>2</sub>	 A 3D perspective view of a square ring resonator structure. It consists of a square ring of a dark gray material (likely metal) on top of a teal-colored rectangular substrate. A small gap in the ring is labeled with the letter 't'. A thin line extends from one side of the ring, possibly representing a feed line.
20	[38]	400 - 500	dielectric particles	 <p>(a)</p> <p>Nanoantennas</p> A 3D perspective view of two light blue, triangular dielectric particles. The particles are oriented such that their hypotenuses are facing each other. Red arrows indicate dimensions: the top edge of the left particle is 214 nm, its height is 20 nm, and its base is 100 nm. The right edge of the right particle is 14 nm. Below the diagram is the label '(a)' and the word 'Nanoantennas' in blue text.



# CHAPTER THREE

## THEORY AND DESIGN CONFIGURATION

### 3.1 Introduction

This chapter, an introduction to the Microstrip antenna and how to divide its layers will be given. Then discuss the design of several shapes of Microstrip Nanoantennas. The exciting ports of all proposed Nanoantennas are named waveguide port because they are considered easy to design and the simplest kind of feeding techniques. The effect of changing various shapes of the Nanoantenna are discussed and analyzed to choose the best one. The performance of the proposed Nanoantennas is evaluated all of the presented Nanoantennas by CST STUDIO SUITE software version 2018.

In this thesis, six designs of Nanoantennas are proposed. The first and second designs have a Hash-shape patch and a Hash-shape Slot patch in which square substrate is used. The third and fourth designs have a Bluetooth-shape patch and a Bluetooth-shape Slot patch; they are etched using suitable substrate dimensions. The fifth and sixth designs have a Wi-Fi-shape patch and a Wi-Fi-shape Slot patch with the same types of substrate. Therefore, the substrate layer (middle layer) that utilized is made of silicon with a relative dielectric constant of  $\epsilon_r = 11.9$  with thickness  $h = 50$  nm.

## 3.2 Microstrip Antenna layers

The Microstrip Antenna consists of three layers:

### 3.2.1 Patch Antenna (first layer)

The first layer is called the patch. Microstrip patch antennas are considered one of the most fundamental and essential kinds of planar Antenna. Huge numbers of the ideas and methods utilized with Microstrip Patch Antennas can be connected straightforward to other planar antennas [15]. Microstrip patch antenna is considered the simplest type of Microstrip Antenna which is essentially composed of three layers as shown in Figure 3.1. This layer is responsible for radiation. It is manufactured from a thin conducting material, for example gold (Au) or copper (Cu) and is printed or etched on the second layer (medium) that is called the dielectric substrate.

The form of patch, as shown in Figure 3.2, may take numerous geometrical shapes: square, rectangular, triangular, elliptical and circular or other various shapes [39].

### 3.2.2 Substrate (second layer)

The dielectric substrate is considered a medium layer that lies between the patch and the ground. So, to plan a minimized size of Microstrip, the dielectric substrate must be utilized with a high dielectric constant value. Hence, a tradeoff must be made between the size of the antennas and its performance. One of the considerations

that has an effect on the substrate material is the dielectric constant on the radiation characteristics. A high dielectric constant results in low radiation from a Microstrip patch antenna [12] [39] [40].

### 3.2.3 Ground (third layer)

This layer is classified as the last layer (third) of Microstrip antenna. So, it is regarded as the corresponding side of the substrate with a conducting material that is called ground plane that represents the third layer [39].

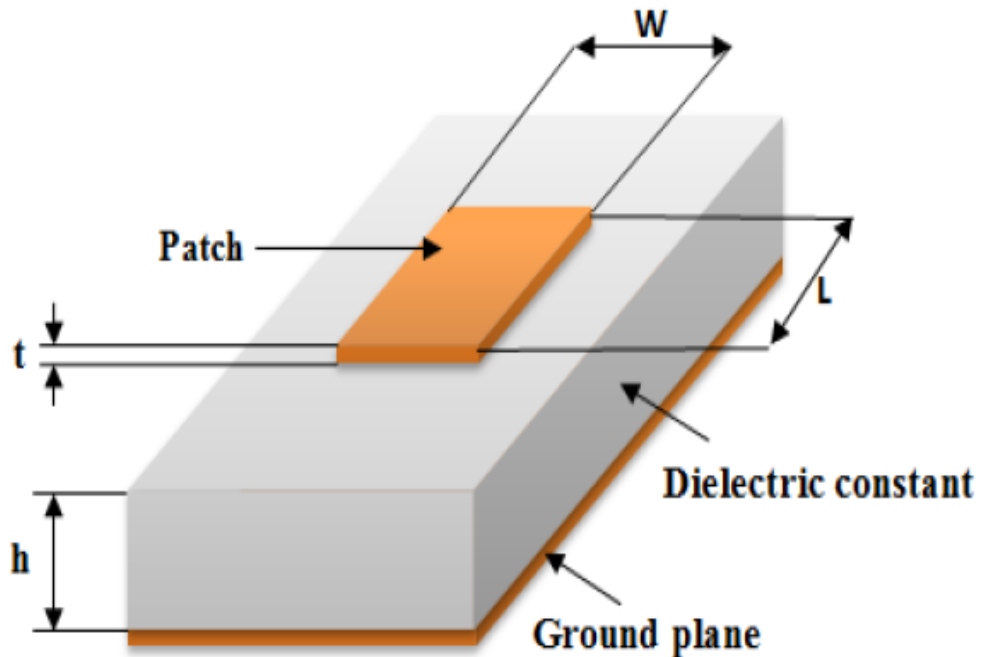


**Figure 3.1: Basic structure of Microstrip [12].**

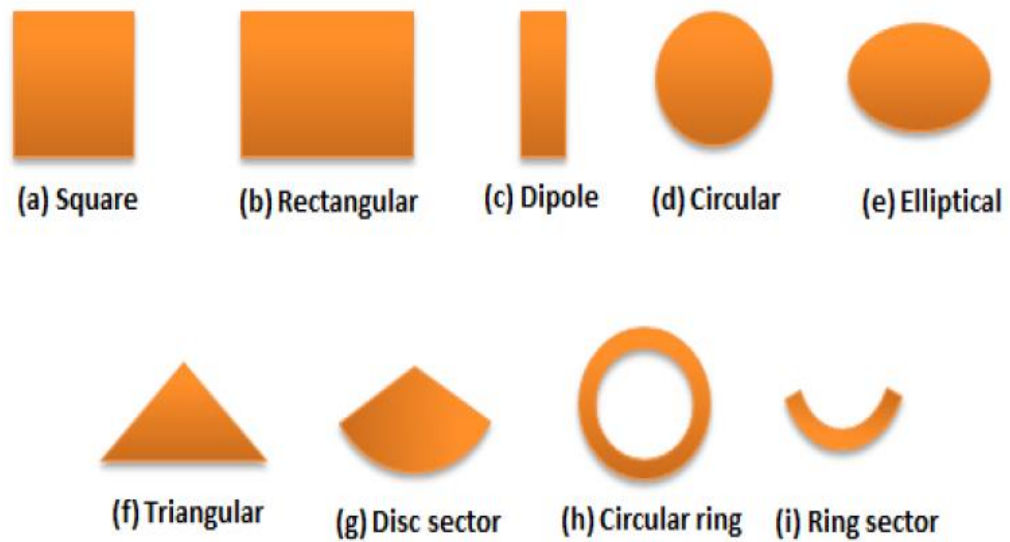


**Figure 3.2: Common shapes of patch [12].**

### 3.3 Feeding Technique

There are many techniques are used in feeding Microstrip patch antenna. These techniques can be characterized into two classes contacting and non-contacting. In the contacting technique, the RF power is directly fed to the radiating patch utilizing a connecting component, for example, a Microstrip line. In the non-contacting technique, electromagnetic field coupling is done to exchange power between the radiating patch and the Microstrip line. Here explaining the most popular feed techniques have been utilized: the Microstrip line, coaxial probe, aperture coupling, proximity coupling and waveguide reflector [41].

### 3.3.1 Microstrip line feed

In this type of feeding, the link of the strip is used directly with the edge of the Microstrip patch as shown in Figure 3.3. The conducting strip is smaller in length and width compared with the patch. This type of feeding arrangement has the advantage that the feed can be etched on the same substrate to provide a suitable power [41].

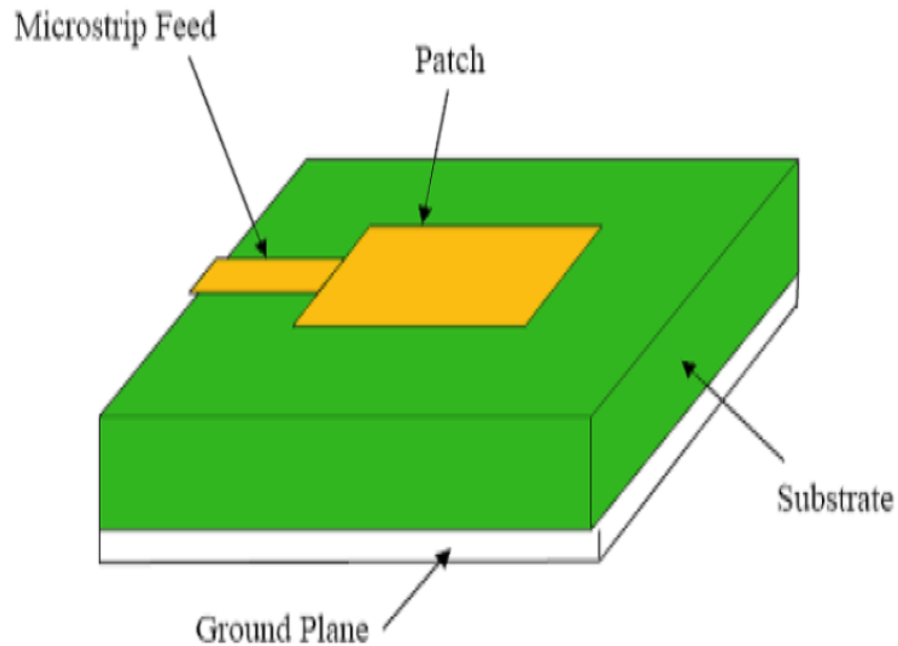


**Figure 3.3: Microstrip Line Feed [41].**

### 3.3.2 Coaxial feed

The Coaxial probe or feed is considered one of the most normal techniques utilized for feeding Microstrip patch antennas. As shown in Figure 3.4, the outer conductor is associated with the ground plane, while the inner conductor of the coaxial connector expands through the dielectric and is soldered to the radiating patch. The main feature of this sort of feeding is that the feed can be put at any ideal position inside the patch so as to acquire impedance matching. This feed technique is easy to manufacture and has low false radiation effects [41].

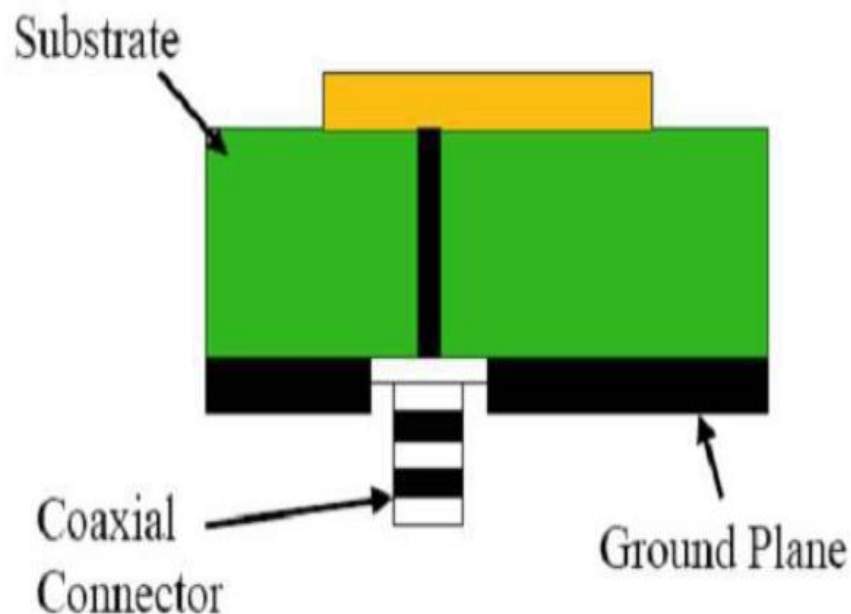


**Figure 3.4: Coaxial feed [41].**

### 3.3.3 Aperture coupled feed

In this type of feeding, as shown in Figure 3.5, the radiating Microstrip patch is etched on the highest point of substrate of the antenna, and the Microstrip feed line is etched on the base of the feed substrate so as to get aperture coupling. The dielectric constants and thickness of these two substrates may be chosen to optimize the distinct electrical functions of radiation [41].

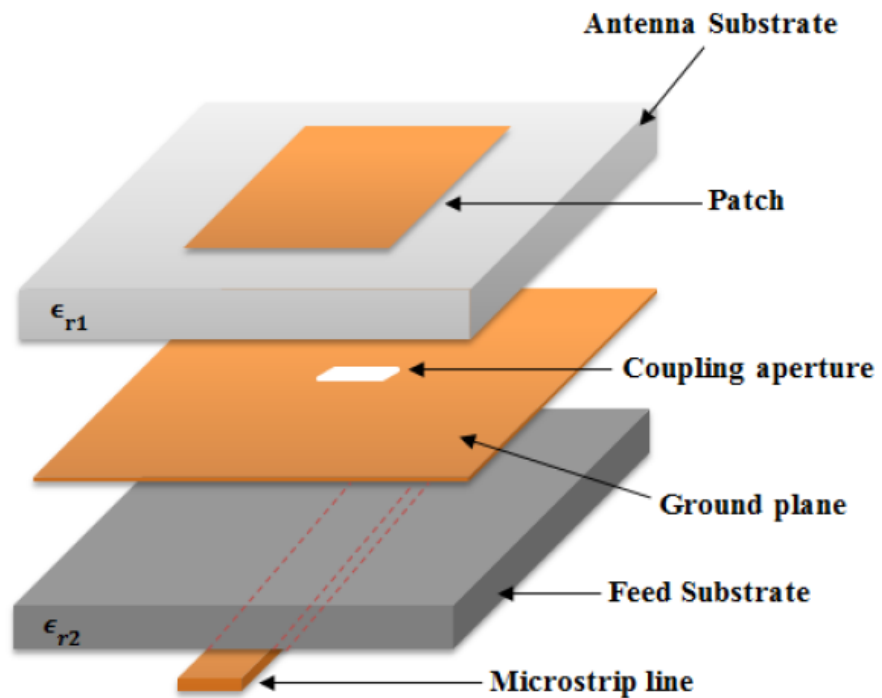


**Figure 3.5: Aperture coupled feed [12].**

### 3.3.4 Proximity coupled feed

This technique is also called the electromagnetic coupling scheme. As shown in Figure 3.6, two dielectric substrates are utilized. Thus the feed line is behind the two substrates and the radiating patch is on top of the highest substrate. The main features of this feeding technique are that it eliminates false feed radiation and provides a high bandwidth, due to the increase in the electrical thickness that is utilized in the Microstrip patch antenna [41].

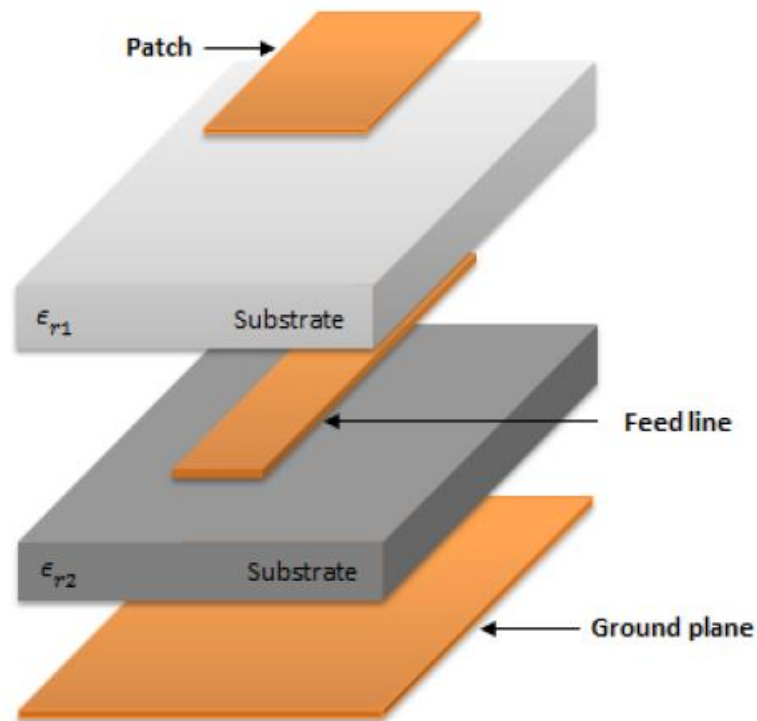


**Figure 3.6: Proximity coupled feed [12].**



### 3.3.5 Co-Planer Waveguide (CPW) feed

This technique is very important for the Microstrip antenna and it is widely utilized. The Co-Planer Waveguide consists of a center feed stripline limited by duplicate ground plane with a small gap separating between them. The main structure is etched on one side of dielectric substrate only as shown in Figure 3.7 [12].

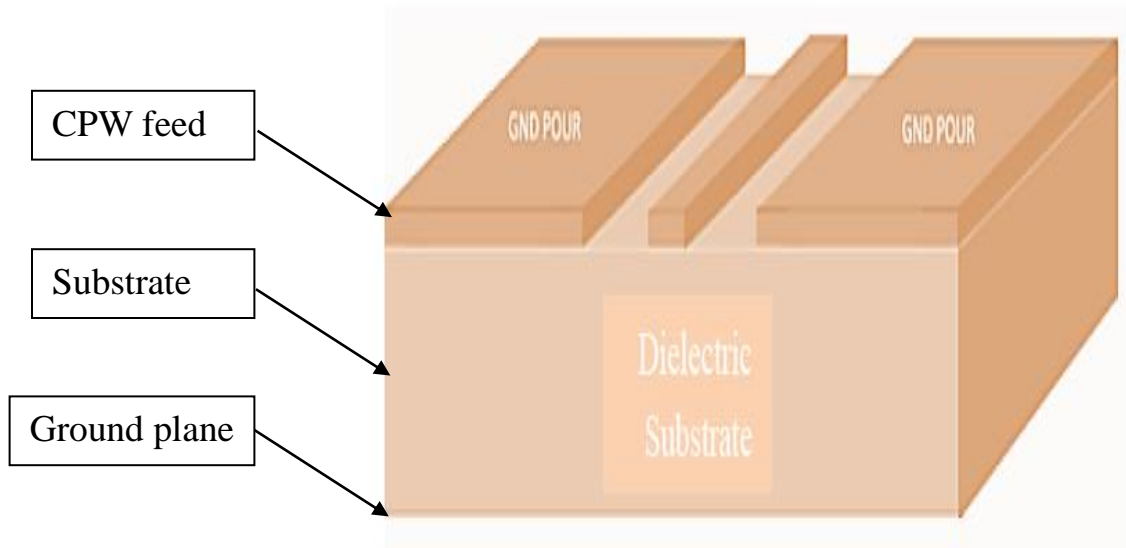


**Figure 3.7: CPW feed [12].**

### 3.3.6 Waveguide feed

This port is considered one of the most famous types and is used for feeding. The characteristic impedance of the waveguide feeding is selected as  $50\Omega$  for the purpose of matching, as shown in Figure 3.8 [42].

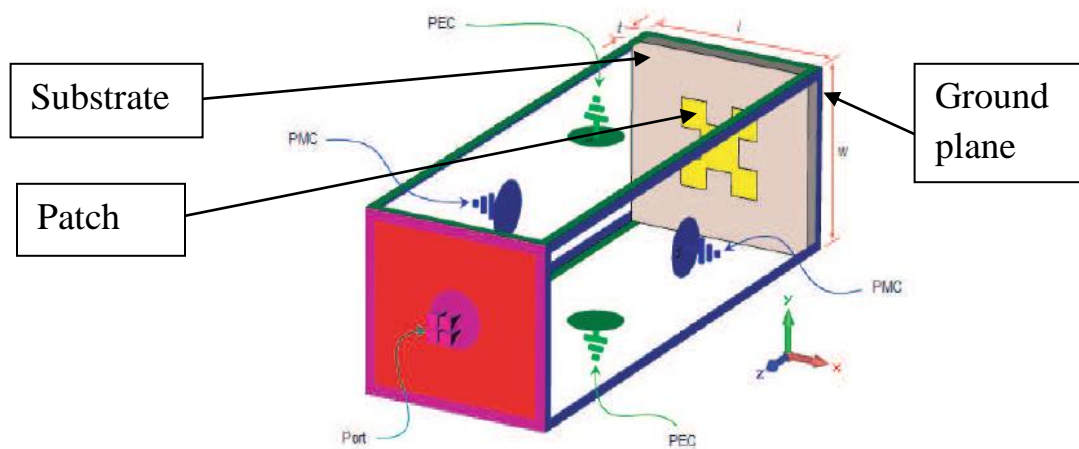


**Figure 3.8: Waveguide feed [43].**

## 3.4 Antenna parameter

### 3.4.1 Reflection Coefficient

The reflection coefficient ( $S_{11}$ ) is defined as “a parameter which quantizes how much of electromagnetic wave or power is reflected from an interface between two different mediums with

different impedances.” It is calculated from the ratio of reflected wave to incident wave [44].  $S_{11}$  is given as:

$$S_{11} = \frac{E^-}{E^+} \dots\dots\dots (3.1)$$

Where:

$E^-$ : Amplitude of reflected wave.  $E^+$ : Amplitude of incident wave.

There is also an important relationship to calculate the Reflection coefficient [13] :

$$\text{Reflection coefficient} = \frac{Z_R - Z_0}{Z_R + Z_0} \dots\dots\dots (3.2)$$

Where:-  $Z_R$  load impedance,  $Z_0$  characteristics impedance

The range of good design (-10 dB to -50 dB).

### 3.4.2 Gain

The gain (G) for any antenna is defined as “the ratio of the intensity, in a given direction, to the radiation intensity that would be obtained if the power accepted by the antenna were radiated isotopically. The radiation intensity corresponding to the isotopically radiated power is equal to the power accepted (input) by the antenna divided by  $4\pi$ .” [1].

The gain can be calculated from equation (3.3)

$$G = \frac{4\pi U}{P_{in}} \dots\dots\dots (3.3)$$

Where:  $P_{in}$ : total input power &  $U$ : radiation intensity

The range of good design (2 dB to 7 dB).

### 3.4.3 Directivity

The directivity ( $D$ ) of an antenna is defined as “the ratio of the radiation intensity in a given direction from the antenna to the radiation intensity averaged over all directions. The average radiation intensity is equal to the total power radiated by the antenna divided by  $4\pi$ . If the direction is not specified, the direction of maximum radiation intensity is implied.” [1] [45]. The directivity can be calculated from equation (3.4). The range of good design (2.5 dB to 7.5 dB).

$$D = \frac{4\pi U}{P_{rad}} \dots\dots\dots (3.4)$$

Where:  $P_{rad}$ : total power radiation,  $U$ : radiation intensity

### 3.4.4 Current distribution

When the source of microwave is connected with Microstrip antenna, the charge will establish distribution in the lower and the upper planes of the antenna.

There are two mechanisms that are used to control the charge distribution: attractive and repulsive. The attractive force is between the opposite charges on the ground plane and patch; it creates a current density at the bottom of the patch inside the dielectric. The repulsive force is between the same charges; it pushes the charges from the bottom of patch around the edge of the patch to the top of the patch. So as to that is create another current density [13].

### 3.4.5 Radiation pattern

The radiation pattern is a variation in the power radiated from the Nanoantenna as a function of the direction away from the Nanoantenna. So, the fields radiated by any antennas with limited dimensions are spherical waves. So, we represent the far-field region with respect to theta and phi (elevation and azimuth angles) [12] [46].

### 3.4.6 Efficiency

We can calculate the radiation efficiency of the proposed Nanoantenna depending on the values of the gain and directivity which can be calculated by equation (3.5) [47]:

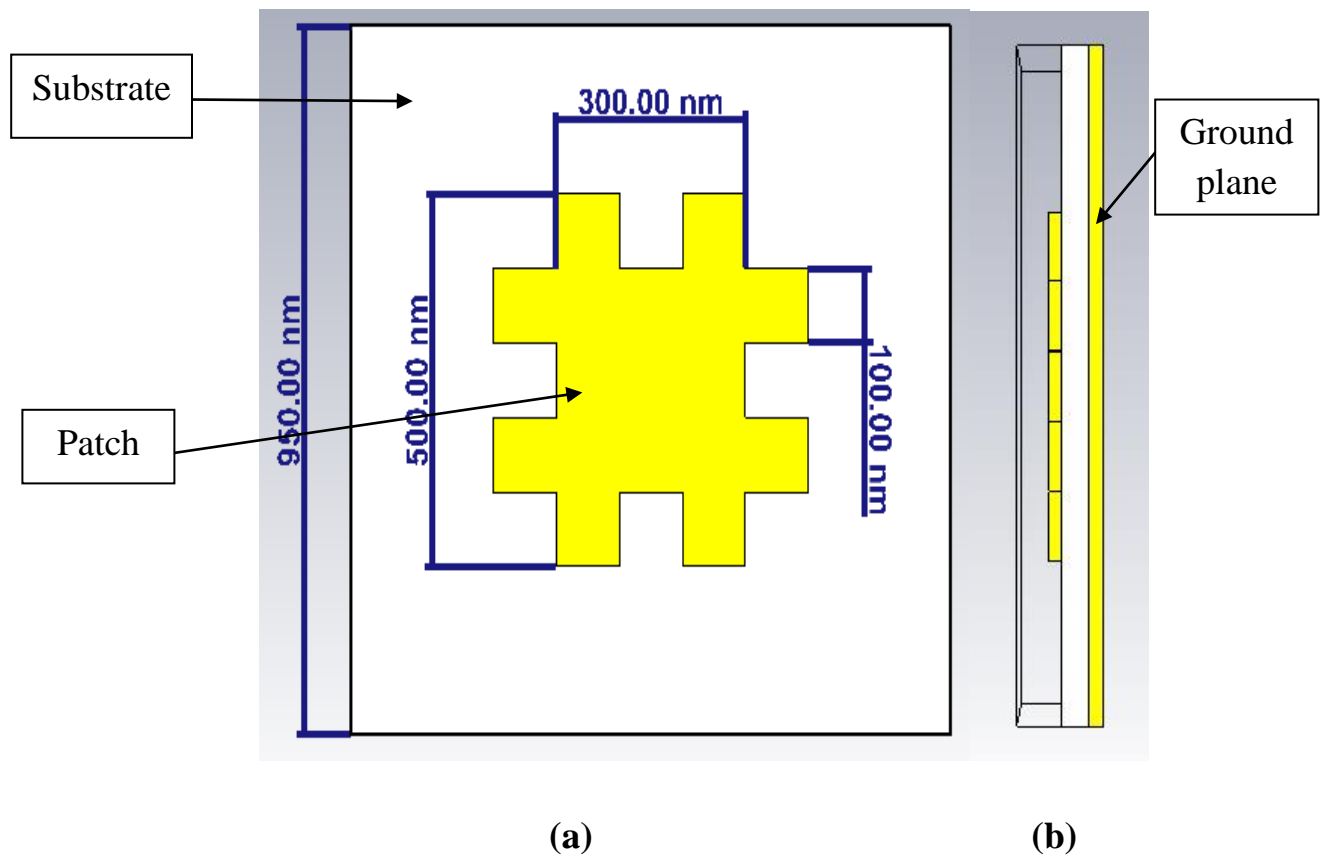
$$\text{Efficiency} = \frac{G}{D} * 100\% \dots\dots\dots (3.5)$$

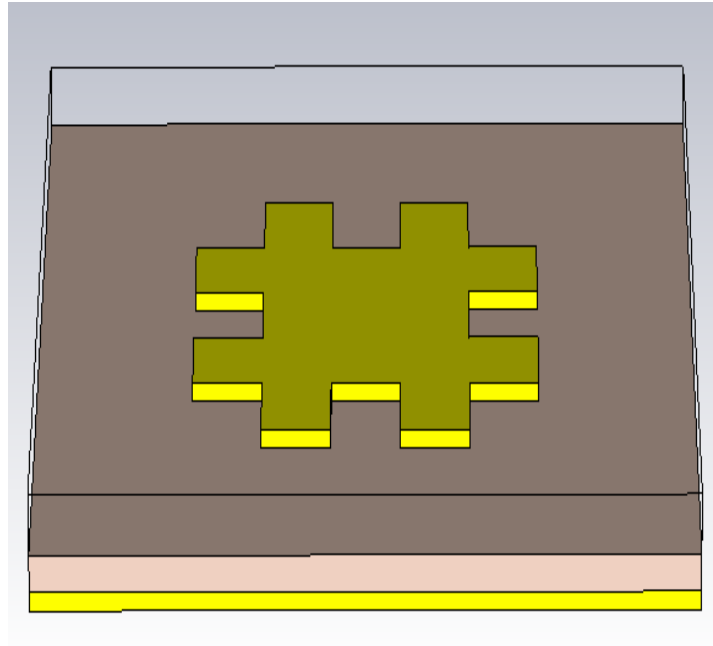
### 3.4.7 Bandwidth

The bandwidth for any antenna is defined as “the range of frequencies within which the performance of the antenna, with respect to some characteristic, conforms to a specified standard.” [1]. Bandwidth of antenna is calculated from the curve of reflection coefficient depending on the -10 dB. It represents a distance from the lower frequency and the higher frequency [48].

### 3.5 The proposed model I: Microstrip Hash-shape Nanoantenna (MHNA)

The first model designed is a Microstrip Hash-shape Nanoantenna which uses a square geometry shape. Thus the substrate and the ground plane takes the square shape with suitable dimensions to achieve good result. This Nanoantenna is designed by using a silicon substrate (middle layer) with dimension of  $(950 \times 950) \text{ nm}^2$  W, L respectively with thickness (h) (50) nm to give the desired results. We have used silicon because it has high dielectric constant  $\epsilon_r=11.9$ . The overall view of MHNA is shown in Figure 3.9.





(c)

**Figure 3.9: a: MHNA front view; b: MHNA side view; c: MHNA perspective view.**

The patch layer (upper layer) material is composed of gold metal. The dimension of Hash-shape patch Nanoantenna is (500) nm for width ( $W_p$ ) and (500) nm for length ( $L_p$ ) with thickness ( $t$ ) (20) nm. The cutoff region in the four corner of patch MHNA is  $(100 \times 100) \text{ nm}^2$ . The purpose of these cutoff corners of new design MHNA is to change the current distribution on the patch that leads to enhance the radiation pattern of MHNA. Moreover, in order to get the best solving for both far-field and reflection coefficient  $S_{11}$  we utilized waveguide excitation port. The ground layer (lower layer) consists of gold with dimension  $(950 \times 950) \text{ nm}^2$ , meanwhile the thickness is (20) nm.

The method of designing the above Nanoantenna in the CST simulator program is done by drawing a square. Then we make four pieces in the corners of the square that is drawn with regard to the mentioned dimensions and thickness. The overall dimensions of MHNA are shown in Table 3.1.

**Table 3.1. MHNA dimensions.**

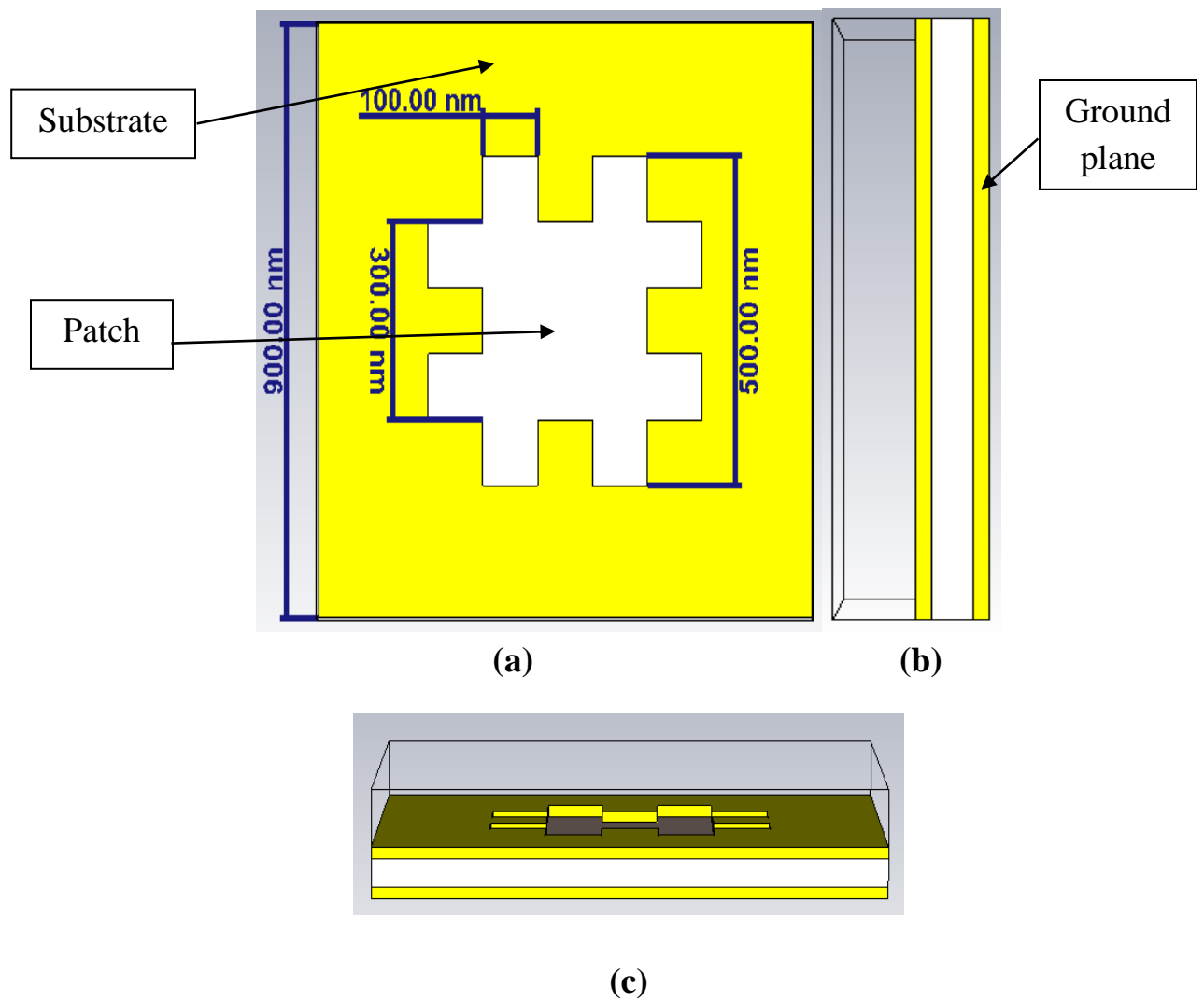
<b>NO.</b>	<b>dimensions</b>	<b>Values (nm)</b>
<b>1</b>	<b>Substrate width, W</b>	<b>950</b>
<b>2</b>	<b>Substrate length, L</b>	<b>950</b>
<b>3</b>	<b>Thickness of Substrate, h</b>	<b>50</b>
<b>4</b>	<b>Ground width, Wg</b>	<b>950</b>
<b>5</b>	<b>Ground length, Lg</b>	<b>950</b>
<b>6</b>	<b>Thickness of Ground, t</b>	<b>20</b>
<b>7</b>	<b>Patch width, Wp</b>	<b>500</b>
<b>8</b>	<b>Patch length, Lp</b>	<b>500</b>
<b>9</b>	<b>Thickness of patch, t</b>	<b>20</b>

### **3.6 The proposed model II: Microstrip Hash-shape Slot Nanoantenna (MHSNA).**

The method of designing the second model Microstrip Hash-shape Slot Nanoantenna similar to the method of drawing the first design with a simple change. Here, we draw a large square with the same dimensions of the substrate and then we draw a small square and choose other material than gold (to cut only) and cut the part that is



chosen. In addition, we draw eight squares and cut them. The final drawing is the shape hash slot. The MHSNA overall view is shown in Figure 3.10. It is considered the inverse of the first design in the case of patch. So, we use silicon in the substrate with dimension of  $(900 \times 900) \text{ nm}^2$  W, L respectively with thickness (h) (50) nm with suitable dimensions to achieve the desired result.



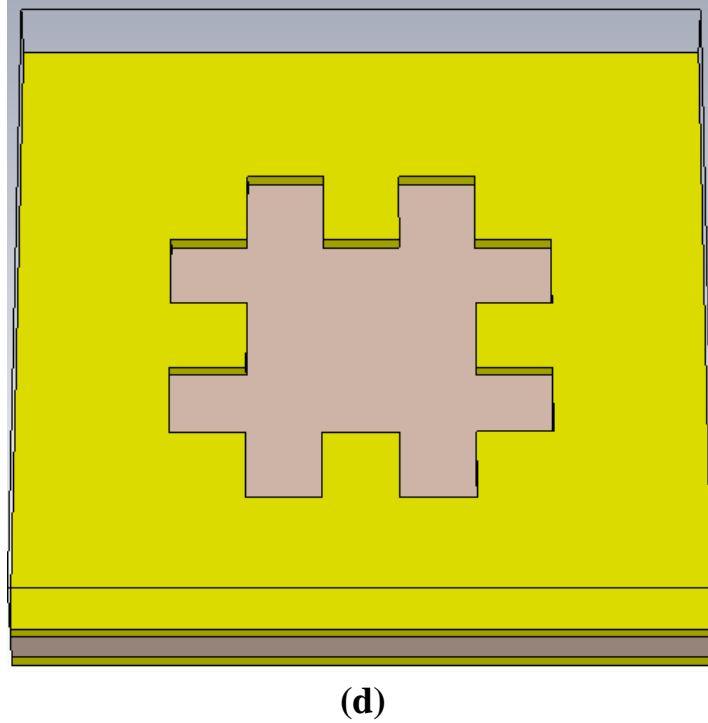


**Figure 3.10: a: MHSNA front view; b: MHSNA side view; c: MHSNA perspective view; d: MHSNA bottom view.**

The ground plane layer is composed of gold with dimension  $(900 \times 900) \text{ nm}^2$  and the thickness is  $(20) \text{ nm}$ . While the upper layer that is called patch layer material is composed of gold metal. The dimension of Hash-shape patch Nanoantenna is  $(500 \times 500) \text{ nm}^2$  for width ( $W_p$ ) and length ( $L_p$ ) with thickness ( $t$ )  $(20) \text{ nm}$ . These dimensions represent the slotted patch. The cutoff region in the four corners of patch MHSNA is  $(100 \times 100) \text{ nm}^2$ . Moreover, we utilize waveguide excitation port. The overall dimensions of MHSNA are shown in Table 3.2.

**Table 3.2. MHSNA dimensions.**

<b>NO.</b>	<b>dimensions</b>	<b>Values (nm)</b>
<b>1</b>	<b>Patch slot width, <math>W_p</math></b>	<b>500</b>
<b>2</b>	<b>Patch slot length, <math>L_p</math></b>	<b>500</b>
<b>3</b>	<b>Thickness of patch, <math>t</math></b>	<b>20</b>
<b>4</b>	<b>Substrate width, <math>W</math></b>	<b>900</b>
<b>5</b>	<b>Substrate length, <math>L</math></b>	<b>900</b>
<b>6</b>	<b>Thickness of Substrate, <math>h</math></b>	<b>50</b>
<b>7</b>	<b>Ground width, <math>W_g</math></b>	<b>900</b>
<b>8</b>	<b>Ground length, <math>L_g</math></b>	<b>900</b>
<b>9</b>	<b>Thickness of Ground, <math>t</math></b>	<b>20</b>

### **3.7 The proposed model III: Microstrip Bluetooth-shape Nanoantenna (MBNA).**

The third model Microstrip Bluetooth-shape Nanoantenna is designed by using a patch Nanoantenna takes the Bluetooth-shape. The substrate layer of this Nanoantenna is designed by utilizing a silicon layer having width ( $W$ ) 900 nm and length ( $L$ ) 900 nm with thickness ( $h$ ) (50) nm to give the optimal results. The dimension of the ground plane is the same dimension of the substrate layer as mentioned above, but the thickness is (20) nm.

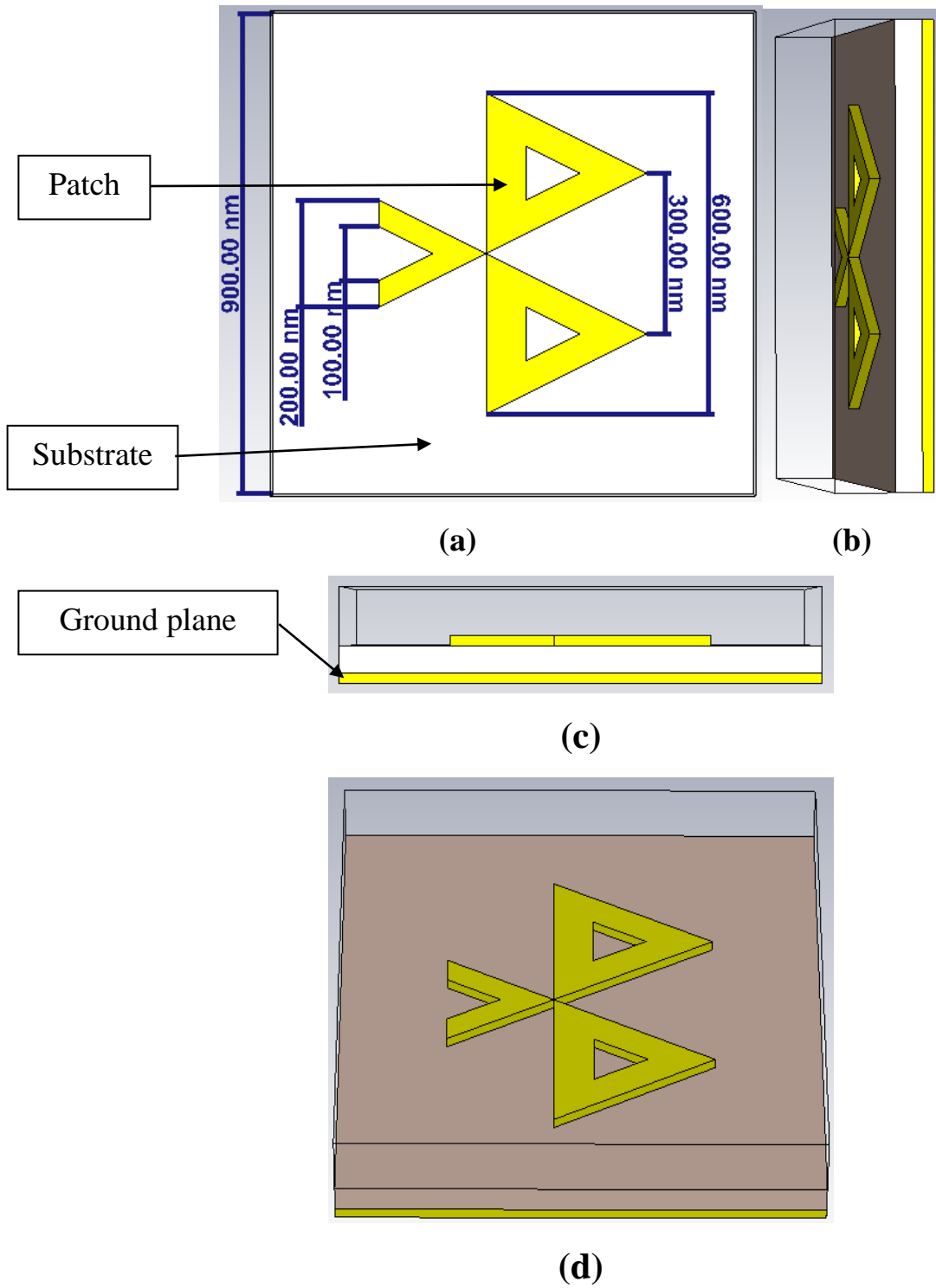


**Figure 3.11: a: MBNA front view; b: MBNA side view; c: MBNA bottom view; d: MBNA perspective view.**

The design method for this Nanoantenna is made by using polygon. Which is found in the modeling shapes section in 2D curve, designing the form of Bluetooth as shown in Figure 3.11. The patch layer is composed of gold metal. The patch dimensions of MBNA is  $(500 \times 600)$  nm<sup>2</sup> for width ( $W_p$ ) and length ( $L_p$ ) respectively. While the thickness ( $t$ ) is (20) nm. These patches take the shape like the three triangular. The cutting regions that are found in the three triangular are very compatible with the size of patch Nanoantenna. Utilizing waveguide excitation port for the above design. The overall dimensions of MBNA are shown in Table 3.3.

**Table 3.3. MBNA dimensions.**

<b>NO.</b>	<b>dimensions</b>	<b>Values (nm)</b>
<b>1</b>	<b>Ground width, <math>W_g</math></b>	<b>900</b>
<b>2</b>	<b>Ground length, <math>L_g</math></b>	<b>900</b>
<b>3</b>	<b>Thickness of Ground, <math>t</math></b>	<b>20</b>
<b>4</b>	<b>Substrate width, <math>W</math></b>	<b>900</b>
<b>5</b>	<b>Substrate length, <math>L</math></b>	<b>900</b>
<b>6</b>	<b>Thickness of Substrate, <math>h</math></b>	<b>50</b>
<b>7</b>	<b>Width of patch, <math>W_p</math></b>	<b>500</b>
<b>8</b>	<b>Length of patch, <math>L_p</math></b>	<b>600</b>
<b>9</b>	<b>Thickness of patch, <math>t</math></b>	<b>20</b>

### 3.8 The proposed model V: Microstrip Bluetooth-shape Slot Nanoantenna (MBSNA).

The fourth design of the Nanoantennas is considered the opposite of the previous design. In other words, the Bluetooth shape used in the patch uses itself but is slot that as shown in Figure 3.12.

Designing the patch with the same dimensions as the substrate and then engrave the Bluetooth shape on it that discussed earlier. The dimensions of Nanoantenna patch are (500) nm for width ( $W_p$ ), (600) nm for length ( $L_p$ ) and thickness ( $t$ ) (20) nm.

The substrate and the ground plane takes the square shape with dimensions  $(950 \times 950) \text{ nm}^2$   $W, L$  respectively and thickness ( $h$ ) (50) nm. This Nanoantenna is designed using silicon as a substrate and use gold in both patch and ground plane.

Also, utilizing a waveguide excitation port for the above design. The overall dimensions of MBSNA are shown in Table 3.4.

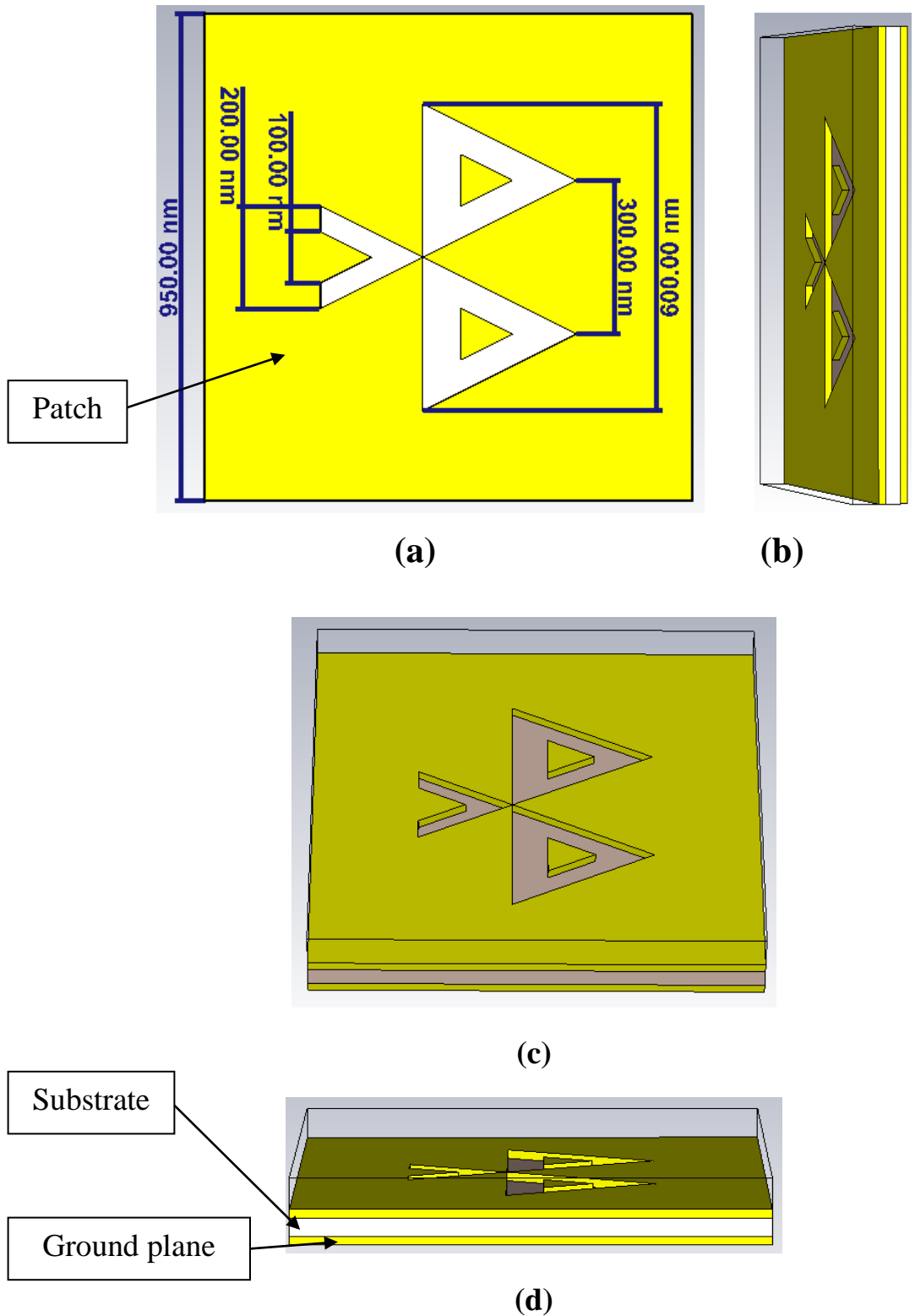


Figure 3.12: a: MBSNA front view; b: MBSNA side view; c: MBSNA perspective view; d: MBSNA bottom view.

**Table 3.4. MBSNA dimensions.**

NO.	dimensions	Values (nm)
1	Ground width, $W_g$	950
2	Ground length, $L_g$	950
3	Thickness of Ground, $t$	20
4	Substrate width, $W$	950
5	Substrate length, $L$	950
6	Thickness of Substrate, $h$	50
7	Width of slot patch, $W_p$	500
8	Length of slot patch, $L_p$	600
9	Thickness of patch, $t$	20

### 3.9 The proposed model VI; Microstrip Wi-Fi-shape Nanoantenna (MWNA).

The fifth proposed design of Microstrip Wi-Fi-shape Nanoantenna is based on four circles in terms of design as shown in Figure 3.13. The above MWNA is composed of three layers: Patch, Substrate and Ground. The gold metal is used in both patches Nanoantenna and ground plane. The substrate layer dimensions are 900, 900 nm  $W, L$  respectively. The dielectric material used in the substrate is Silicon with thickness ( $h$ ) 50 nm. The dielectric constant for silicon  $\epsilon_r=11.9$ . Whereas the ground layer dimensions are  $1100 \times 1100 \text{ nm}^2$ , the thickness ( $t$ ) is 20 nm.



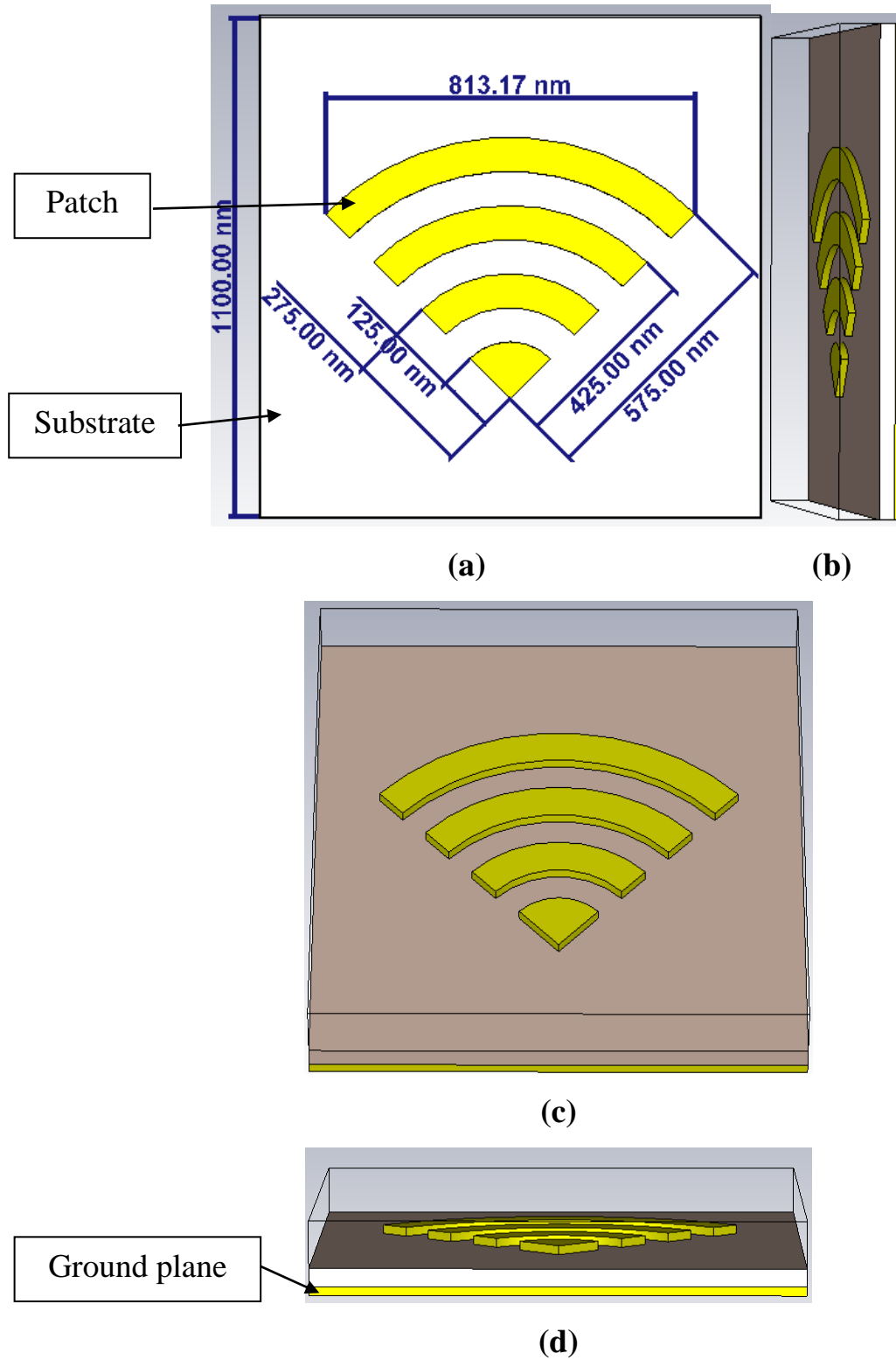


**Figure 3.13: a: MWNA front view; b: MWNA side view; c: MWNA perspective view; d: MWNA bottom view.**

The design method that used in this Nanoantenna is based on four circles: First Patch circle  $R_1=125$  nm. Second Patch circle  $R_2=275$  nm. Third Patch circle  $R_3=425$  nm and Fourth Patch circle  $R_4=525$  nm. The distance between the circles is 150 nm with thickness (t) 20 nm. These patches take the shape of Wi-Fi-shape. It can be designed depending on the circles. The ground plane consists of gold with dimension  $(1100 \times 1100)$  nm<sup>2</sup> and the thickness was (20) nm. The port that was used is waveguide excitation. All dimensions of MWNA are shown in Table 3.5.

**Table 3.5. MWNA dimensions.**

<b>NO.</b>	<b>dimensions</b>	<b>Values (nm)</b>
<b>1</b>	<b>Thickness of patch, t</b>	<b>20</b>
<b>2</b>	<b>First Patch circle R1</b>	<b>125</b>
<b>3</b>	<b>Second Patch circle R2</b>	<b>275</b>
<b>4</b>	<b>Third Patch circle R3</b>	<b>425</b>
<b>5</b>	<b>Fourth Patch circle R4</b>	<b>525</b>
<b>6</b>	<b>Distance between circles</b>	<b>150</b>
<b>7</b>	<b>Substrate width, W</b>	<b>1100</b>
<b>8</b>	<b>Substrate length, L</b>	<b>1100</b>
<b>9</b>	<b>Thickness of Substrate, h</b>	<b>50</b>
<b>10</b>	<b>Thickness of Ground, t</b>	<b>20</b>
<b>11</b>	<b>Ground width, Wg</b>	<b>1100</b>
<b>12</b>	<b>Ground length, Lg</b>	<b>1100</b>

### 3.10 The proposed model VII; Microstrip Wi-Fi-shape Slot Nanoantenna (MWSNA).

The sixth proposed design of Nanoantenna, which is called MWSNA, is shown in Figure 3.14. It is designed using silicon substrate with dimension  $(1000 \times 1000) \text{ nm}^2$ , thickness (h) 50 nm and the dielectric constant is  $\epsilon_r=11.9$ .

The ground layer dimensions are  $1000 \times 1000 \text{ nm}^2$ , while the thickness (t) is 20 nm. Gold metal is used in the designs of ground layer and patch layer.

In the design process of patch Nanoantenna, taking the inverse of the previous design (MWNA). Thus the Wi-Fi-shape slot patch Nanoantenna consists of four circles: first Patch circle  $R_1=125 \text{ nm}$ ; second Patch circle  $R_2=275 \text{ nm}$ ; third Patch circle  $R_3=425 \text{ nm}$  and fourth Patch circle  $R_4=525 \text{ nm}$ . The distance between the circles is 150 nm with thickness (t) 20 nm. So we design the patch Nanoantenna with the same size as the substrate and the ground plane. Then another material is used for cutting purpose. Finally, we cut from the drawing the shape of Wi-Fi to maintain engraved slot. Ground plane dimensions are the same as the substrate, the thickness is (20) nm. Dimensions of MWSNA are shown in Table 3.6.

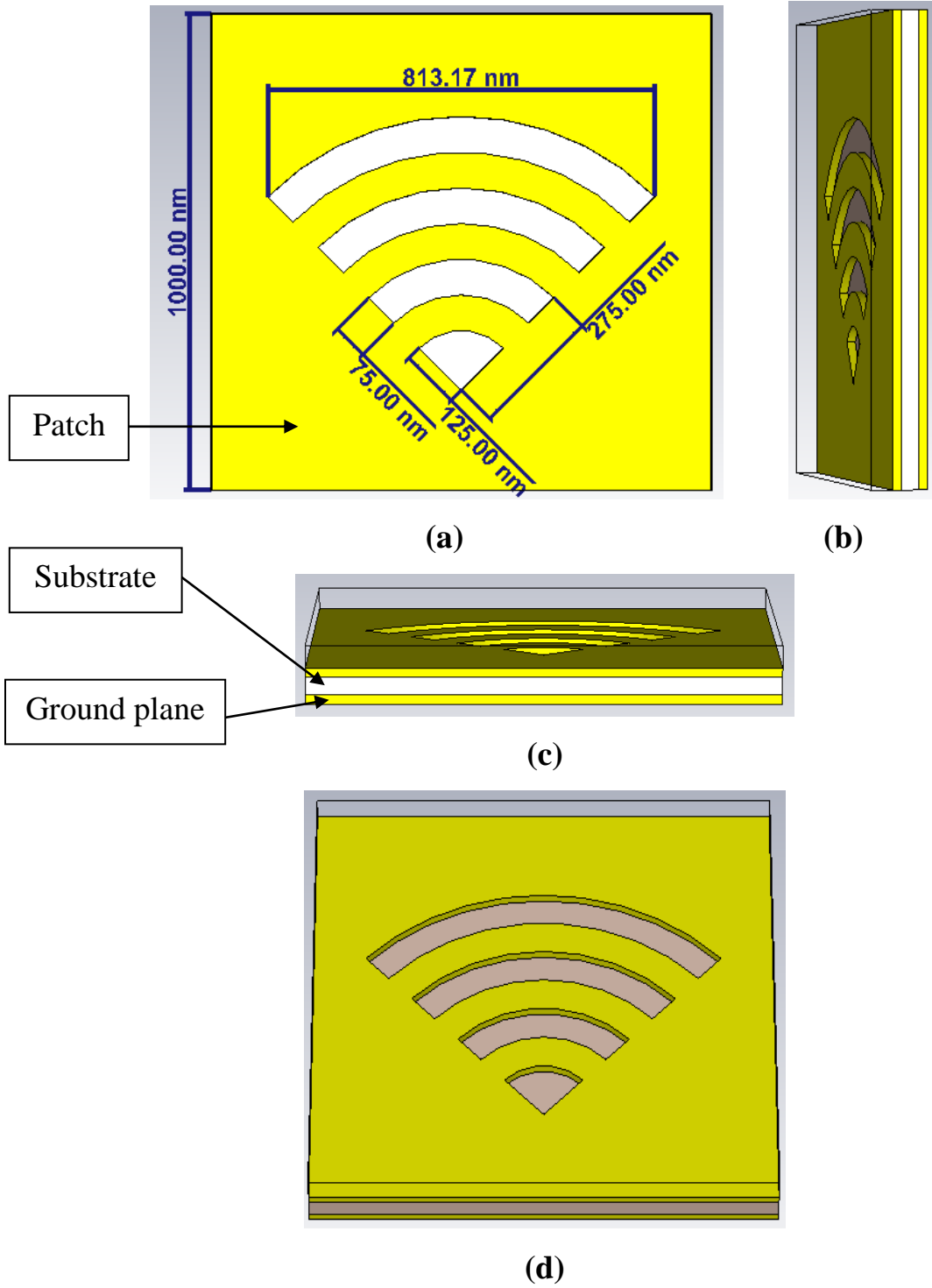


**Figure 3.14: a: MWSNA front view; b: MWSNA side view; c: MWSNA bottom view; d: MWSNA perspective view.**

**Table 3.6. MWSNA dimensions.**

<b>NO.</b>	<b>dimensions</b>	<b>Values (nm)</b>
<b>1</b>	<b>First slot Patch circle R1</b>	<b>125</b>
<b>2</b>	<b>Second slot Patch circle R2</b>	<b>275</b>
<b>3</b>	<b>Third slot Patch circle R3</b>	<b>425</b>
<b>4</b>	<b>Fourth slot Patch circle R4</b>	<b>525</b>
<b>5</b>	<b>Thickness of patch, t</b>	<b>20</b>
<b>6</b>	<b>Distance between slots</b>	<b>150</b>
<b>7</b>	<b>Substrate width, W</b>	<b>1000</b>
<b>8</b>	<b>Substrate length, L</b>	<b>1000</b>
<b>9</b>	<b>Thickness of Substrate, h</b>	<b>50</b>
<b>10</b>	<b>Thickness of Ground, t</b>	<b>20</b>
<b>11</b>	<b>Ground width, Wg</b>	<b>1000</b>
<b>12</b>	<b>Ground length, Lg</b>	<b>1000</b>

### **3.11 Analysis Formulation of the Microstrip Nanoantenna Structures.**

For all designs, and through the equations of length and width of the Microstrip Antenna, we are able to calculate the length and width using equations (3-1) and (3-2), so, the slightly manipulate the extracted values to suit our new design [1].

Actual width (W):

$$W = \frac{v_o}{2f_r} \sqrt{\frac{2}{\epsilon_r + 1}} \dots\dots\dots (3.1)$$

$v_o$ : free space velocity of light.

$f_r$ : resonant frequency.

$\epsilon_r$ : dielectric constant.

Actual length (L):

$$L = \frac{1}{2f_r \sqrt{\mu_0 \epsilon_0} \sqrt{\epsilon_{\text{reff}}}} \dots\dots\dots (3.2)$$

$\epsilon_{\text{reff}}$ : Effective dielectric constant.

$\mu_0$ :  $4\pi \times 10^{-7}$  H/m (permeability)

$\epsilon_0$ :  $8.8541878128(13) \times 10^{-12}$  F·m<sup>-1</sup> (permittivity)

The effective dielectric constant for Microstrip antenna is given by [49]:

$$\epsilon_{\text{reff}} = \frac{\epsilon_r + 1}{2} + \frac{\epsilon_r - 1}{2} \left( \frac{1}{\sqrt{1 + \frac{12h}{w_f}}} \right) \dots\dots\dots (3.3)$$

$h$ : thickness

$w_f$ : strip width

# **CHAPTER FOUR**

## **RESULTS, DISCUSSIONS AND PERFORMANCE EVALUATIONS**

### **4.1 Introduction**

In this chapter, the parameters of the Nanoantenna design will be discussed generally. It includes the reflection coefficient, Nanoantenna gain, Nanoantenna directivity, far-field radiation pattern, bandwidth and 3-D far-field of designs.

After discussing the parameters, making a comparison between the Hash-shape and Hash-shape Slot Nanoantenna, Bluetooth-shape and Bluetooth-shape Slot Nanoantenna and Wi-Fi-shape and Wi-Fi-shape Slot Nanoantenna. Finally, all designs model are compared to choose the best ones.

### **4.2 Characteristics of the Microstrip Hash-shape Nanoantenna and Microstrip Hash-shape Slot Nanoantenna.**

#### **4.2.1 Reflection Coefficient for MHNA & MHSNA.**

For the two designs MHNA and MHSNA, the reflection coefficients are illustrated in Figure 4.1 and Figure 4.2 respectively. Reflection coefficients indicates that the first proposed Microstrip Hash-shape Nanoantenna resonates at 129.44 THz with  $S_{11}$  -45.71

dB, while the second proposed Microstrip Hash-shape Slot Nanoantenna resonates at 129.74 THz with reflection coefficient ( $S_{11}$ ) -14.19 dB. This gives a slight difference between the two frequency bands as a result of the change in the shape of the patch.

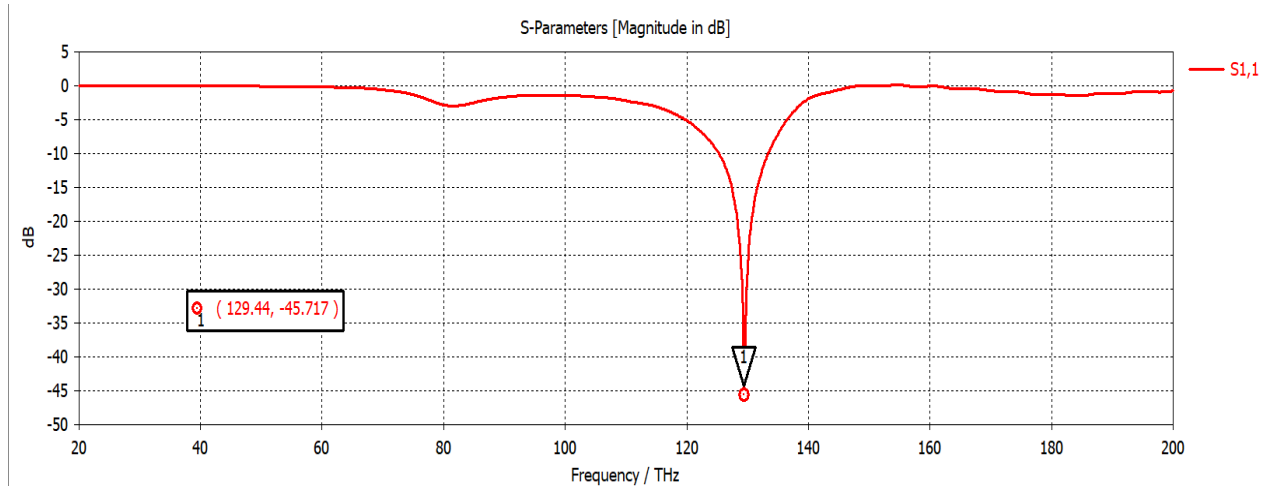


**Figure 4.1:  $S_{11}$  of MHNA.**

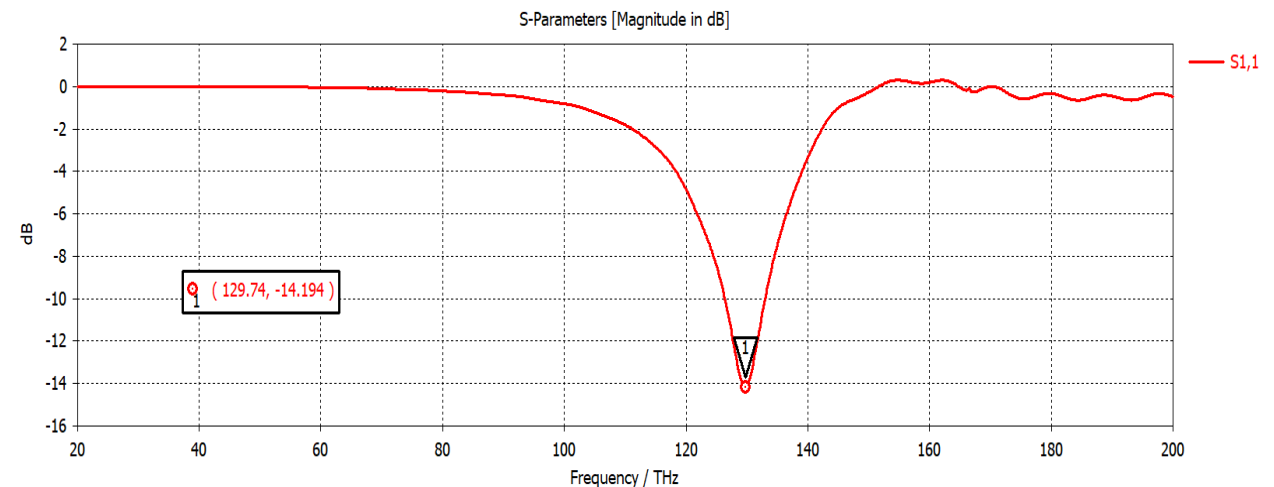
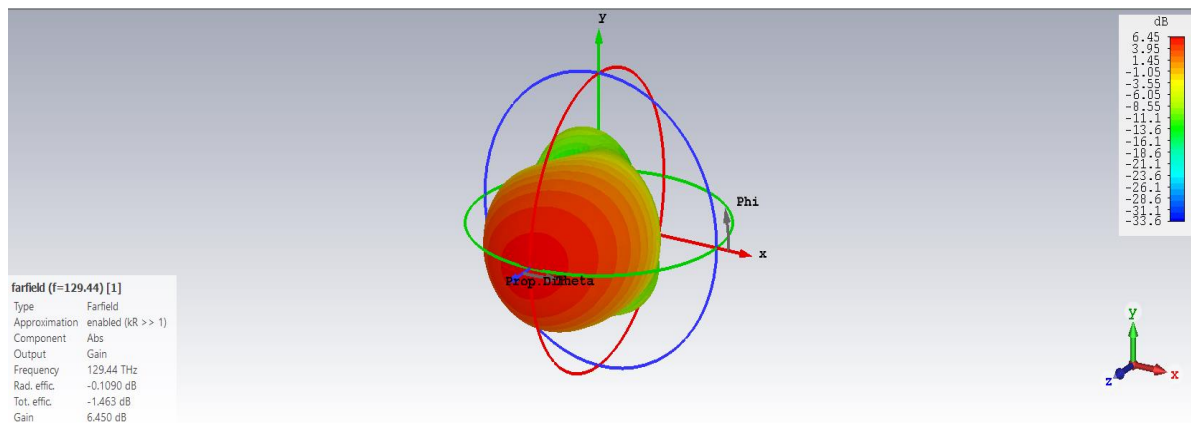


**Figure 4.2:  $S_{11}$  of MHSNA.**

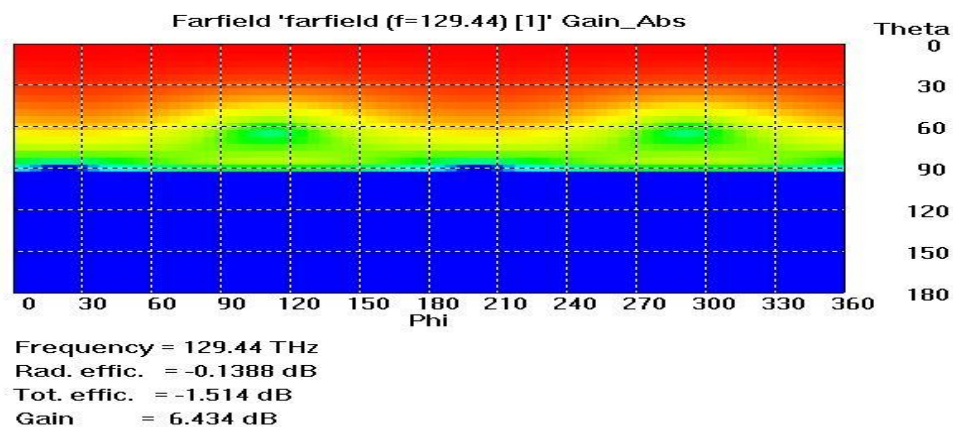


## 4.2.2 Gain for MHNA & MHSNA.

The 3D & 2D plots for the gain of the MHNA and MHSNA are shown in Figure 4.3 and Figure 4.4 respectively. So, the max value of the gain is 6.45 dB at the resonant frequency 129.44 THz for the MHNA, while the gain of the MHSNA is 5.73 dB at the resonant frequency 129.74 THz. This gives an indication that the gain of the first design larger than gain of second design by 0.72 dB.

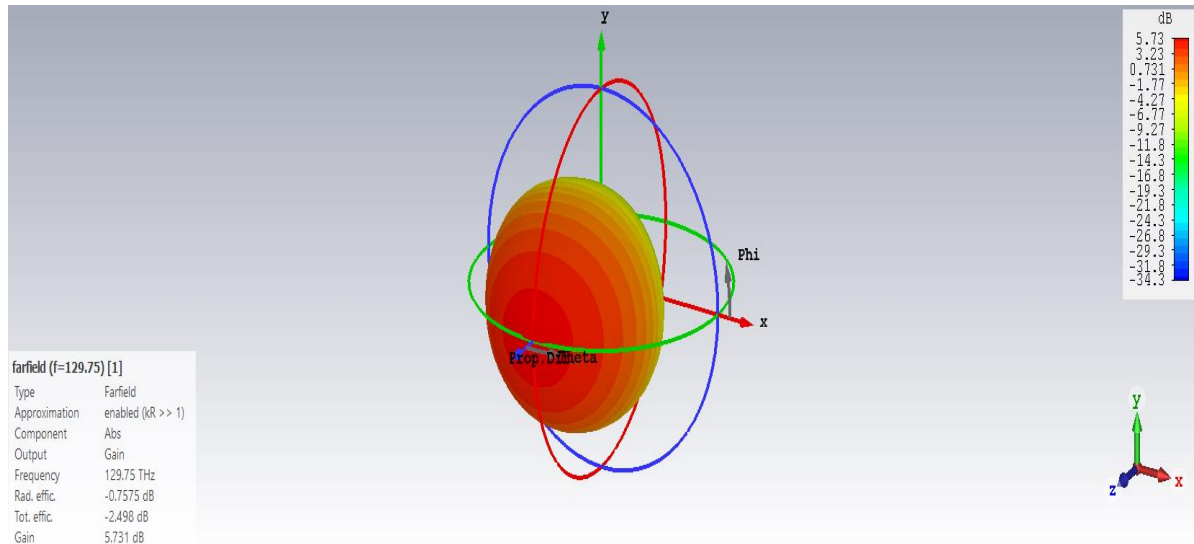


(a)

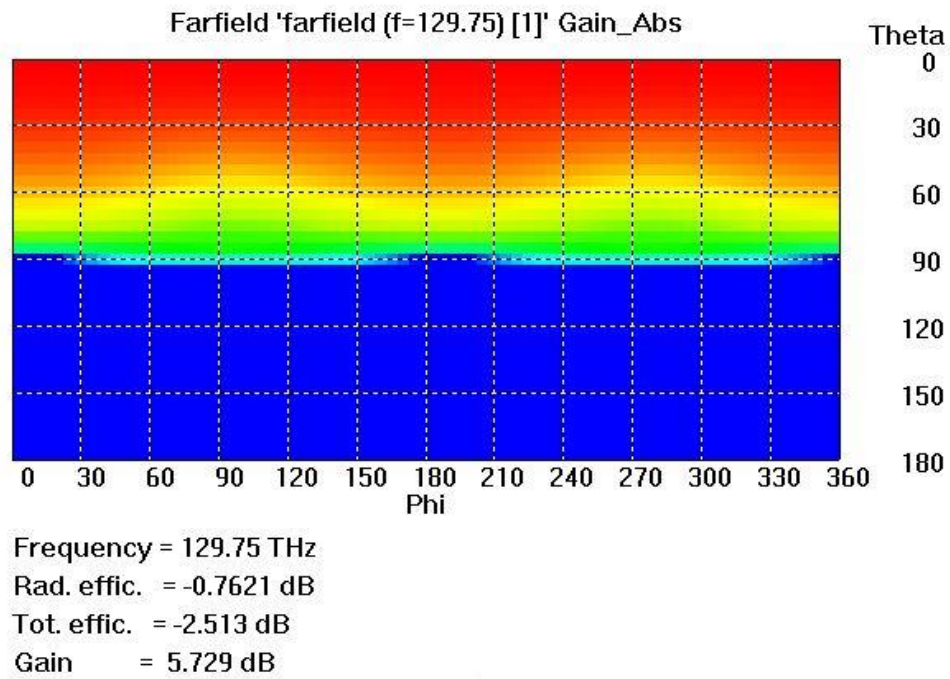


(b)

Figure 4.3: Gain of MHNA (a) 3D and (b) 2D.



(a)



(b)

Figure 4.4: Gain of MHSNA (a) 3D and (b) 2D.

### 4.2.3 Directivity for MHNA & MHSNA.

The 3-D plot for Directivity are illustrated in Figure 4.5 for the MHNA and Figure 4.6 for MHSNA. The value of the directivity is 6.56 dB at the resonant frequency 129.44 THz while the value of the directivity at the resonant frequency 129.74 THz is 6.49 dB. Note that the MHNA design has more directivity than the MHSNA design due to the form of the patch.

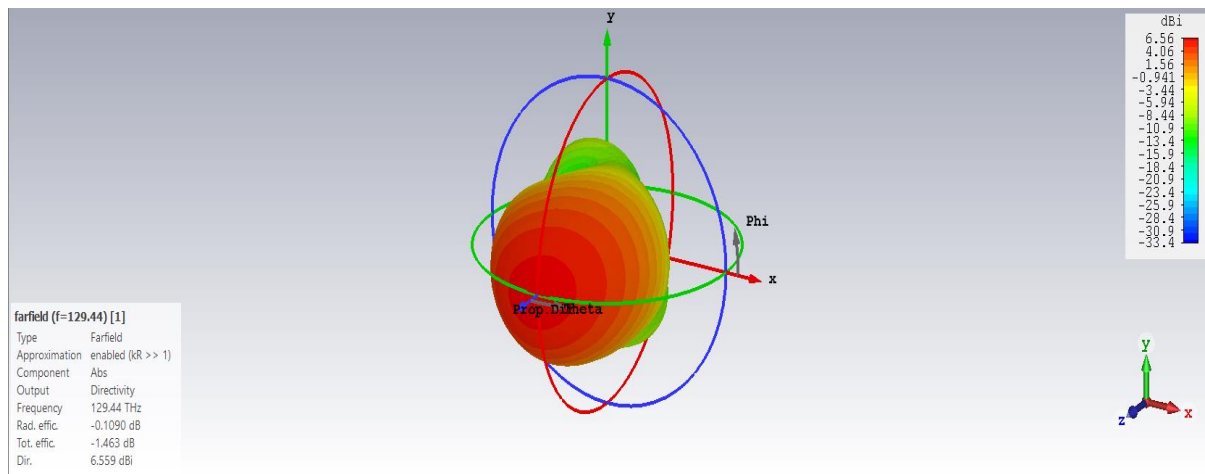


**Figure 4.5: Directivity of MHNA.**

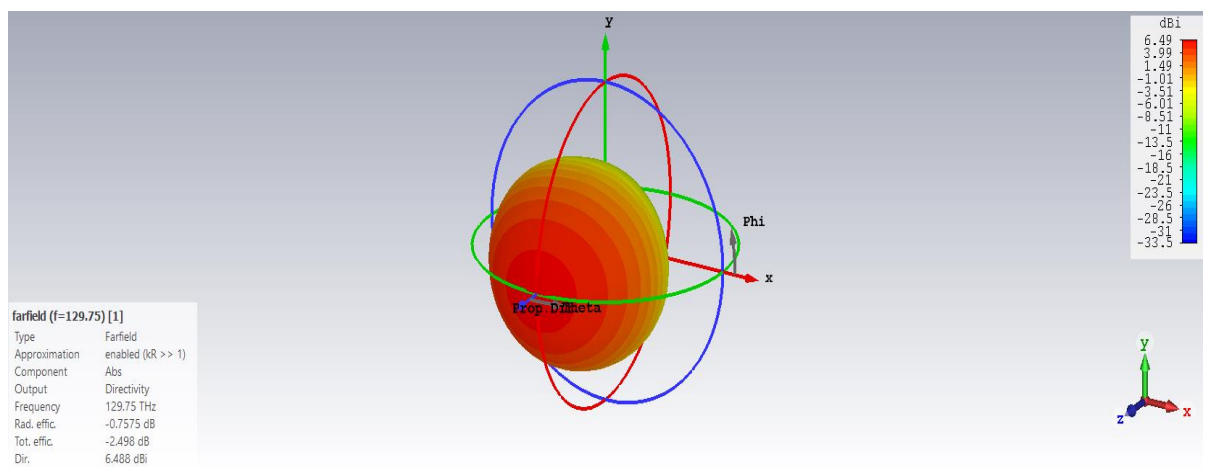


**Figure 4.6: Directivity of MHSNA.**

#### 4.2.4 Current Distribution for MHNA & MHSNA.

In these proposed Nanoantennas, to get more insight about the EM characteristics, the current distributions generated in the Nanoantenna have been simulated in the two designs.

In MHNA, the form of current distribution at resonant frequency 129.44 THz is shown in Figure 4.7 (a). Note that the current distribution form is distributed from inside the patch and is spread circularly outward. While the MHSNA design has a resonant frequency 129.74 THz current distributed around the slot of the Hash outward as shown in Figure 4.7 (b).

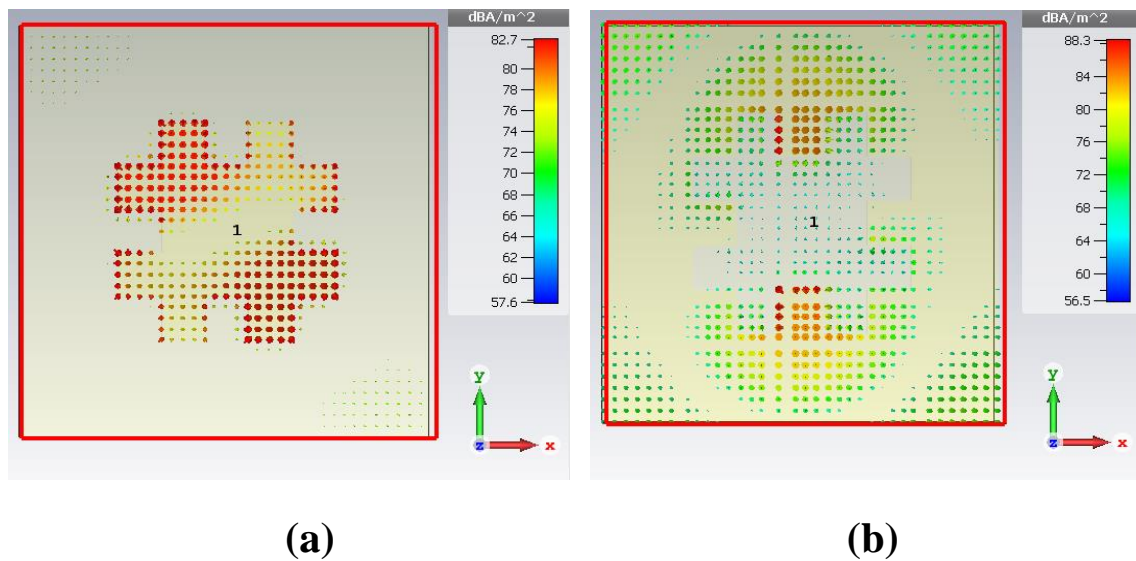


**Figure 4.7: Current distribution, (a) MHNA & (b) MHSNA.**

### 4.2.5 Radiation Patterns for MHNA & MHSNA.

The polar plot for the MHNA and MHSNA radiation pattern are shown in Figures 4.8 and 4.9 respectively.

For the MHNA, in the x-y plane ( $\theta = 90^\circ$ ), the main lobe magnitude is (5.35) dB, the main lobe direction is ( $293^\circ$ ), and the angular width is ( $89.9^\circ$ ), in the y-z plane ( $\varphi = 90^\circ$ ) the main lobe magnitude is (19.8) dB, the main lobe direction is ( $0^\circ$ ), and the angular width is ( $57.9^\circ$ ), in the x-z plane ( $\varphi = 0^\circ$ ) the main lobe magnitude is (19.8) dB, the main lobe direction is ( $0^\circ$ ), and the angular width is ( $73.1^\circ$ ).

In the MHSNA, the x-y plane ( $\theta = 90^\circ$ ) the main lobe magnitude is (-1.17) dB, the main lobe direction is ( $276^\circ$ ), and the angular width is ( $86.3^\circ$ ), in the y-z plane ( $\varphi = 90^\circ$ ) the main lobe magnitude is (18.8) dB, the main lobe direction is ( $0^\circ$ ), and the angular width is ( $64.8^\circ$ ), in the x-z plane ( $\varphi = 0^\circ$ ) the main lobe magnitude is (18.8) dB, the main lobe direction is ( $0^\circ$ ), and the angular width is ( $78.4^\circ$ ).

All values described above are shown in Table 4.1.

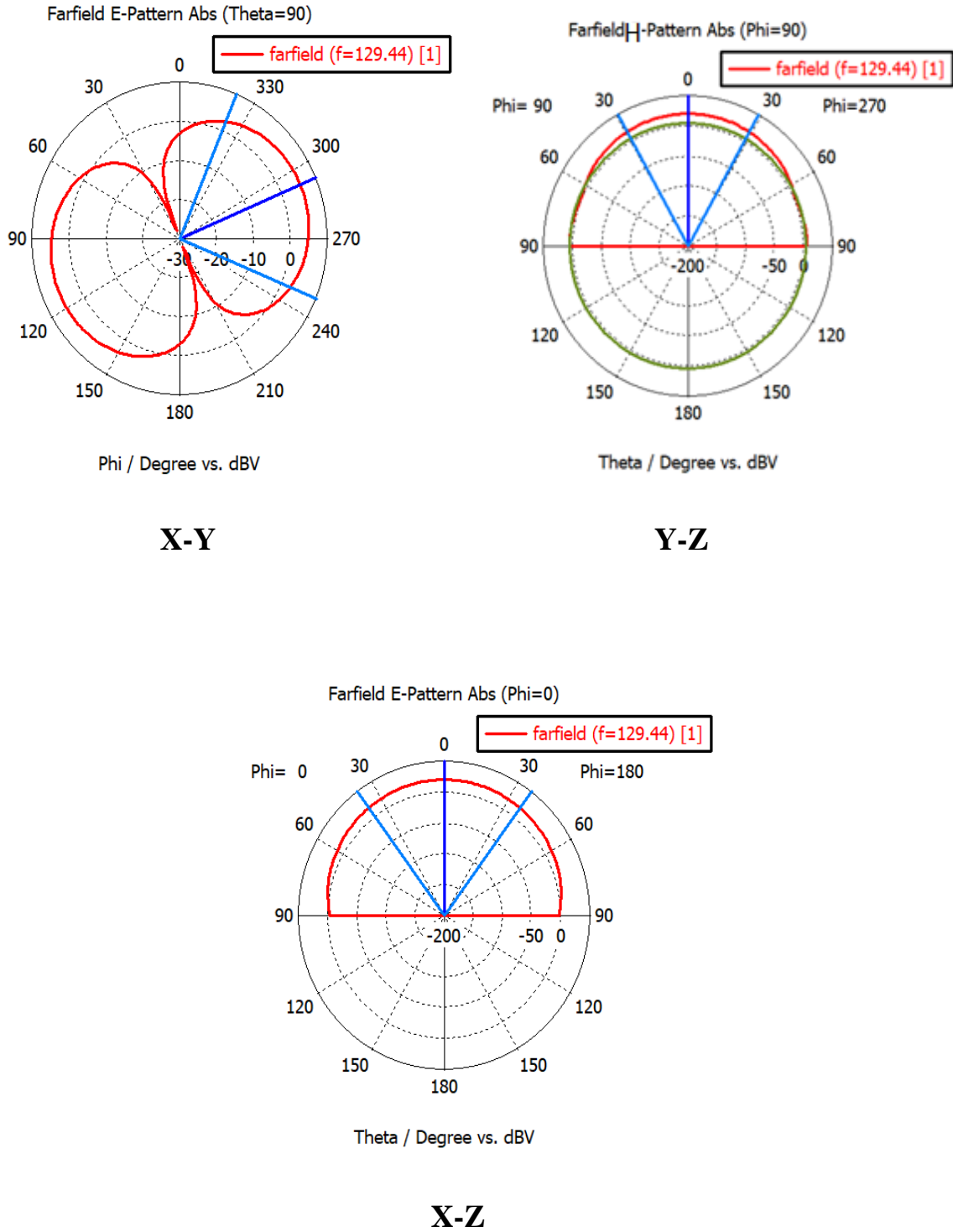


Figure 4.8: Radiation pattern of the MHNA at  $f=129.44$  THz.

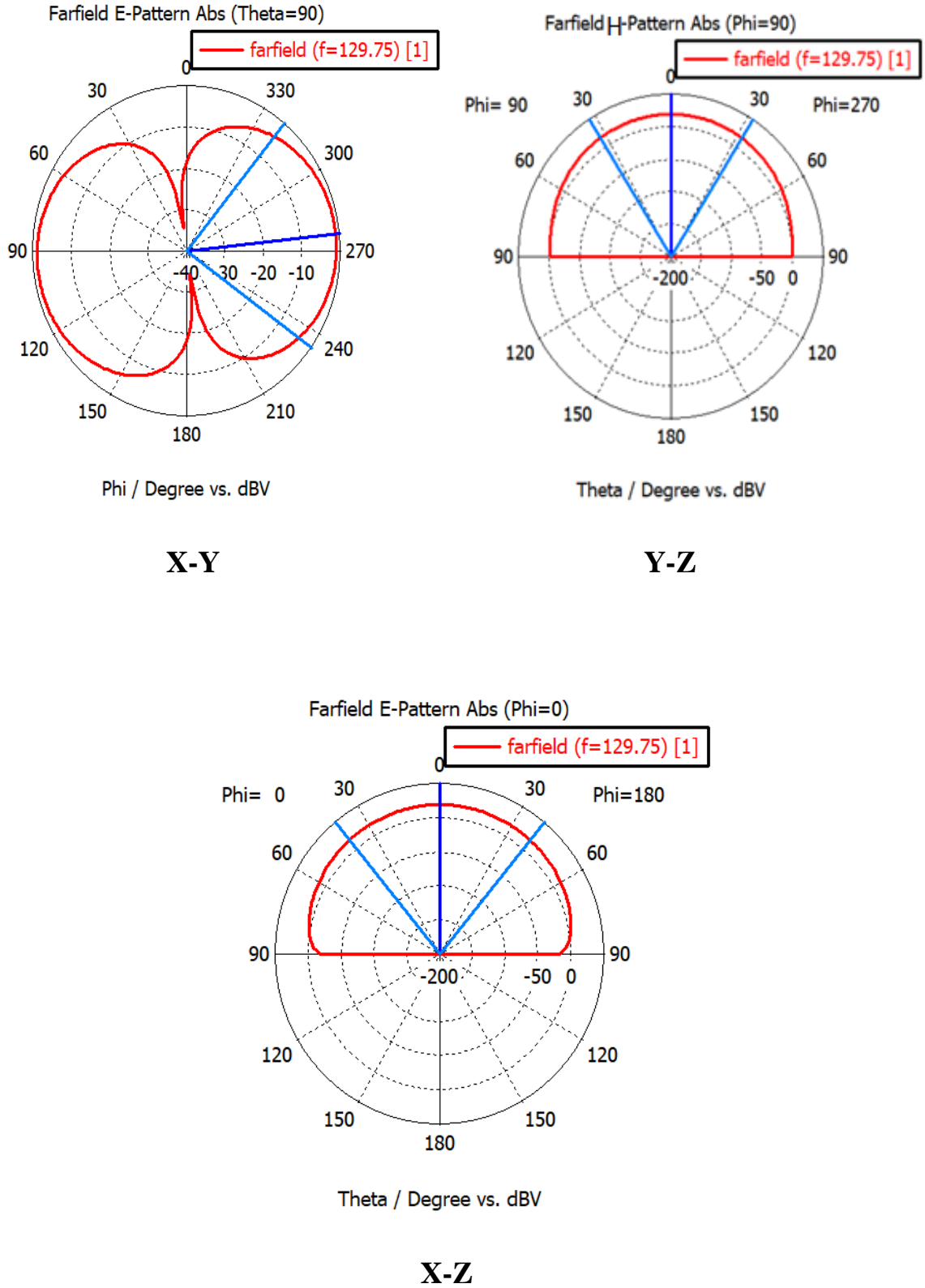


Figure 4.9: Radiation pattern of the MHSNA at  $f=129.74$  THz.

**Table 4.1: Characteristics of the far-field radiation pattern for the MHNA & MHSNA.**

Freq. (THz)	Parameter	x-y plane	y-z plane	x-z plane
129.44	Main lobe magnitude (dB)	5.35	19.8	19.8
	Main lobe direction (deg.)	293	0	0
	Angular width (deg.)	89.9	57.9	73.1
	Side lobe level (dB)	0	-15.2	0
129.74	Main lobe magnitude (dB)	-1.17	18.8	18.8
	Main lobe direction (deg.)	276	0	0
	Angular width (deg.)	86.3	64.8	78.4
	Side lobe level (dB)	0	0	0

#### 4.2.6 Efficiency for MHNA & MHSNA.

The efficiency of MHNA is 98.32 %. It is calculated from the relationship between the gain and directivity (which has previously mentioned). The efficiency of MHSNA is 88.28 %. So, based on these values, the MHNA design is more acceptable than the MHSNA design.

#### 4.2.7 Bandwidth for MHNA & MHSNA.

Depending on Figure 4.10, the bandwidth shows that the Nanoantenna frequency band starts at frequency 125.3 THz to frequency 133.3 THz, producing a bandwidth of approximately 8



THz in the MHNA design. However, Figure 4.11, shows that the Nanoantenna frequency band starts at frequency 126.39 THz and ends at frequency 132.99 THz, producing a bandwidth of approximately 6.6 THz. This gives another indicator of the MHNA design producing the bandwidth much larger than the MHSNA design.

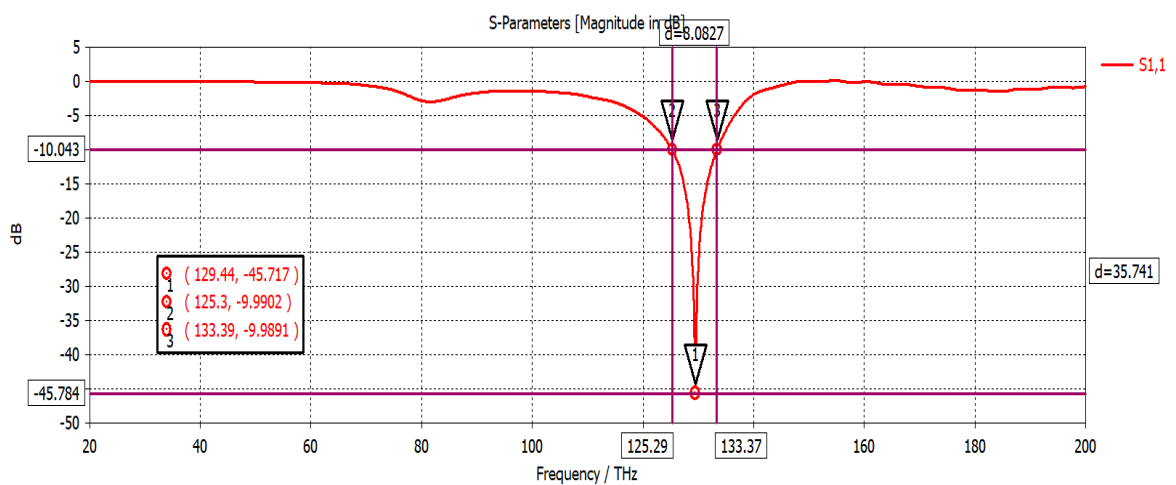


**Figure 4.10: Bandwidth of MHNA.**

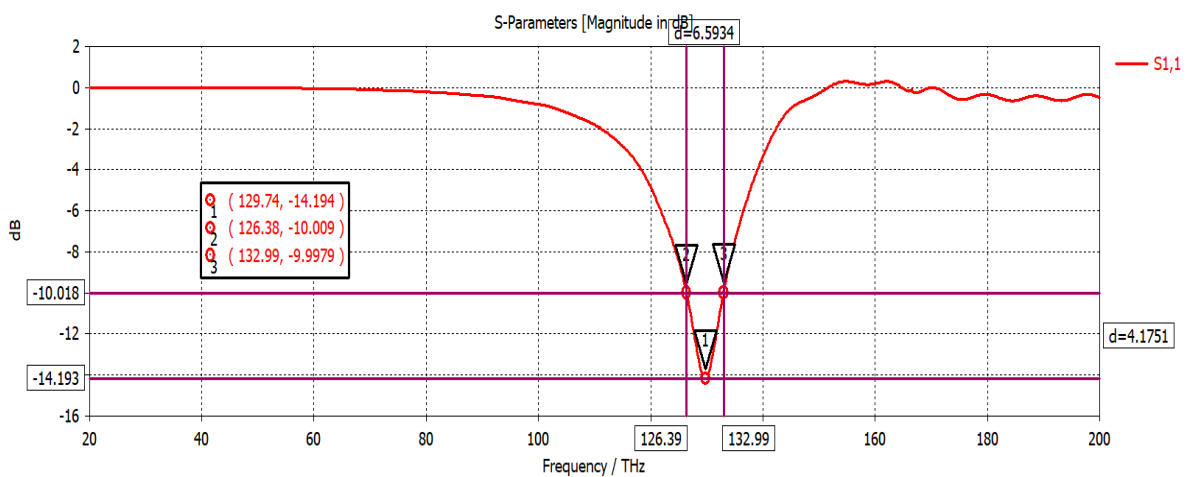


**Figure 4.11: Bandwidth of MHSNA.**

### 4.2.8 Validation between MHNA, MHSNA and other references.

In this part of thesis, the references [50] and [51] with the two proposed Nanoantennas (MHNA & MHSNA) in terms of the parameters will be compared as shown in table 4.2. Their results are calculated and extracted in this chapter. Where observed in the reference that used in the comparison that there is resonated at a high frequency while the reflection coefficient is somewhat acceptable.

The directivity is smaller compared to the two proposed Nanoantenna designs. Also, there is a high-bandwidth mention in the references compared to the two proposed Nanoantenna designs, but the dielectric constant of the silicon that is used by the reference  $\epsilon=4.4$  while the dielectric constant for the proposed Nanoantenna designs is  $\epsilon=11.9$ .

**Table 4.2: Comparison between MHNA, MHSNA and references.**

Name	Sub. type	$S_{11}$	f(THz)	G(dB)	D(dB)	Eff.	BW
[50]	Silicon $\epsilon=11.9$	-46.45	8.685	2.03	---	---	2
[51]	Glass	-16	31.5	5.73	---	---	4
<b>MHNA</b>	Silicon $\epsilon=11.9$	-45.71	129.44	6.45	6.56	98.32	8
<b>MHSNA</b>	Silicon $\epsilon=11.9$	-14.19	129.74	5.73	6.49	88.28	6.6

### 4.3 Characteristics of the Microstrip Bluetooth-shape Nanoantenna and Microstrip Bluetooth-shape Slot Nanoantenna.

#### 4.3.1 Reflection Coefficient for MBNA & MBSNA.

In these designs, the layout of the MBNA and MBSNA are identified as shown in Figures 4.12 and 4.13 respectively. The Microstrip Bluetooth-shape Nanoantenna resonates at 120 THz with reflection coefficient  $S_{11} = -27.19$  dB. But reflection coefficient for the Microstrip Bluetooth-shape Slot Nanoantenna resonates at 133 THz with reflection coefficient  $S_{11} -25.18$  dB. This shows how accurate the resonant frequency is as a transient -10 dB in the  $S_{11}$  Figures below.

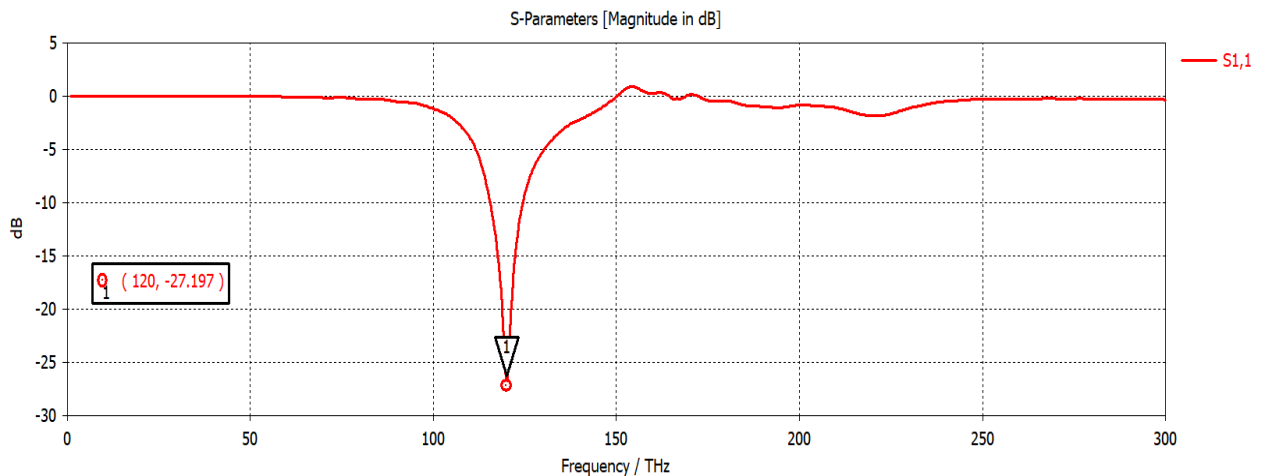


Figure 4.12:  $S_{11}$  of MBNA.

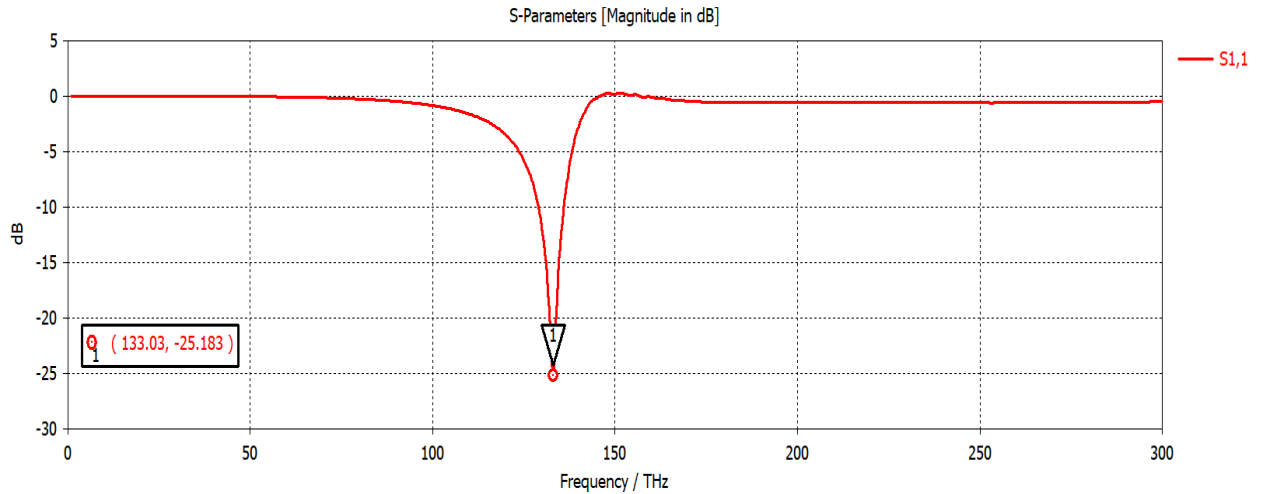
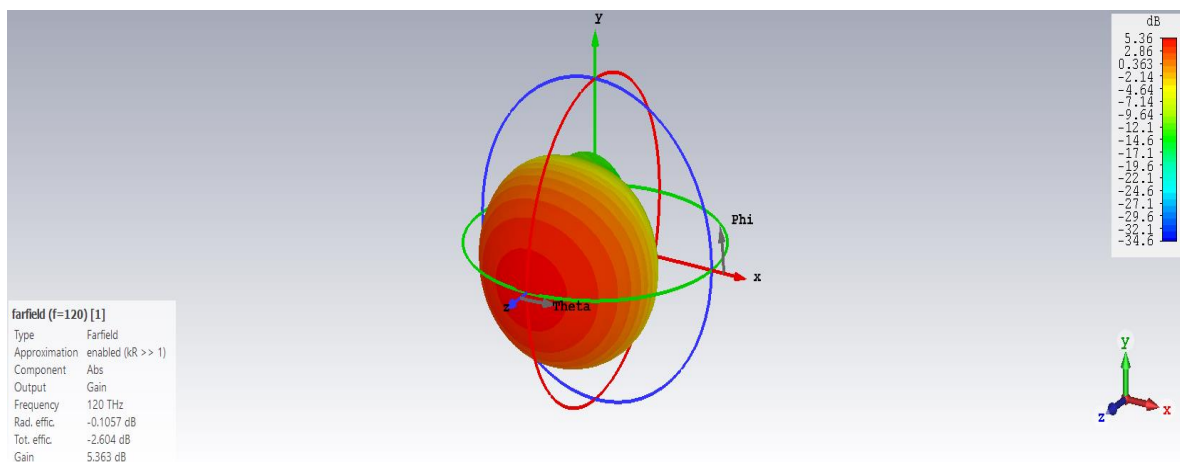


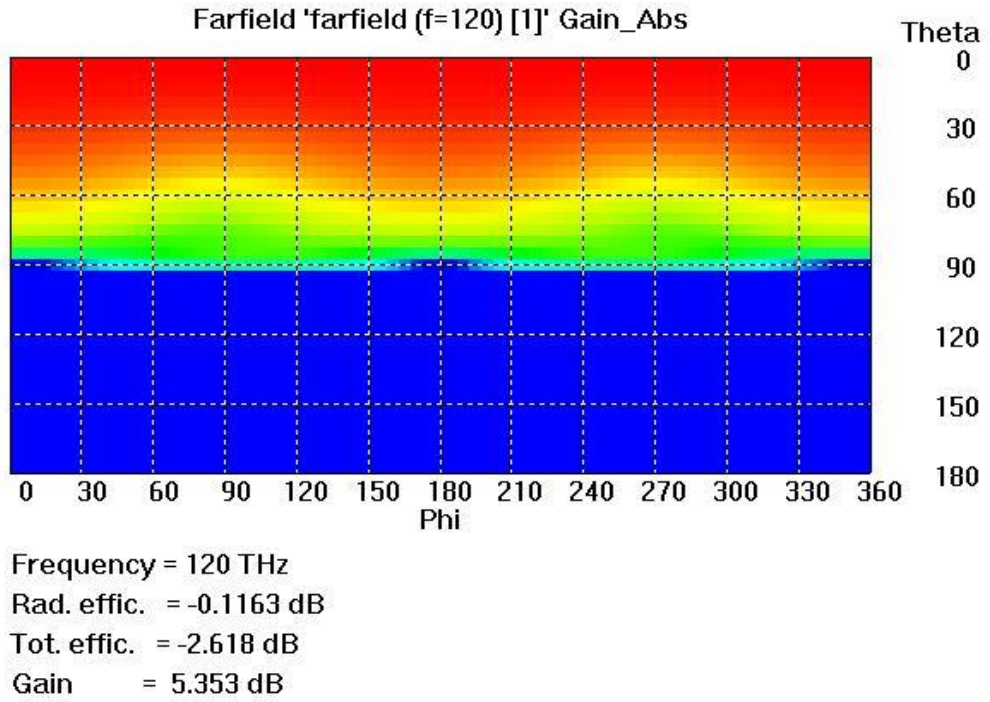
Figure 4.13: S<sub>11</sub> of MBSNA.

### 4.3.2 Gain for MBNA & MBSNA.

The shape of the MBNA gain is shown in Figure 4.14 where its value is 5.36 dB, while the plot for gain of the MBSNA is 6.71 dB as shown in Figure 4.15. It is considered higher than the MBNA design because of the different shape of the patch in the two designs.

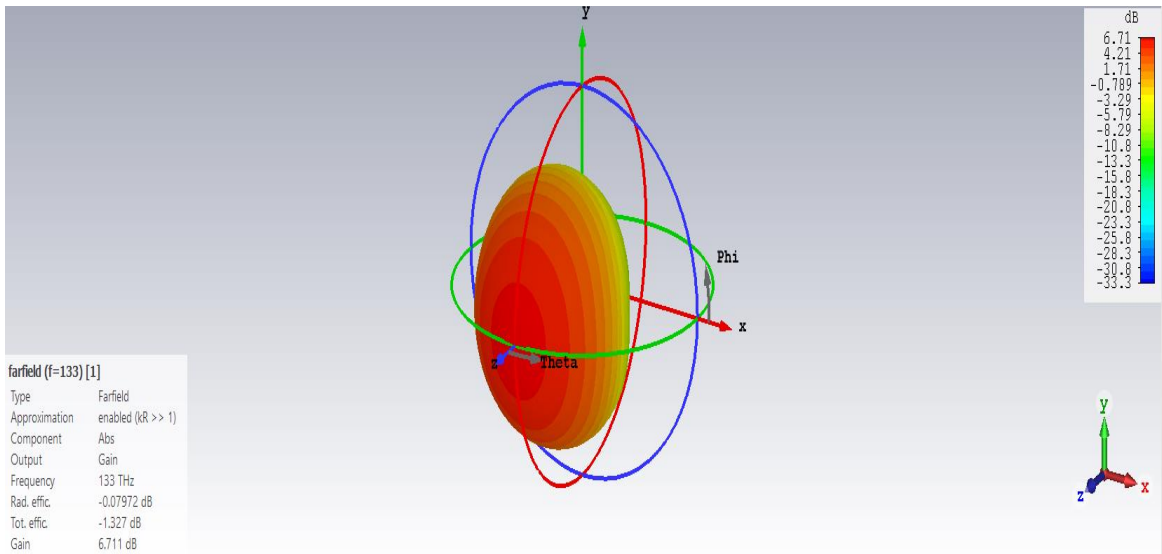


(a)

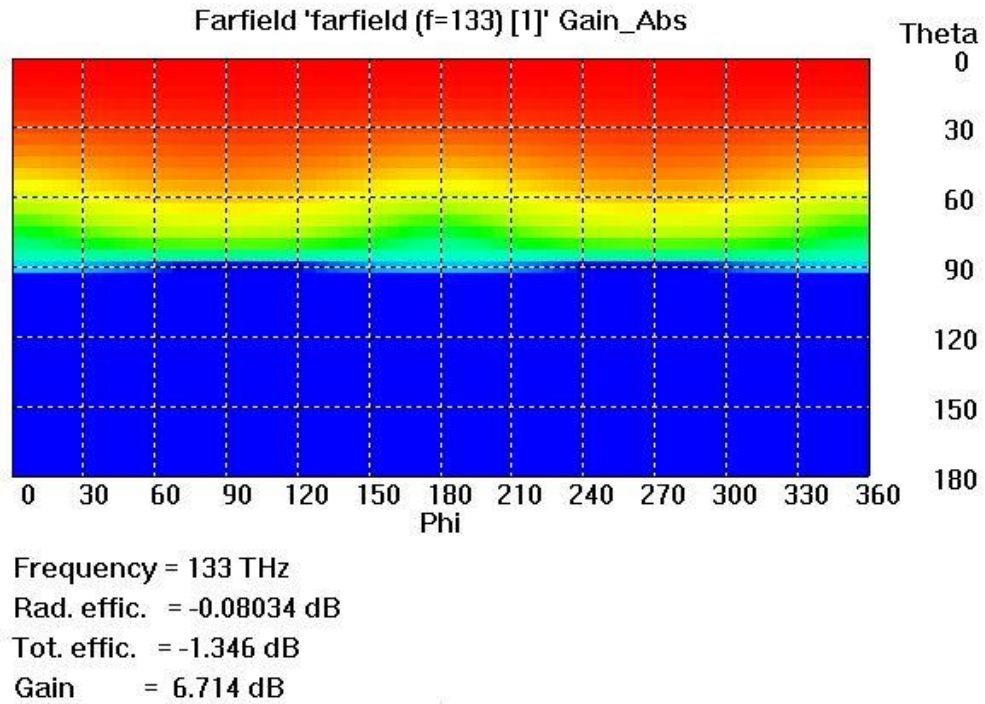


(b)

Figure 4.14: Gain of MBNA (a) 3D and (b) 2D.



(a)



(b)

**Figure 4.15: Gain of MBSNA (a) 3D and (b) 2D.**

### 4.3.3 Directivity for MBNA & MBSNA.

In these designs, the value of the Directivity to the MBNA design is 5.47 dB as shown in Figure 4.16, while in the MBSNA design the value is 6.79 dB as illustrated in Figure 4.17.

From the results above, we notice that the MBSNA design has a higher directivity than the MBNA design and this makes it more suitable in terms of reaching the radiation as far as possible.

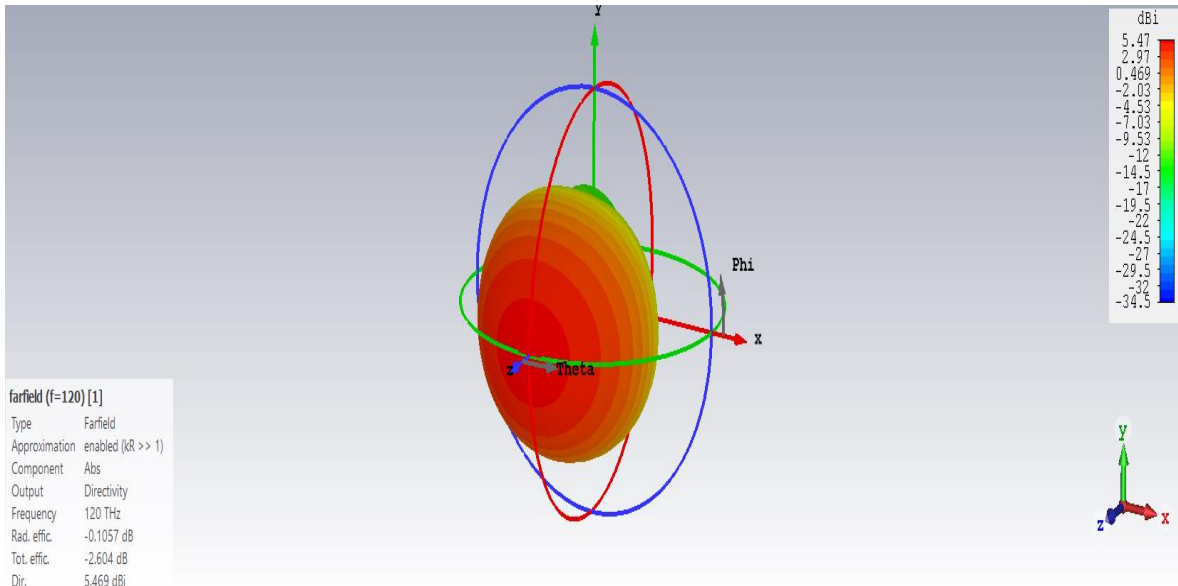


Figure 4.16: Directivity of MBNA.

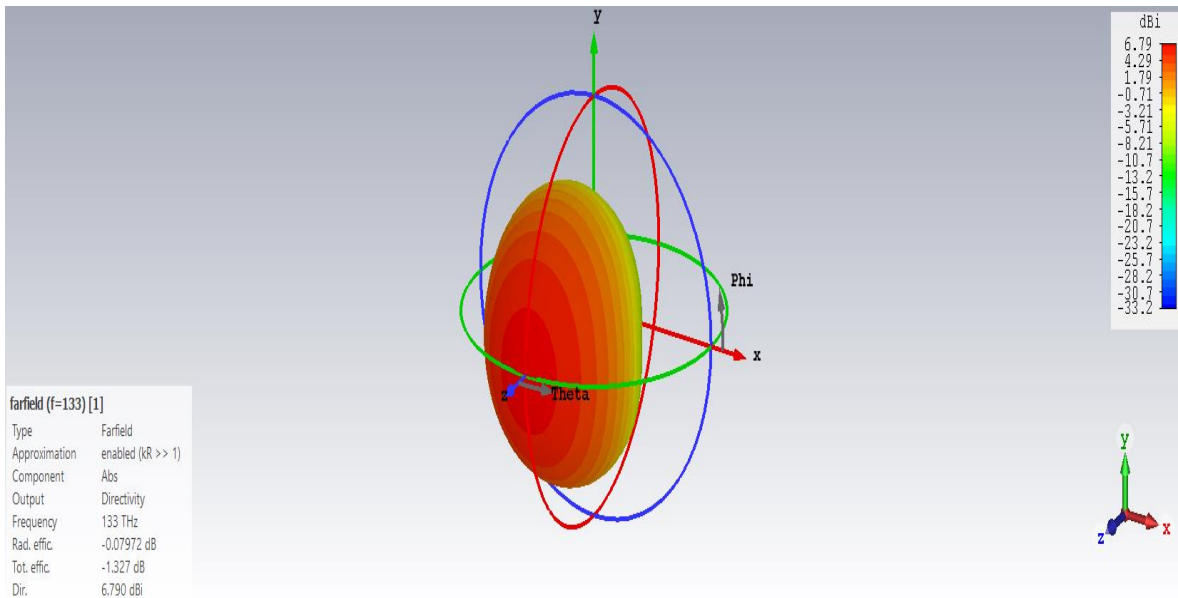
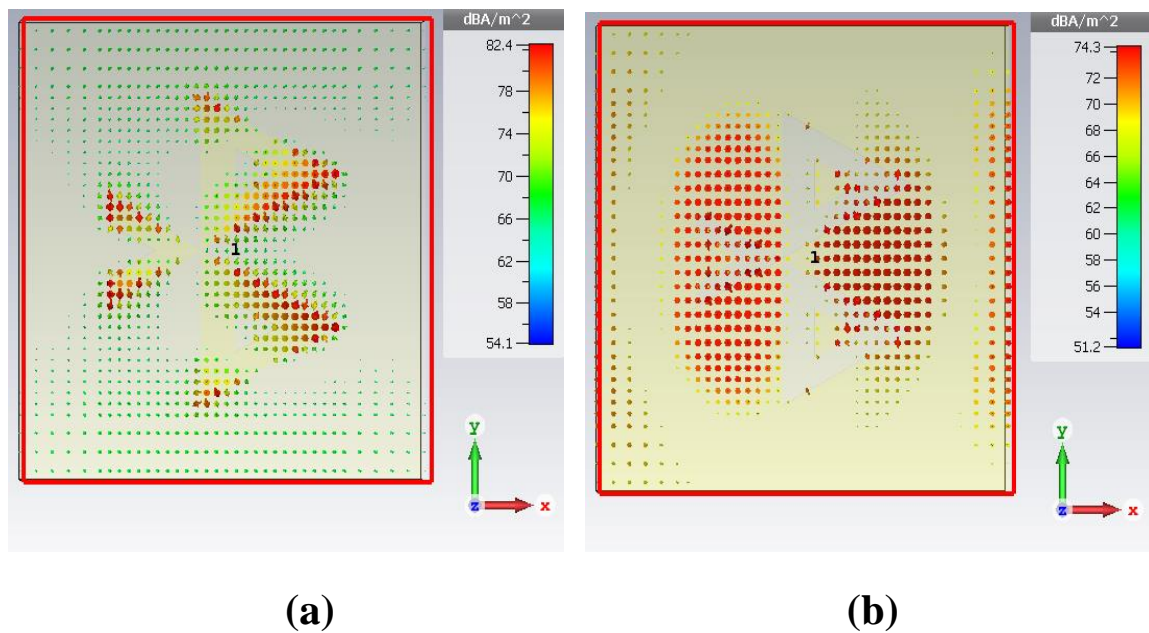


Figure 4.17: Directivity of MBSNA.

### 4.3.4 Current Distribution for MBNA & MBSNA.

The current distribution for the MBNA is illustrated in Figure 4.18 (a). It is clear, based on the figure below, that the form of distribution of the current spreads from the patch to the outside in a rotational manner according to the form of Bluetooth.

The distribution of current for the MBSNA design is shown in Figure 4.18 (b). Here, the current flows around the Bluetooth-shape and never spreads in the slot. So, the current will be spread around the slot depending on the method of spreading.



**Figure 4.18: Current distribution of (a) MBNA & (b) MBSNA.**



### 4.3.5 Radiation Patterns for MBNA & MBSNA.

The radiation patterns for the MBNA is shown in Figure 4.19. For the resonant frequency 120 THz of the MBNA design, in the x-y plane ( $\theta = 90^\circ$ ), the value of main lobe magnitude is (-12.7) dB. The main lobe direction is ( $258^\circ$ ) and the angular width is ( $80.3^\circ$ ). While in the y-z plane ( $\varphi = 90^\circ$ ), the main lobe magnitude is (19.8) dB. The main lobe direction is ( $0^\circ$ ) and the angular width is ( $62.9^\circ$ ). But the x-z plane ( $\varphi = 0^\circ$ ) the main lobe magnitude is (19.8) dB. The main lobe direction is ( $0^\circ$ ) and the angular width is ( $79.8^\circ$ ).

Here, the radiation values for the resonant frequency of 133 THz of the MBSNA design will be reviewed. Figure 4.20 shows the radiation process in three cases. The first case is x-y plane ( $\theta = 90^\circ$ ) contain main lobe magnitude is (-18.7) dB; main lobe direction is ( $0^\circ$ ) and the angular width is ( $88.9^\circ$ ). The second case is y-z plane ( $\varphi = 90^\circ$ ) contain main lobe magnitude is (6.79) dB, main lobe direction is ( $0^\circ$ ) and the angular width is ( $76.5^\circ$ ). The last case is x-z plane ( $\varphi = 0^\circ$ ) contain main lobe magnitude is (6.79) dB, main lobe direction is ( $0^\circ$ ) and the angular width is ( $61.5^\circ$ ). Overall values of radiation to the MBNA & MBSNA are shown in Table 4.3.

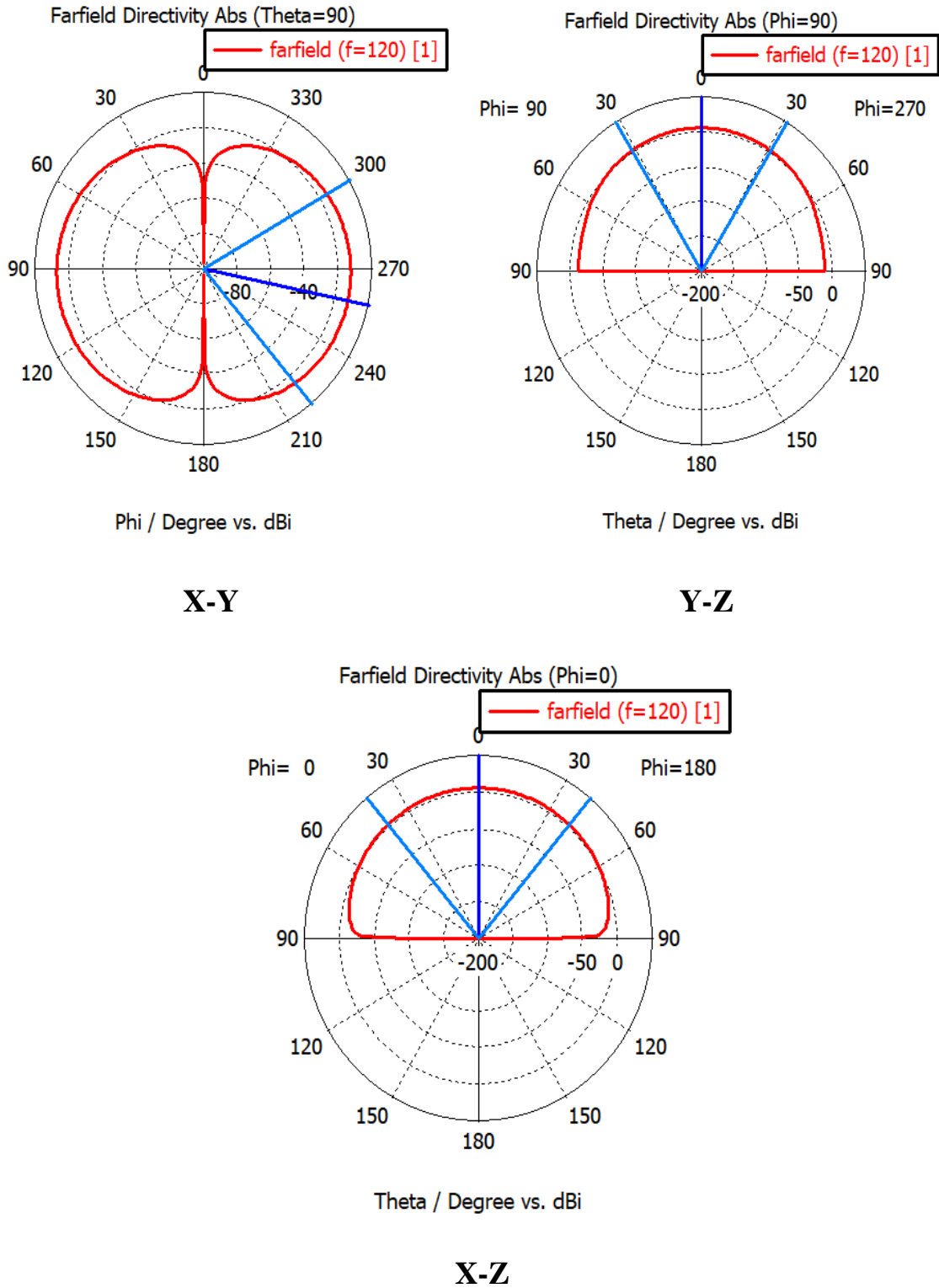


Figure 4-19: Radiation pattern of the MBNA at f=120 THz.

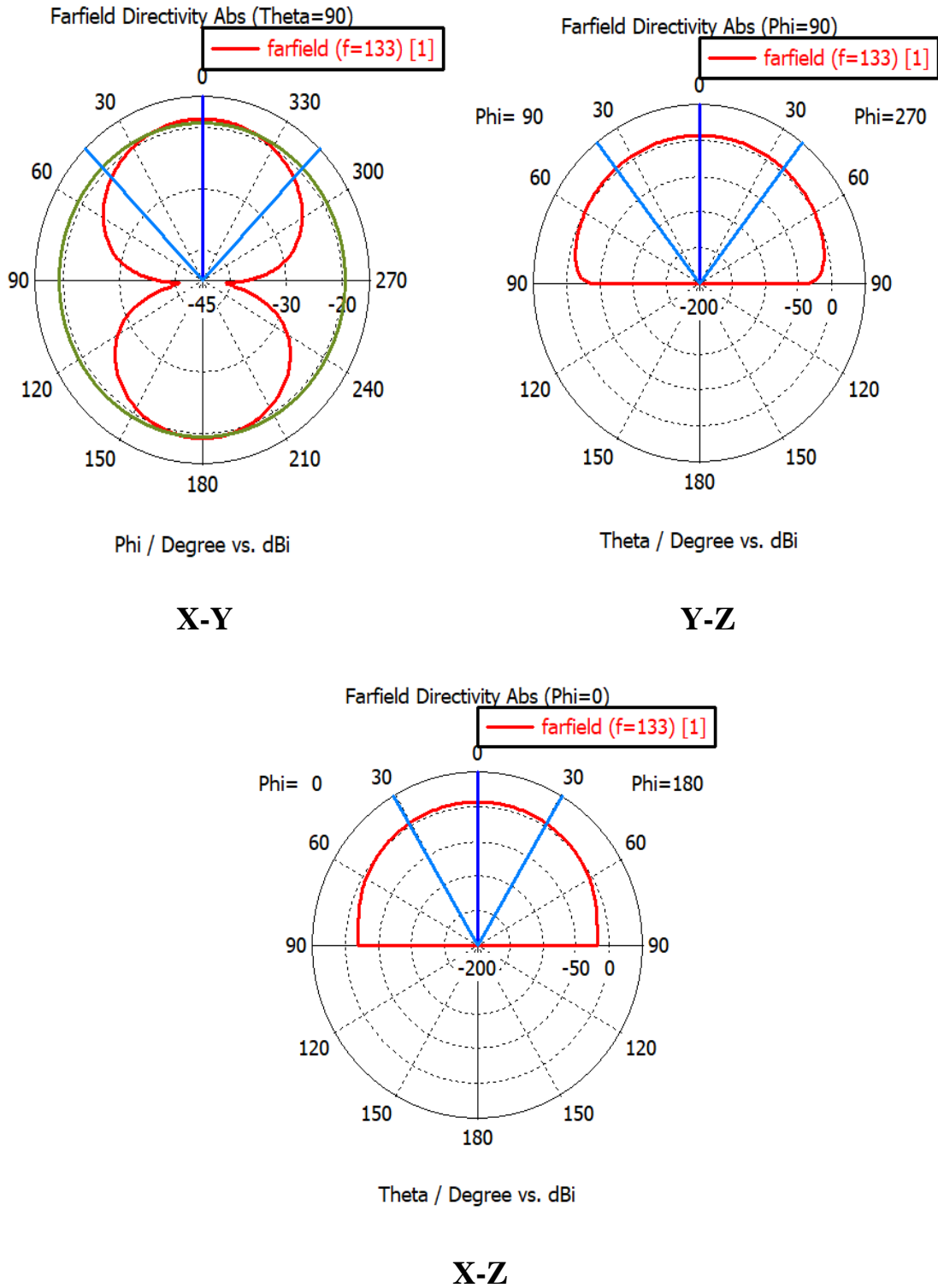


Figure 4-20: Radiation pattern of the MBSNA at f=133 THz.

**Table 4.3: Characteristics of the far-field radiation pattern for the MBNA & MBSNA.**

Freq. (THz)	Parameter	x-y plane	y-z plane	x-z plane
120	Main lobe magnitude (dB)	-12.7	5.47	5.47
	Main lobe direction (deg.)	258	0	0
	Angular width (deg.)	80.3	62.9	79.8
	Side lobe level (dB)	0	0	0
133	Main lobe magnitude (dB)	-18.7	6.79	6.79
	Main lobe direction (deg.)	0	0	0
	Angular width (deg.)	88.9	76.5	61.5
	Side lobe level (dB)	-0.6	0	0

#### 4.3.6 Efficiency for MBNA & MBSNA.

There is a relationship between the gain and directivity, as mentioned in Chapter Three, shows how to extract the efficiency of the Nanoantenna. So the efficiency of the MBNA design is 97.63 %, but the efficiency of MBSNA design is 98.82 %. Since we find the efficiency of the MBSNA design is higher than the MBNA design, this gives us preference in terms of efficiency.

#### 4.3.7 Bandwidth for MBNA & MBSNA.

The diagram bandwidth of the two designs is illustrated in Figures 4.21 and 4.22. So the value of bandwidth to the MBNA design is 8.93 THz in the range that starts from frequency 115.54 THz and

ends at frequency 124.47 THz. However, in MBSNA design the frequency is 7 THz and the range begins from 128.97 THz to 135.97 THz. The results make the MBNA design includes a wide range of frequencies over the MBSNA design.

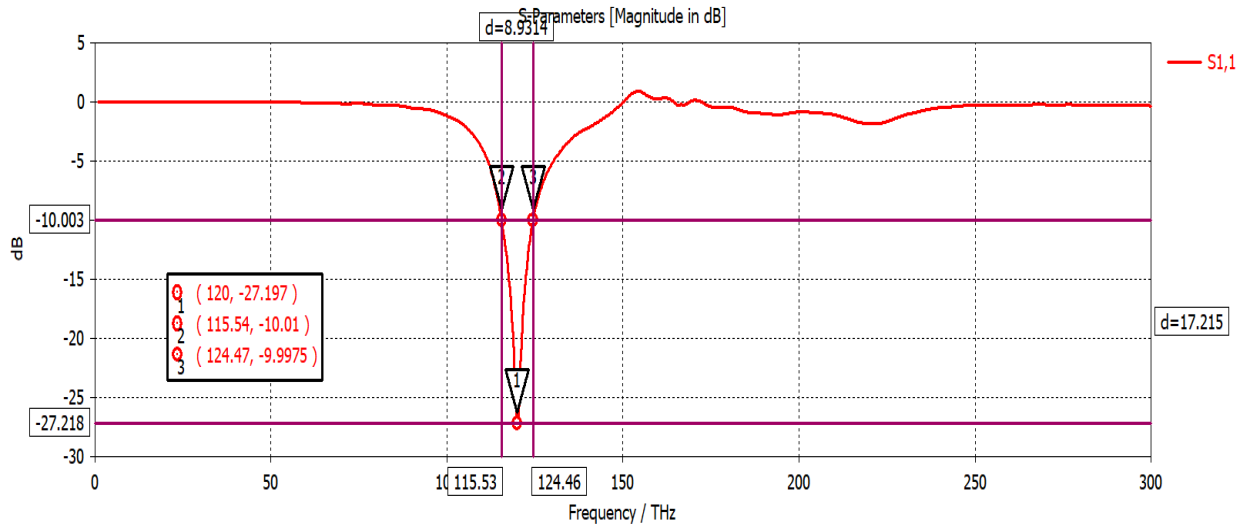


Figure 4.21: Bandwidth of MBNA.

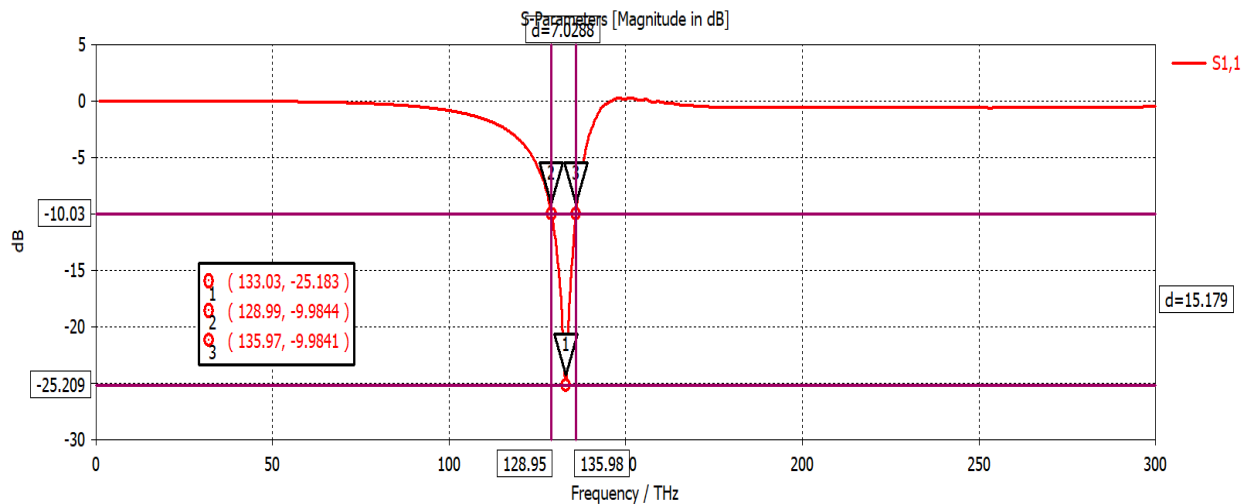


Figure 4.22: Bandwidth of MBSNA.

### 4.3.8 Validation between MBNA, MBSNA and other references.

The second comparison of our work that compare a references [52] and [53] with two proposed Nanoantennas (MBNA & MBSNA) in terms of the parameters that were calculated and extracted their results in this chapter as shown in table 4.4, where we observed in the reference we used in the comparison that there is resonated at a low frequency while the reflection coefficient was somewhat acceptable.

In the dielectric substrate in the reference Silicon nitrate with Quartz is used, while the dielectric substrate for the proposed Nanoantenna designs only silicon is used. The directivity is small compared with the two proposed Nanoantenna designs. Also, there is a low-bandwidth in the reference compared to the two proposed Nanoantenna designs.

**Table 4.4: Comparison between MBNA, MBSNA and references.**

Name	Sub. type	$S_{11}$	f(THz)	G(dB)	D(dB)	Eff.	BW
[52]	Silicon nitrate + Quartz	-14 to -22	5 to 10	---	3.8	---	2
[53]	Polyimide $\epsilon=3.5$	-35	0.75	5.09	5.71	89.14	---
<b>MBNA</b>	Silicon $\epsilon=11.9$	-27.19	120	5.36	5.47	97.63	8.93
<b>MBSNA</b>	Silicon $\epsilon=11.9$	-25.18	133	6.71	6.79	98.82	7

## 4.4 Characteristics of the Microstrip Wi-Fi-shape Nanoantenna and Microstrip Wi-Fi-shape Slot Nanoantenna.

### 4.4.1 Reflection Coefficient for MWNA & MWSNA.

The reflection coefficient shape is shown in Figures 4.23 and 4.24 for the two designs MWNA and MWSNA respectively. The value of the first one is -31.33 dB resonates at 106 THz but the second is -18.27 dB resonates at 126.28 THz. Here, the MWNA design can be considered more accurate than MWSNA design due to the descent of the frequency to the lower value in the  $S_{11}$  parameter.

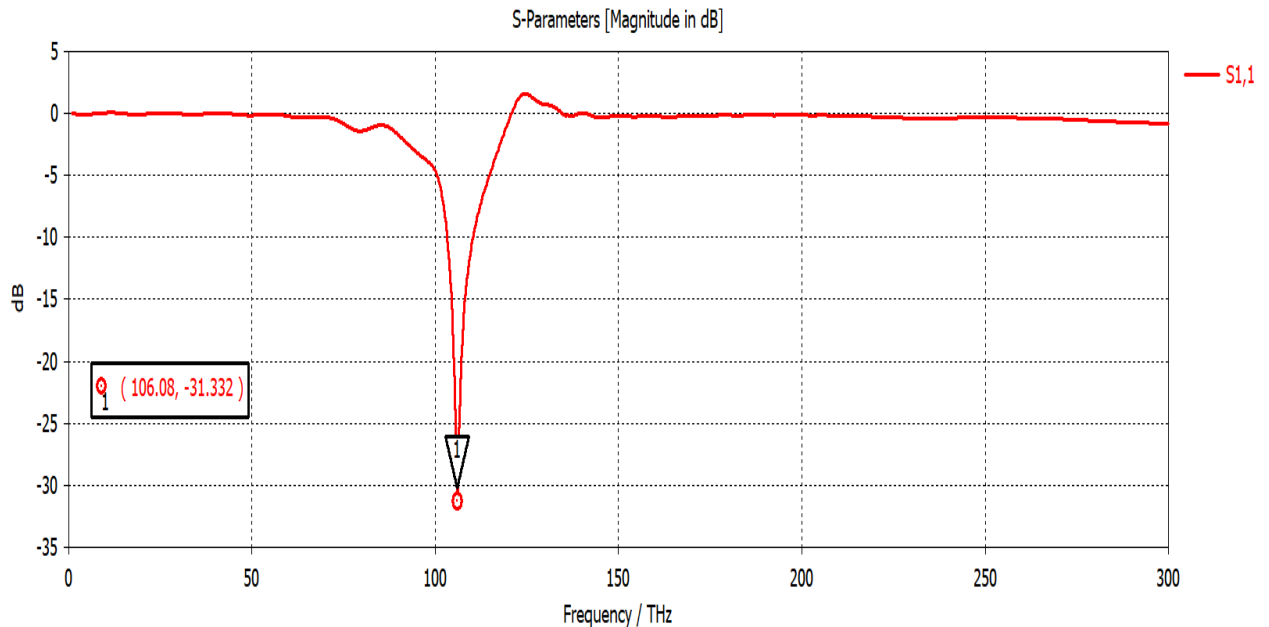
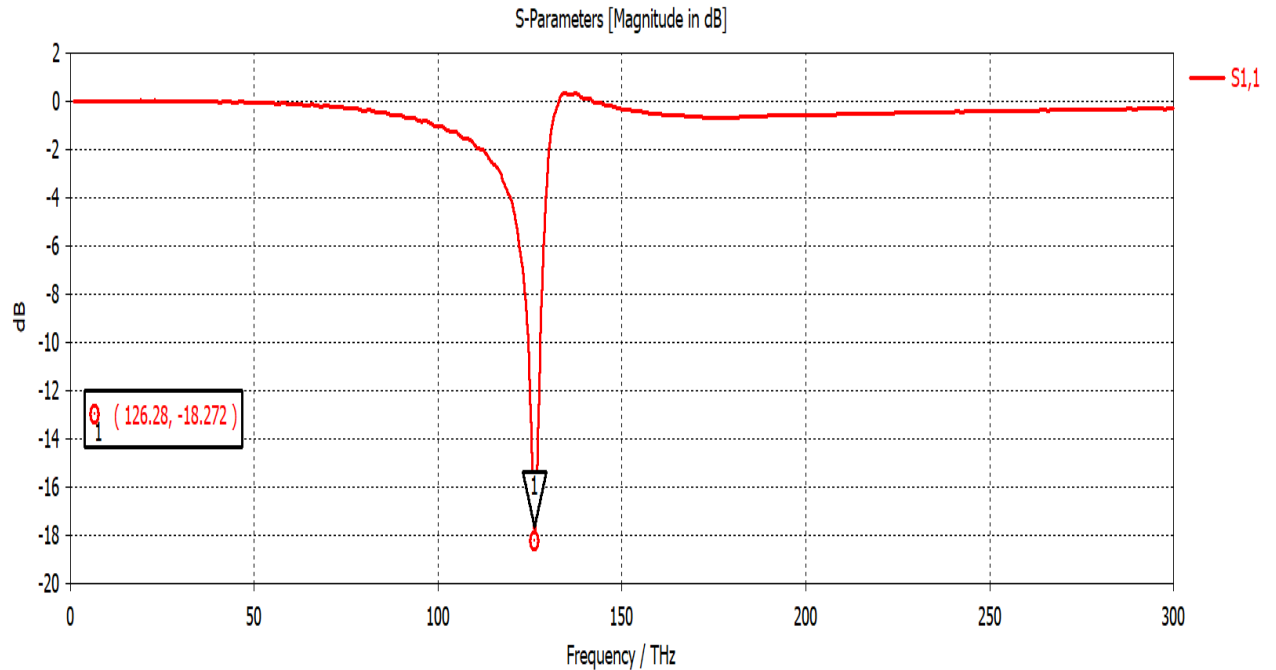


Figure 4.23:  $S_{11}$  of MWNA.

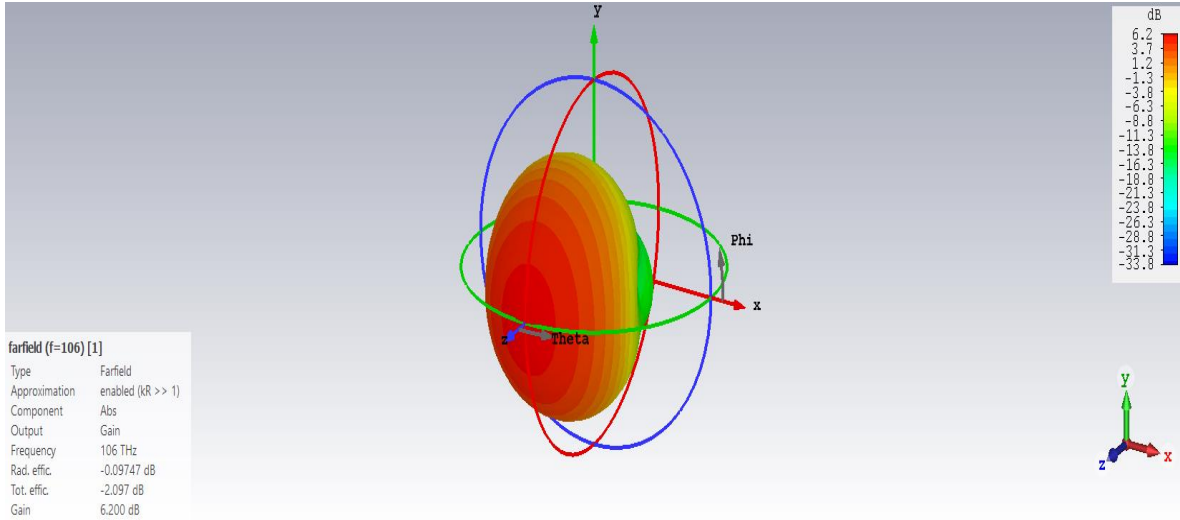


**Figure 4.24:  $S_{11}$  of MWSNA.**

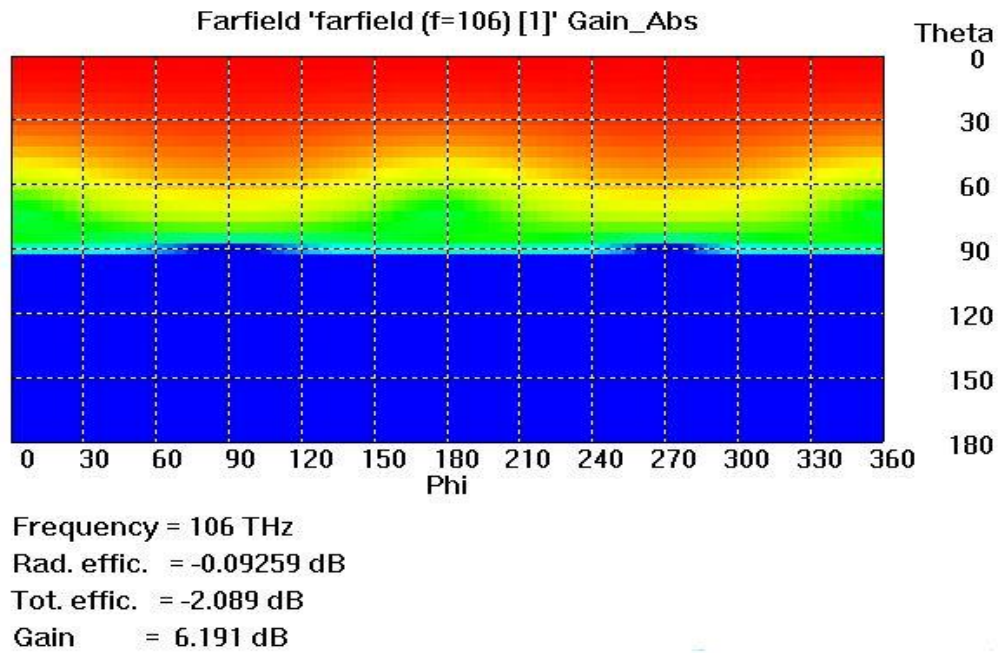
#### 4.4.2 Gain for MWNA & MWSNA.

The form of gain for the two designs MWNA and MWSNA is shown in Figures 4.25 and 4.26 respectively. The value of the gain to the MWNA design is 6.2 dB at the resonant frequency 106 THz. While the value of the gain of the MWSNA design is 6.57 dB at the resonant frequency 126.28 THz. In this case, the gain for the MWSNA design is more valuable than the MWNA design. Thus, the former design is preferred.



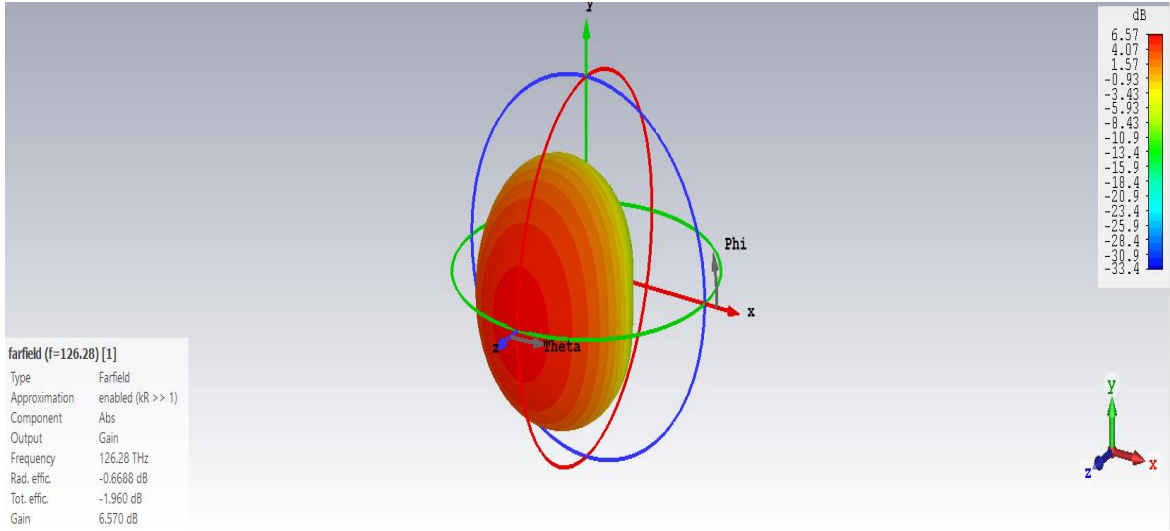


(a)

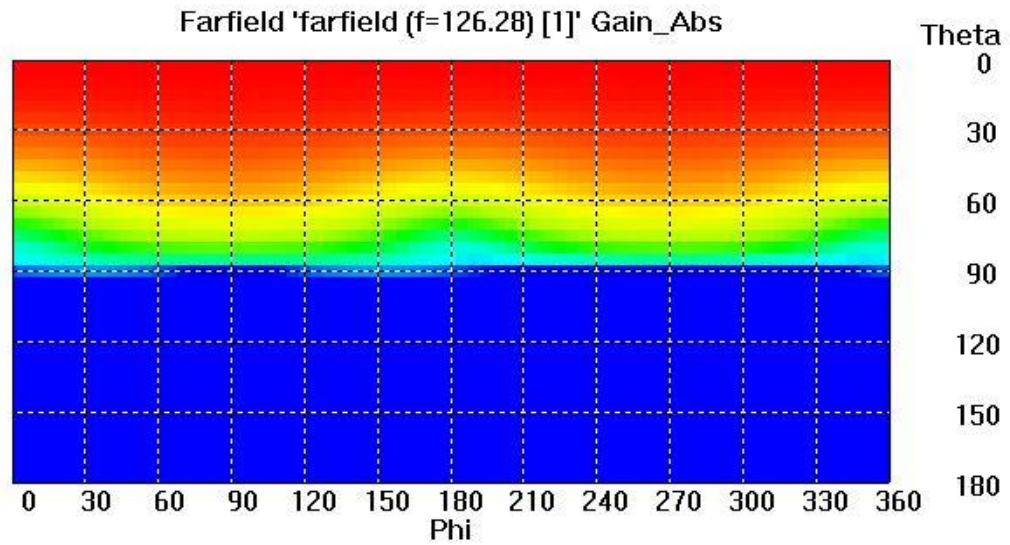


(b)

Figure 4.25: Gain of MWNA (a) 3D and (b) 2D.



(a)



Frequency = 126.28 THz  
 Rad. effic. = -0.6653 dB  
 Tot. effic. = -1.985 dB  
 Gain = 6.583 dB

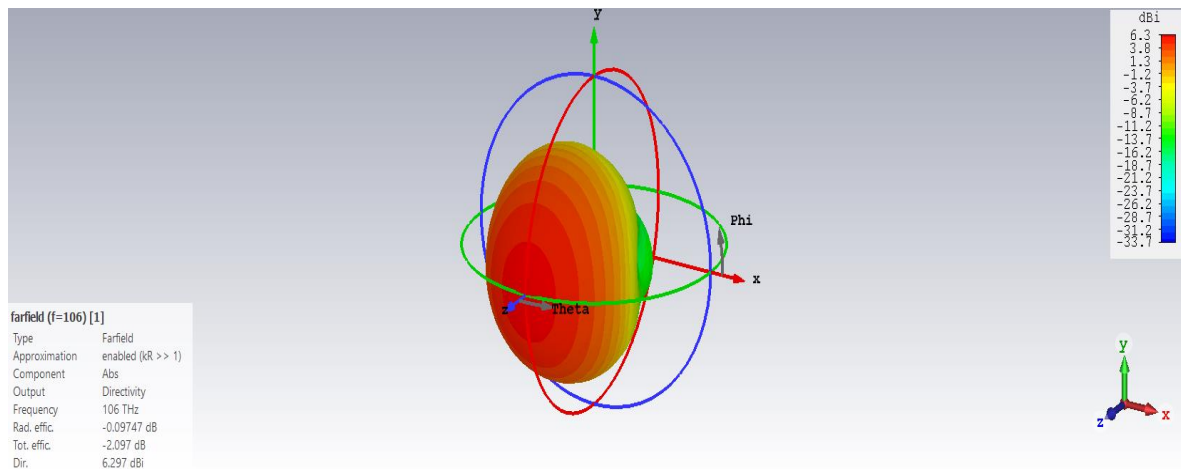
(b)

Figure 4.26: Gain of MWSNA (a) 3D and (b) 2D.

### 4.4.3 Directivity for MWNA & MWSNA.

The value of directivity to the MWNA is 6.3 dB, while the value of directivity to the MWSNA is 7.24 dB. These values are illustrated in Figures 4.27 and 4.28 respectively.

In these two designs we note that the directivity value is high and excellent. But in the MWSNA design, the highest guidance in all the designs that are designed in this thesis.



**Figure 4.27: Directivity of MWNA.**

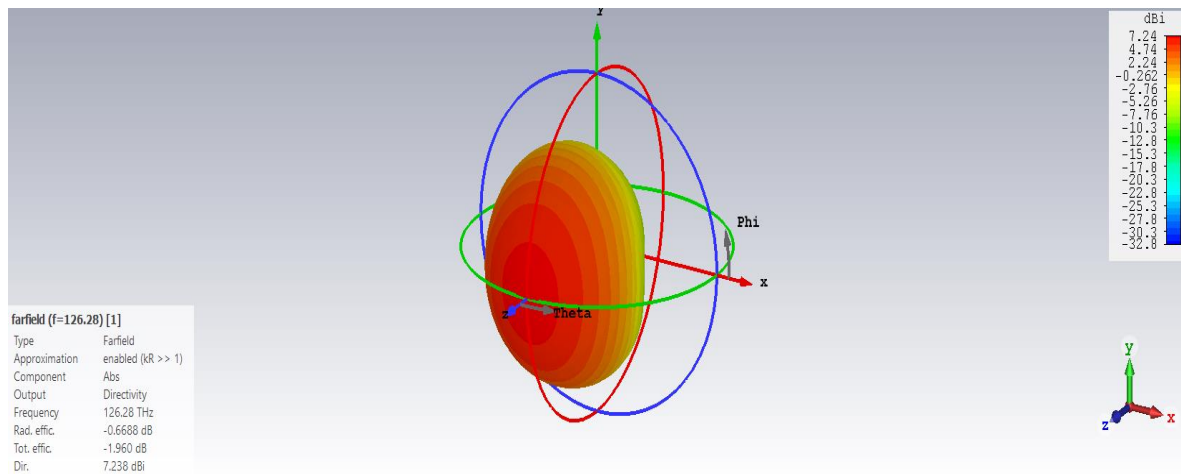


**Figure 4.28: Directivity of MWSNA.**

#### 4.4.4 Current Distribution for MWNA & MWSNA.

The simulated current distribution of the MWNA & MWSNA designs at different frequencies is illustrated in Figure 4.29. So, Figure 4.29 (a) shows the current distribution at the resonant frequency 106 THz. We notice the spread of the current from the middle of the patch towards the edges and in a manner similar to the shape of the circle.

In Figure 4.29 (b), the form of current distribution at the resonant frequency 126.28 THz is centered from the upper half of the Nanoantenna and distributed from the patch without flow in the Wi-Fi-shape slot. It is obvious that most of the current concentration is in the upper patch of the MWSNA.

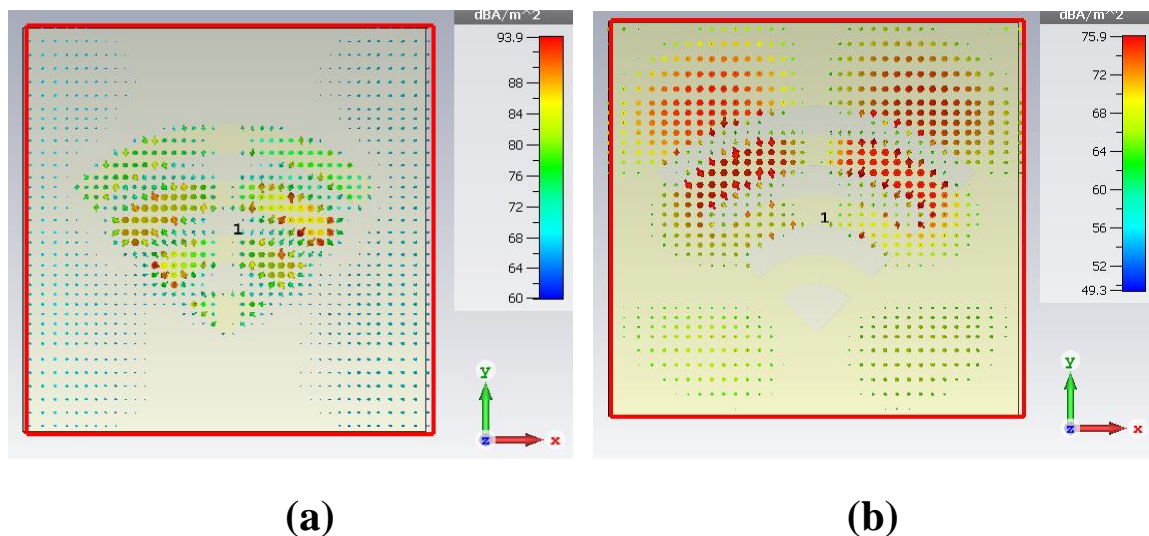


**Figure 4.29: Current distribution of (a) MWNA & (b) MWSNA.**

#### 4.4.5 Radiation Patterns for MWNA & MWSNA.

As mentioned earlier, the radiation pattern is a variation in the power radiated from the Nanoantenna as a function of the direction away from the Nanoantenna. Overall values of radiation to the MWNA & MWSNA are shown in Table 4.5. The radiation patterns for the MWNA is shown in Figure 4.30. Resonant frequency of the MWNA design is 106 THz, in the x-y plane ( $\theta = 90^\circ$ ); the value of main lobe magnitude is (-13.1) dB; the main lobe direction is ( $194^\circ$ ) and the angular width is ( $86.4^\circ$ ). While in the y-z plane ( $\varphi = 90^\circ$  represent E-plane), the main lobe magnitude is (6.3) dB, the main lobe direction is ( $0^\circ$ ) and the angular width is ( $77.8^\circ$ ), but the x-z plane ( $\varphi = 0^\circ$  represent H-plane) the main lobe magnitude is (6.3) dB; the main lobe direction is ( $0^\circ$ ) and the angular width is ( $59.4^\circ$ ).

The MWSNA design of the radiation pattern resonates to its resonant frequency 126.28 THz as in Figure 4.31. The radiation process contains three planes. The first plane is x-y plane ( $\theta = 90^\circ$ ); contain main lobe magnitude is (-20.8) dB, main lobe direction is ( $148^\circ$ ) and the angular width is ( $64.5^\circ$ ). The second plane is y-z plane ( $\varphi = 90^\circ$ ); contain main lobe magnitude is (7.24) dB; main lobe direction is ( $1^\circ$ ) and the angular width is ( $76.4^\circ$ ). The last plane is x-z plane ( $\varphi = 0^\circ$ ) contain main lobe magnitude is (7.24) dB; main lobe direction is ( $0^\circ$ ) and the angular width is ( $60.7^\circ$ ).

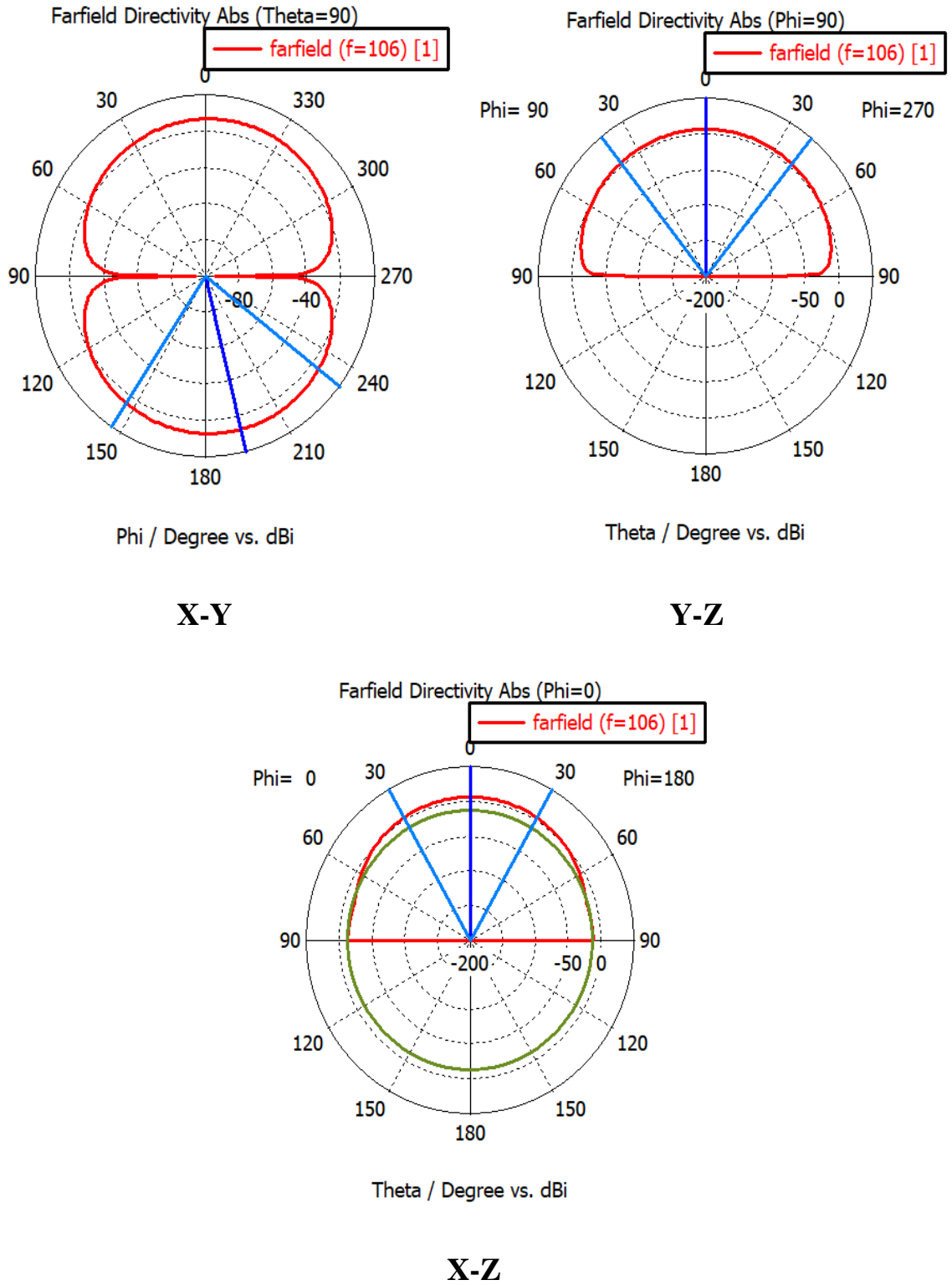


Figure 4-30: Radiation pattern of the MWNA at  $f=106$  THz.

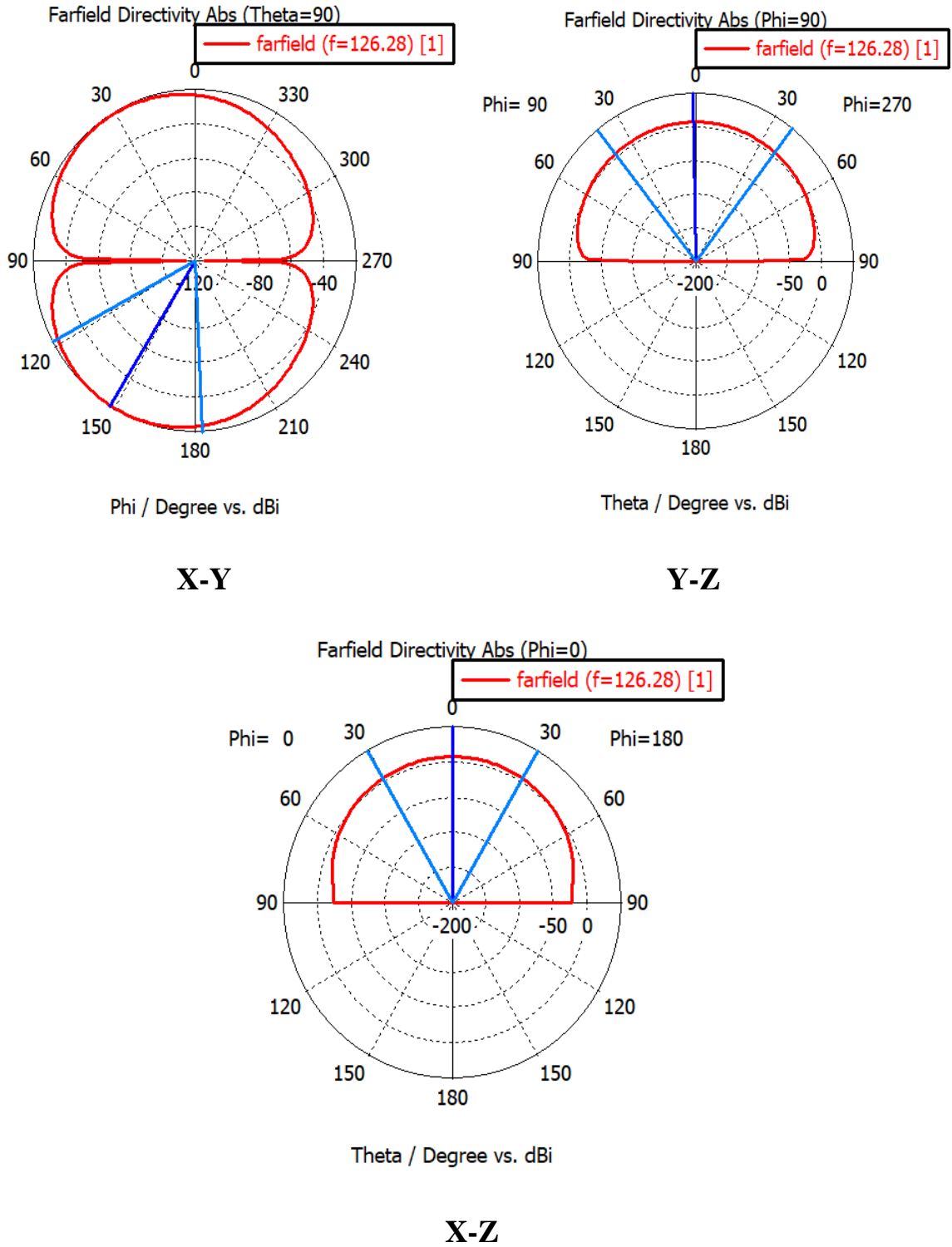


Figure 4-31: Radiation pattern of the MWSNA at f=126.28 THz.



**Table 4.5: Characteristics of the far-field radiation pattern for the MWNA & MWSNA.**

Freq. (THz)	Parameter	x-y plane	y-z plane	x-z plane
106	Main lobe magnitude(dB)	-13.1	6.3	6.3
	Main lobe direction(deg.)	194	0	0
	Angular width(deg.)	86.4	77.8	59.4
	Side lobe level (dB)	0	0	-19.7
126.28	Main lobe magnitude(dB)	-20.8	7.24	7.24
	Main lobe direction(deg.)	148	1	0
	Angular width(deg.)	64.5	76.4	60.7
	Side lobe level (dB)	0	0	0

#### 4.4.6 Efficiency for MWNA & MWSNA.

The value of efficiency to the MWNA design is 98.41 %. It is calculated depending on the relationship between the gain and directivity. Hence, the value of the efficiency in MBSNA design is 90.74 %. In these two designs, we find that the MWNA design is more efficient than the MWSNA design based on the results extracted from the above designs.

#### 4.4.7 Bandwidth for MWNA & MWSNA.

Depending on the diagram shown in Figures 4.32 and 4.33 for the MWNA and MWSNA respectively. The range of bandwidth



starts from 103.31 THz and ends at frequency 110.31 THz for the MWNA design producing a bandwidth 7 THz. However, the range of bandwidth to the MWSNA design starts from frequency 124.53 THz and ends at frequency 127.85 THz, producing a bandwidth approximately 3.32 THz. When comparing the two designs, it appears that the MWNA design has a wider range of frequencies which can be used in several applications. In the MWSNA design range is very few, making applications limited.

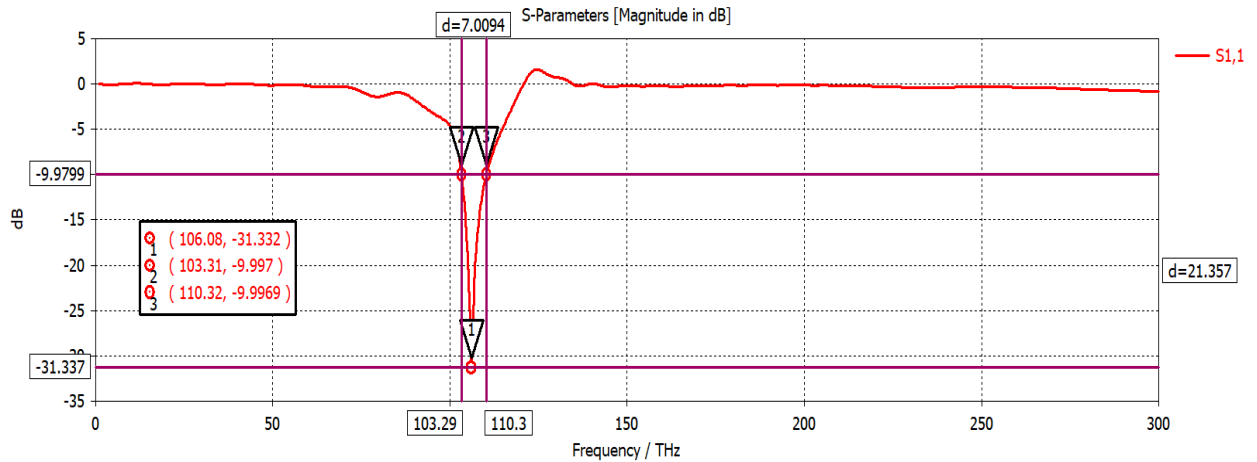


Figure 4.32: Bandwidth of MWNA.

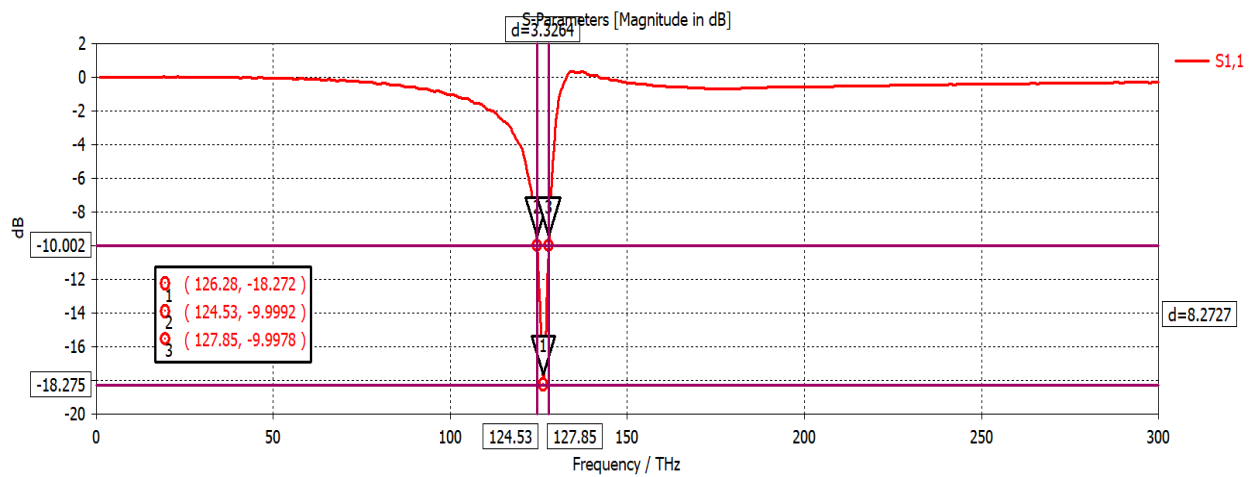


Figure 4.33: Bandwidth of MWSNA.

#### 4.4.8 Validation between MWNA, MWSNA and other references.

The third comparison that compared a reference and two proposed Nanoantennas (MWNA & MWSNA) in terms of the parameters with results that calculated in this chapter as shown in table 4.6, where we observed in the reference we used in the comparison that there is resonated at a low frequency while the reflection coefficient was good.

In the dielectric substrate of the reference, silicon dioxide  $\text{SiO}_2$  is used. In the dielectric substrate for the proposed Nanoantenna designs only silicon is used. The directivity and gain are small compared with the two proposed Nanoantenna designs. Also, there is a low-bandwidth in the reference compared to the two proposed Nanoantenna designs. In terms of efficiency the Nanoantenna is considered very close between reference and the two proposed Nanoantenna designs.

**Table 4.6: Comparison between MWNA, MWSNA and references.**

Name	Sub. type	$S_{11}$	f(THz)	G(dB)	D(dB)	Eff.	BW
[54]	$\text{SiO}_2$ $\epsilon=4$	-27.57	12.2 to 13.8	5.3	5.32	99.33	1.8
[55]	Crystal $\epsilon=9.1$	-23	0.69	4.5	6.2	72.58	---
<b>MWNA</b>	Silicon $\epsilon=11.9$	-31.33	106	6.2	6.3	98.41	7
<b>MWSNA</b>	Silicon $\epsilon=11.9$	-18.27	126.28	6.57	7.24	90.74	7

## 4.5 Comparison between overall six proposed designs.

In this part of the chapter, we compare the proposed six Nanoantennas in terms of parameters: reflection coefficient  $S_{11}$ , resonant frequency, gain, directivity, efficiency, bandwidth and application.

We observe the  $S_{11}$  varying from -14 dB to -45 dB depending on the frequency band. All values are considered acceptable because they exceed the -10 dB. The resonant frequencies bands start from 106 THz and end 133 THz.

The values of the gain start at 5.36 dB and end 6.71 dB while the values of the directivity start at 5.47 dB and end 7.24 dB. The gain and directivity of the six proposed Nanoantennas are very good compared with the previous work.

The values of the efficiency of the six proposed Nanoantennas are very good compared with the previous work, therefore we obtain the high efficiency 98.82 % to the MBSNA, while the low efficiency is 88.28 % to the MHSNA. The MBNA has the highest bandwidth while the MHSNA has the lowest bandwidth.

Table 4.7, comparison between the sixth proposed Nanoantennas.

Name	$S_{11}$	f(THz)	G(dB)	D(dB)	Eff.	BW	Applications
MHNA	-45.71	129.44	6.45	6.56	98.32	8	Spectroscopy for Imaging [56] [57] [58]
MHSNA	-14.19	129.74	5.73	6.49	88.28	6.6	Spectroscopy for Imaging [56] [57] [58]
MBNA	-27.19	120	5.36	5.47	97.63	8.93	Imaging and Sensing [38] [57] [58]
MBSNA	-25.18	133	6.71	6.79	98.82	7	Sensing [57] [58]
MWNA	-31.33	106	6.2	6.3	98.41	7	Communication Security Sensing [28] [57] [58]
MWSNA	-18.27	126.28	6.57	7.24	90.74	3.3	Visible region & Mid infrared (IR) [59] [57] [58]

In the Figure 4.34 below show the values of the six proposed nanoantennas.

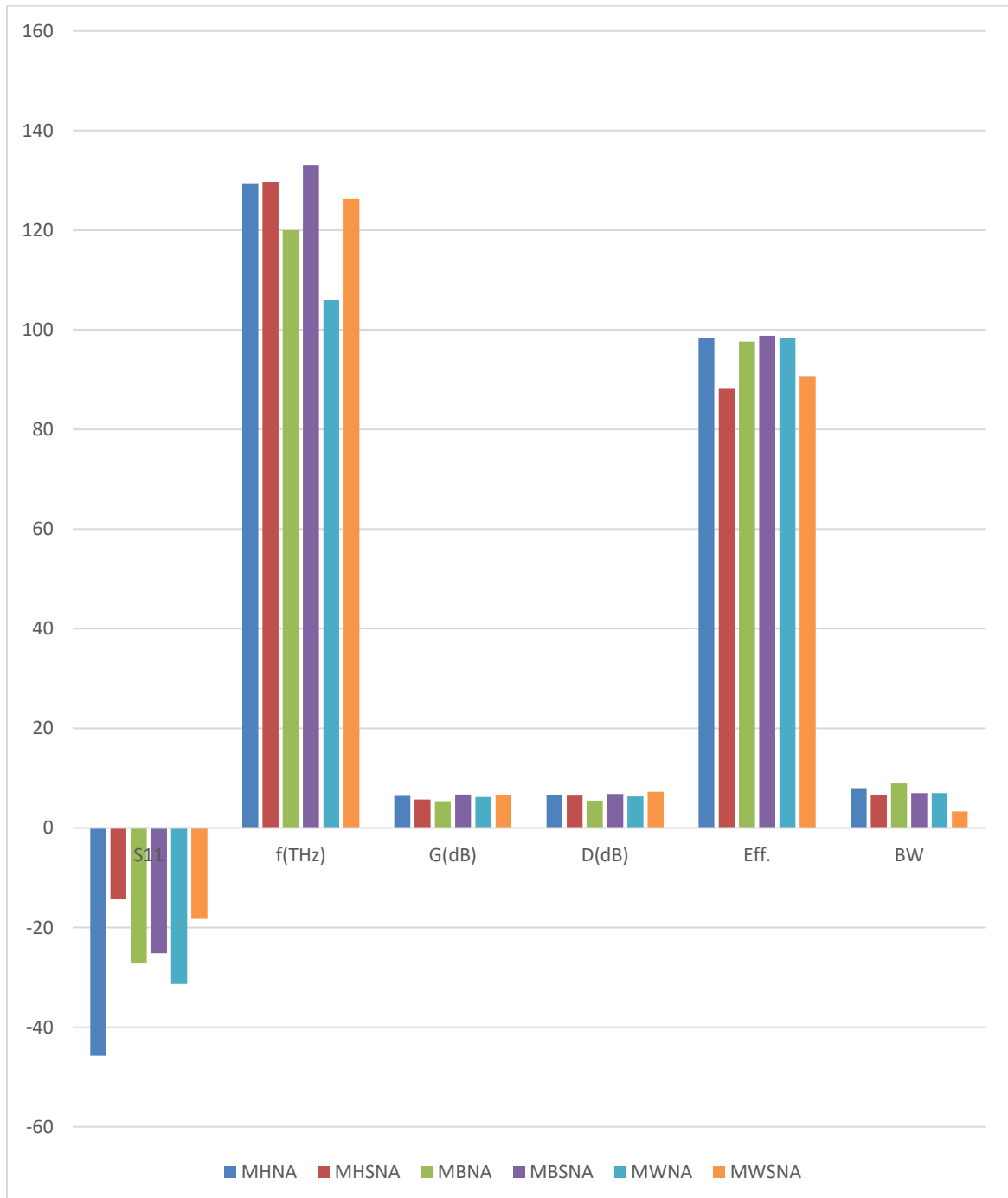


**Figure 4.34: values of six proposed nanoantennas.**

# CHAPTER FIVE

## CONCLUSIONS AND SUGGESTIONS FOR FUTURE WORK

### 5.1 Introduction

In this chapter, the most important goals of the work will be reviewed, as well as the conclusion obtained from the proposed designs. Besides, highlight on the recommendations for the future work.

### 5.2 Conclusion

In this section, the associated comments about the six-design methodologies of Microstrip patch antennas are presented. These six Nanoantennas are proposed with different geometrical shapes to demonstrate the effect of the geometrical shape of the patch layer of Microstrip Nanoantenna on the antenna performance, such as reflection coefficient  $S_{11}$ , bandwidth, Directivity, current distribution, efficiency and gain. So, the first and second Microstrip Nanoantenna designs take the form of Hash-shape and Hash-shape Slot. So they are called Microstrip Hash-shape Nanoantenna (MHNA) and Microstrip Hash-shape Slot Nanoantenna (MHSNA). These Nanoantennas give a range of bandwidth (125.3 - 133.3) THz and (126.39 - 132.99) THz respectively.

The third and fourth Microstrip Nanoantenna designs take the form of Bluetooth-shape and Bluetooth-shape Slot. Thus they are called Microstrip Bluetooth-shape Nanoantenna (MBNA) and Microstrip Bluetooth-shape Slot Nanoantenna (MBSNA). These Nanoantennas give a range of bandwidth of (115.54 - 124.47) THz and (128.97 - 135.97) THz respectively. Also, the fifth and sixth Microstrip Nanoantenna designs take the form of Wi-Fi-shape and Wi-Fi-shape Slot. They are called Microstrip Wi-Fi-shape Nanoantenna (MWNA) and Microstrip Wi-Fi-shape Slot Nanoantenna (MWSNA). Indeed, these Nanoantennas operate in the range of bandwidth from (103.31 - 110.31) THz and (103.31 - 110.31) THz respectively.

Finally, concluding that the best design is the MBNA according to the highest bandwidth and the MWSNA according to the highest directivity.

### **5.3 Suggestions for the Future Work**

The suggestions for the future scope can be reviewed as follows:-

1. Design other shapes of Microstrip patch Nanoantenna and obtain their characteristics, trying to enlarge the gain and bandwidth.

2. Use another type of feeding technique and compare the results with the results that are presented in this work.
3. Design a Microstrip Nanoantennas array to modify the gain to be suitable for applications that need high Bandwidth.
4. Try to fabricate one of the designs mentioned in the previous work because fabrication is not available currently neither in Iraq nor in neighboring countries.
5. Try to make a mathematical analysis of the Microstrip Nanoantenna designs.



## References

- [1] Constantine A. Balanis, *Antenna Theory Analysis and Design*, New Jersey: John Wiley & Sons, Inc., Fourth Edition 2016.
- [2] Dheif I. Abood and Refat T. Hussain, "Wideband Nano Fractal Antenna Design," *MSc thesis, Department of Electrical Engineering, University of Technology*, 2015.
- [3] Riffat T. Hussien and Dheif I. Abood, "A Wideband Hybrid Plasmonic Fractal Patch Nanoantenna," *International Journal of Electronics and Communication Engineering & Technology (IJECECT)*, vol. 5, no. 9, pp. 1-8, 2014.
- [4] A. Krasnok et.al, "Optical Nanoantennas," *Phys.-Usp*, vol. 56, no. 6, pp. 539-564, 2013.
- [5] S. Cakmakyapan and N. Cinel, "Validation of electromagnetic field enhancement in near-infrared through Sierpinski fractal nanoantennas," *Opt. Express*, vol. 22, no. 16, p. 19504, 2014.
- [6] Zeev Iluz and Amir Boag, "Wideband dual Vivaldi nano-antenna with high radiation efficiency over the infrared frequency band," in *Microwaves Communications Antennas and Electronic Systems (COMCAS), IEEE International Conference*, 2011.
- [7] A. Alú and N. Engheta, "Wireless at the Nanoscale: Optical Interconnects using Matched Nanoantennas," *Phys. Rev.*, 2010.
- [8] Lukas Novotny, "Effective wavelength scaling for optical antennas," *Physical Review Letters*, p. 266802, 2007.
- [9] Lingli Zhan and KeXiu Dong, "Design of Resonant Optical Nano-antenna for 1.55 $\mu\text{m}$  wavelength," Crown city, 2011.

- [10] Javier Alda et.al, "Nano-antennas for optoelectronics and nanophotonics," *SPIE—The International Society for Optical Engineering*, 2006.
- [11] Ivan Wang and Y. Du, "Directional field enhancement of dielectric nano optical disc antenna arrays," *ScienceDirect Elsevier B.V. All rights reserved*, 2011.
- [12] Shereen A. Shandal, Mahmood F. Mosleh and Mohammed A. Kadim, "Design and Implementation of Wideband Fractal Microstrip Antenna," *M.Sc. Thesis, Middle Technical University, Electrical Engineering Technical College*, p. 16, 2018.
- [13] Saif Nadhem, "Design and Analysis of Slotted Patch Antenna for Wideband Applications," *M.Sc. Thesis, Al-Mustansiriyah University, Department of Electrical Engineering*, 2016.
- [14] Debatosh Guha and Yahia M. M. Antar, "Microstrip and Printed Antennas: New Trends, Techniques And Applications," *India: John Wiley & Sons Ltd*, 2011.
- [15] Zhi Ning Chen and Michael Y. W. Chia, "Broadband Planar Antennas Design and Applications," *Institute for Infocomm Research, Singapore*, 2006.
- [16] Shengjie Zhai, "Hybrid Plasmonic Nanoantennas: Fabrication, Characterization and Application," *PhD dissertation, University of Nevada*, 2012.
- [17] Andreas Pospischil et.al, "CMOS-compatible graphene photodetector covering all optical communication bands," *Vienna University of Technology, Institute of Photonics*, 2014.
- [18] Mairead Bevan, "Electromagnetic Analysis of Horn Antennas in the Terahertz region," *M.Sc Thesis, Ireland, NUI Maynooth, Department of Experimental Physics*, May 2013.

- [19] A. Kawakami et al, "Fabrication of Nano-Antennas for Superconducting Infrared Detectors," *IEEE TRANSACTIONS ON APPLIED SUPERCONDUCTIVITY*, vol. 21, no. 3, JUNE 2011.
- [20] Kumud RanjanJha and G.Singh, "Performance analysis of an open-loop resonator loaded terahertz microstrip antenna," *Science Direct, Elsevier, MicroelectronicsJournal*, vol. 42, 2011.
- [21] Mario Bareib et al, "Nano Antenna Array for Terahertz Detection," *IEEE Transactions on Microwave Theory and Techniques*, vol. 59, no. 10, October 2011.
- [22] Lechen Yang et al., "Analysis of photonic crystal and multi-frequency terahertz microstrip patch antenna," *Science Direct, Elsevier, Physica B*, vol. 431, no. 11–14, 2013.
- [23] Junsei Horikawa et al, "Study of Mid-Infrared Superconducting Detector with Phased Array Nano-Slot Antenna," *IEEE Transactions on Applied Superconductivity*, 2013.
- [24] Evgeny G. Mironov et al, "Titanium Nano-Antenna for High-Power Pulsed Operation," *IEEE Journal of Lightwave Technology*, vol. 31, no. 15, AUGUST 1, 2013.
- [25] Ameneh Nejati et al., "Effect of photonic crystal and frequency selective surface implementation on gain enhancement in the microstrip patch antenna at terahertz frequency," *Science Direct, Elsevier, Physica B*, vol. 449, no. 113–120, May 2014.
- [26] B. Mehta and M. E. Zaghloul, "Tuning the Scattering Response of the Optical Nano Antennas Using Graphene," *IEEE Photonics Journal*, vol. 6, no. 1, February 2014.
- [27] Amandeep Singh and Surinder Singh, "A trapezoidal microstrip patch antenna on photonic crystal substrate substratefor high speed THz applications," *Science Direct, Elsevier, Photonics and Nanostructures –*

*Fundamentals and Applications*, no. 490, p. 11, 2015.

- [28] Behzad Ashrafi et al, "Integrated Optical Phased Array Nano-Antenna System Using a Plasmonic Rotman Lens," *IEEE Journal of Lightwave Technology*, 2015.
- [29] Fatemeh Taghian et al, "Enhanced Thin Solar Cells Using Optical Nano-Antenna Induced Hybrid Plasmonic Travelling-Wave," *IEEE Journal of Lightwave Technology*, 2015.
- [30] Luke Zakrajsek et al, "Lithographically Defined Plasmonic Graphene Antennas for Terahertz-band Communication," *IEEE Antennas and Wireless Propagation Letters*, 2015.
- [31] Mai et al., "Novel Wire-Grid Nano-Antenna Array with Circularly Polarized Radiation for Wireless Optical Communication Systems," *IEEE Journal of Lightwave Technology*, 2017.
- [32] Divesh Mittala and Ekambir Sidhu, "THz Rectangular Microstrip Patch Antenna employing Polyimide substrate for Video Rate Imaging and Homeland Defence Applications," *International Journal for Light and Electron Optics*, vol. 17, no. 5, 2017.
- [33] Ritesh Kumar, "Design and analysis of novel microstrip patch antenna on photonic crystal in THz," *Science Direct, Elsevier, Physica B: Condensed Matter*, vol. 545, no. 107-112, 2018.
- [34] Qudsia Rubani et al., "Design and Analysis of a Terahertz Antenna for Wireless Body Area Networks," *International Journal for Light and Electron Optics*, vol. 18, no. 5, October 2018.
- [35] Abdel-Karim S.O. Hassan et al, "Optimization of a Novel Nano Antenna With Two Radiation Modes Using Kriging Surrogate Models," *IEEE Photonics Journal*, vol. 10, no. 4, August 2018.
- [36] Yuyao Chen et al, "Meander Line Nanoantenna Absorber for Subwavelength Terahertz Detection," *IEEE Photonics Journal*, vol. 10,

no. 4, August 2018.

- [37] Seyed Arash and Gholamreza Moradi, "An improved method to null-fill H-plane radiation pattern of graphene patch THz antenna utilizing branch feeding microstrip line," *Science Direct, Elsevier, Optik - International Journal for Light and Electron Optics*, vol. 181, no. 21–27, 2019.
- [38] Gȯktug̃ Is,ıklar et.al, "Design and Analysis of Nanoantenna Arrays for Imaging and Sensing Applications at Optical Frequencies," *Advanced Electromagnetics*, vol. 8, no. 2, FEBRUARY 2019.
- [39] Seevan Fahmi Abdulkareem, "Design and Fabrication of Printed Fractal Slot Antennas for Dual-band Communication Applications," *M.Sc. Thesis, University of Technology, Department of Electrical Engineering, Oct, 2013*.
- [40] Girish Kumar, and K. P. Ray, "Broadband Microstrip Antennas," *Artech House, Inc., Boston, London, 2003*.
- [41] Sourabh Bisht et.al, "Study The Various Feeding Techniques of Microstrip Antenna Using Design and Simulation Using CST Microwave Studio," *International Journal of Emerging Technology and Advanced Engineering*, vol. 4, no. 9, 2008.
- [42] Kai Zhang et al, "Design and Optimization of Broadband Single-Layer Reflectarray," *IEEE* , 2014.
- [43] F. Zubir et al, "Design and Analysis of Microstrip Reflectarray Antenna with minkowski shape Radiation Element," *Progress In Electromagnetics Research*, vol. 24, pp. 317-331, 2010.
- [44] Adeel Afridi, "Design and Analysis of Plasmonic Nanoantennas with Ground Plane and Impedance Matching," *Msc thesis in Koc University*, p. 17, August 16, 2016.

- [45] WU YU-MING, "Analysis and Design of Nanoantennas," *Harbin Institute of Technology*, p. 27, 2010.
- [46] Constantine A. Balanis, *Advanced Engineering Electromagnetics*, United States of America: John Wiley & Sons, Inc., Second Edition 2012.
- [47] Sikiru Zakariyya, "Modeling of Miniaturized, Multiband and Ultra-Wideband Fractal Antenna," *Msc thesis in Eastern Mediterranean University*, p. 4, September 2015.
- [48] N.Anusha et al, "Design and Investigation of Terahertz Antenna Using Different Configurations," in *International Conference on Electronics, Communication and Aerospace Technology ICECA*, Vizianagaram,India, 2017.
- [49] David M. Pozar, *Microwave Engineering*, United Stateso America: John Wiley & Sons,Inc, Third Edition 2005.
- [50] Tan Thet Ming and Goh Chin Hock, "Rounded Bowtie Nanoantenna for Solar Energy Harvester," *Journal of Built Environment, Technology and Engineering*, vol. 2, march 2017.
- [51] Isa Kocakarın and Korkut Yegin, "Glass Superstrate Nanoantennas for Infrared Energy Harvesting Applications," *Hindawi Publishing Corporation, International Journal of Antennas and Propagation*, p. 7, 2013.
- [52] N.Anusha et al, "Design and Investigation of Terahertz Antenna Using Different Configurations," in *IEEE International Conference on Electronics, Communication and Aerospace Technology ICECA*, 2017.
- [53] S. Anand et al, "Graphene nanoribbon based terahertz antenna on polyimide substrate," *ScienceDirect, ELSEVIER, Optik*, vol. 125, 2014.
- [54] Rajni Bala and Anupma Marwaha, "Characterization of graphene for performance enhancement of patch antenna in THz region,"

*ScienceDirect, ELSEVEIR, Optik*, 2015.

- [55] G. Singh, "Design considerations for rectangular microstrip patch antenna on electromagnetic crystal substrate at terahertz frequency," *ScienceDirect, ELSEVIER, Infrared Physics & Technology*, 2009.
- [56] Isha Malhotra et al., "Terahertz antenna technology for imaging applications: a technical review," *International Journal of Microwave and Wireless Technologies*, vol. 173, no. 9, Feb 2018.
- [57] L. Businaro et al., "Mid-infrared nanoantenna arrays on silicon and CaF<sub>2</sub> substrates for sensing applications," *Science Direct, Elsevier, Microelectronic Engineering.*, vol. 97, no. 5, p. 197–200, 2012.
- [58] Marco P. Fischer et al., "Plasmonic mid-infrared third harmonic generation in germanium nanoantennas," *Official journal of the CIOMP, Light: Science & Applications*, vol. 7, no. 106, 2018.
- [59] Davide Ramaccia et al., "Electrical and Radiation Properties of a Horn Nano-Antenna at Near Infrared Frequencies," *IEEE, In University, Rome, Italy*, vol. 11, pp. 2407-2410, 2011.
- [60] Cst.com, "CST - Computer Simulation Technology," 2014. [Online]. Available: <https://www.cst.com/>. [Accessed 5 1 2019].



جمهورية العراق  
وزارة التعليم العالي والبحث العلمي  
جامعة الفرات الاوسط التقنية  
الكلية التقنية الهندسية- نجف



# تصميم جديد ودراسة تحليلية للهوائي النانوي الشريطي الدقيق

رسالة مقدمة الى  
قسم هندسة تقنيات الاتصالات  
كجزء من متطلبات نيل درجة ماجستير تقني في هندسة تقنيات الاتصالات

تقدم بها

بسام رؤوف محمد علي الاسدي  
بكالوريوس في هندسة تقنيات الاتصالات

إشراف

الاستاذ الدكتور عبد الكاظم جعفر الياسري

الاستاذ المساعد الدكتور فارس محمد علي الجعيفري

ايلول / 2019



## الخلاصة

العديد من التطبيقات العلمية للاستشعار عن بعد اثار اهتمام الباحثين في مجال تصميم الهوائي النانوي الشريطي الدقيق بنطاق ترددات التيراهيرتز. ونتيجة لاختراع مكونات جديدة في تقنية النانو وكذلك التقنيات الطيفية الضوئية ادى هذا إلى تطوير التطبيقات في منطقة التيراهيرتز.

الهدف الرئيسي من هذه الرسالة هو تصميم ومحاكاة وتحليل هوائي نانوي جديد نوع شريطي دقيق يعمل في منطقة التيراهيرتز ويغطي الكثير من نطاقات الاتصالات البصرية أو نطاقات الترددات من (80-300) تيراهيرتز.

في هذا العمل ، هناك العديد من العناصر الهندسية مثل التغذية وأبعاد الرقعة ومستوي الارضية. حيث يتم إدراج فتحات بأحجام وأشكال مختلفة في الهوائيات النانوية.

في هذه الرسالة ، تم تصميم ومحاكاة ستة تصاميم هوائيات نانوية شريطية دقيقة ، اذ تم الحصول على العديد من نطاقات التردد التي تعمل في منطقة التيراهيرتز. جميع الركائز العازلة للتصاميم الستة تتكون من العازل السيليكون لأنه يحتوي على ثابت عزل عالي  $\epsilon = 11.9$  ، نوع التغذية المستخدم لإثارة تلك الهوائيات النانوية هو تغذية موجية عند 50 اوم. جميع التصاميم للهوائيات النانوية تكون أبعاد الركيزة لها في حدود (950 x 950) نانومتر بسمك 50 نانومتر بينما البعد من المستوى الأرضي في نطاق (950 x 950) نانومتر و بسمك 20 نانومتر. ابعاد الطبقة الاولى تكون في حدود (450 x 450) نانومت و بسمك 20 نانومتر. من أجل تقييم أداء كل هوائي من الهوائيات المقترحة ، تم استخدام محاكي البرمجيات والماتح تجاريا CST STUDIO SUITE 2018.

التصميمان الاول والثاني للهوائي الشريطي الدقيق يتخذان شكل الهاش والهاش المفتوح ، لذلك يطلق عليهما الهوائي النانوي الهاش الشريطي الدقيق و الهوائي النانوي الهاش المفتوح الشريطي الدقيق ، اذ تم الحصول على مجموعة من النطاقات الترددية من (125.3 - 133.3) تيراهيرتز و (126.39 - 132.99) تيراهيرتز على التوالي. التصميمان الثالث والرابع من الهوائيات النانوية يتخذان شكل البلوتوث و البلوتوث المفتوح ، لذلك يطلق عليهما اسم الهوائي النانوي بلوتوث الشريطي الدقيق و الهوائي النانوي بلوتوث مفتوح الشريطي الدقيق ، توفر هذه الهوائيات مجموعة من النطاقات الترددية من (115.54 - 124.47) تيراهيرتز و (128.97 - 135.97) تيراهيرتز على التوالي. اخيرا يأخذ التصميمان الخامس والسادس شكل الواي فاي و الواي فاي المفتوح ، لذلك يطلق عليهما اسم الهوائي النانوي واي فاي الشريطي الدقيق و الهوائي النانوي واي فاي مفتوح الشريطي الدقيق ، حيث تعمل هذه الهوائيات في النطاقات الترددية من (103.31 - 110.31) تيراهيرتز و (103.31 - 110.31) تيراهيرتز على التوالي.